EVALUATION OF GRAVITY DATA FOR THE STOKES-HELMERT SOLUTION TO THE GEODETIC BOUNDARY-VALUE PROBLEM

PAVEL NOVÁK

December 2000

EVALUATION OF GRAVITY DATA FOR THE STOKES-HELMERT SOLUTION TO THE GEODETIC BOUNDARY-VALUE PROBLEM

Pavel Novák

Department of Geodesy and Geomatics Engineering
University of New Brunswick
P.O. Box 4400
Fredericton, N.B.
Canada
E3B 5A3

December 2000

PREFACE

This technical report is a reproduction of a dissertation submitted in partial fulfillment of the requirements for the degree of Doctor of Philosophy in the Department of Geodesy and Geomatics Engineering, December 1999. The research was supervised by Dr. Petr Vaníček, and funding was provided by the Natural Sciences and Engineering Research Council of Canada, Natural Resources Canada, and a Geomatics for Informed Decisions (GEOIDE) project.

As with any copyrighted material, permission to reprint or quote extensively from this report must be received from the author. The citation to this work should appear as follows:

Novák, P. (2000). *Evaluation of Gravity Data for the Stokes-Helmert Solution to the Geodetic Boundary-Value Problem.* Ph.D. dissertation, Department of Geodesy and Geomatics Engineering Technical Report No. 207, University of New Brunswick, Fredericton, New Brunswick, Canada, 133 pp.

Abstract

The theory of an approximate solution to the gravimetric geoid has been known for about 150 years. Its revision from the view of gravity information available today, which would allow for the solution to the magic one-centimetre geoid, is the main topic of this dissertation. Built on basic principles of potential theory, a proper definition of the geodetic boundary-value problem is presented, including its possible approximations both in gravity and geometric spaces, leading to practical solutions. Based on these formulations, appropriate gravity data as an input for the solution to the geodetic boundary-value problem are defined.

Due to the non-existence of the solution in the real topographical space, a model space, based on the second Helmert condensation, is introduced. A transformation of observed values of gravity, both of terrestrial and spatial origin, into the Helmert space is accomplished by a series of gravity reductions and corrections. The latter originate in the existence of masses above the desired equipotential surface, i.e., the geoid. Effects of topographical and atmospheric masses on gravity potential and gravity are defined, and formulae for their practical numerical evaluations are presented.

Derived gravity data can be used for practical computations of geoidal heights. Based on spherical and ellipsoidal approximations of the geoid, appropriate integration kernels are derived and their practical evaluations discussed. The solution based on the spherical approximation of the geoid is tested using synthetic gravity data. The solution is then transformed back into the real space.

Derived formulae are subsequently used for numerical evaluations with real data over a test region in the Canadian Rocky Mountains which represents one of the most complex parts of both the earth's surface and gravity fields. Series of plots and tables are presented to justify the role of the proper gravity reductions in preparation of the accurate gravimetric geoid.

Effects of the second Helmert condensation of topographical masses on the geoid can reach values at a metre level. Their correct evaluation is therefore critical for the determination of the precise gravimetric geoid. An improved modelling of the topography using a spherical approximation reduces significantly errors of the geoid solutions. The effect of distant topography, neglected in geoid computations world-wide, helps to remove the low-frequency bias present in the current models of the regional gravimetric geoid.

Values of atmospheric corrections to the geoid are significantly smaller due to the smaller values of the atmospheric mass density. Since their combined effect can still reach several decimetres, they have to be also accounted for in evaluations of the precise gravimetric geoid. Some of the atmospheric effects, although important from the theoretical point of view, contribute very little to the geoid and can safely be neglected in practical computations.

The accuracy analysis of the discrete Stokes integration proves an insufficient discretization of the gravity field used in the current geoid computations in Canada. Assuming errorless discrete gravity data with a regular spacing of $5'$, an expected error in the geoid due to Stokes's integration can reach several centimetres.

Acknowledgments

Contents

List of Tables

List of Figures

List of Symbols

a	...	major semiaxis of the reference ellipsoid
a'	...	radius of Brillouin's sphere
a_c	...	centrifugal acceleration
a_g	...	gravitational acceleration
b	...	minor semiaxis of the reference ellipsoid
b'	...	complex argument of Legendre's functions
e	...	first numerical eccentricity of the reference ellipsoid
f	...	polar flattening of the reference ellipsoid
g	...	magnitude of gravity
h	...	geodetic height
m	...	geodetic parameter
m	...	order of the harmonic series expansion
n	...	degree of the harmonic series expansion
r	...	geocentric radius in spherical coordinates
r_c	...	geocentric radius of the co-geoid in spherical coordinates
r_e	...	geocentric radius of the ellipsoid in spherical coordinates
r_g	...	geocentric radius of the geoid in spherical coordinates
r_s	...	geocentric radius of the topography in spherical coordinates
r_t	...	geocentric radius of the telluroid in spherical coordinates
t_n	...	modification coefficients to Stokes's function
u	...	geocentric radius in ellipsoidal coordinates

u'	...	complex argument of Legendre's functions
u_c	...	geocentric radius of the co-geoid in ellipsoidal coordinates
u_e	...	geocentric radius of the ellipsoid in ellipsoidal coordinates
x	...	first Cartesian coordinate
y	...	second Cartesian coordinate
z	...	third Cartesian coordinate
A^a	...	gravitation of atmospheric masses
A^{ar}	...	gravitation of atmospheric roughness
A^{ca}	...	gravitation of condensed atmospheric masses
A^{car}	...	gravitation of condensed atmospheric roughness
A^{cas}	...	gravitation of condensed atmospheric shell
A^t	...	gravitation of topographical masses, i.e., whole topography
A^{tr}	...	gravitation of topographical roughness, i.e., terrain
A^{ts}	...	gravitation of topographical shell
A^{ct}	...	gravitation of condensed topographical masses
A^{ctr}	...	gravitation of condensed topographical roughness, i.e., condensed terrain
A^{cts}	...	gravitation of condensed topographical shell
$D\Delta g$	...	downward continuation of gravity anomaly
E	...	linear eccentricity of the reference ellipsoid
G	...	universal gravitational constant
H	...	orthometric height
H^N	...	normal height
J_2	...	dynamic form factor of the earth
M	...	meridian radius of curvature of the reference ellipsoid
M	...	mass of the earth
N	...	prime vertical radius of curvature of the reference ellipsoid
N	...	geoidal height
N_ℓ	...	reference spheroid (low-frequency geoid)

N^{ℓ}	...	residual (high-frequency) geoid
N^h	...	Helmert's geoid (co-geoid)
$N^{h,\ell}$	...	Helmert's residual geoid
P	...	atmospheric pressure
P_n	...	Legendre's polynomial of the first kind
$P_{n,m}$	...	associated Legendre's function of the first kind
Q_n	...	truncation coefficient of Stokes's integral
Q_n	...	Legendre's polynomial of the second kind
$Q_{n,m}$	...	associated Legendre's function of the second kind
R	...	radius of the reference sphere
$R_{n,m}$	...	Paul's coefficient
T	...	molecular-scale temperature of atmospheric masses
T	...	disturbing gravity potential
T^h	...	Helmert's disturbing gravity potential
V^a	...	gravitational potential of atmospheric masses
V^{ar}	...	gravitational potential of atmospheric roughness
V^{as}	...	gravitational potential of atmospheric shell
V^{ca}	...	gravitational potential of condensed atmospheric masses
V^{car}	...	gravitational potential of condensed atmospheric roughness
V^{cas}	...	gravitational potential of condensed atmospheric shell
V^{ct}	...	gravitational potential of condensed topographical masses
V^{ctr}	...	gravitational potential of condensed topographical roughness
V^{cts}	...	gravitational potential of condensed topographical shell
V^t	...	gravitational potential of topographical masses
V^{tr}	...	gravitational potential of topographical roughness
V^{ts}	...	gravitational potential of topographical shell
W	...	actual gravity potential
W_c	...	centrifugal potential associated with the earth rotation

W_g	. . .	gravitational potential of the earth
U	. . .	normal gravity potential
U_c	. . .	centrifugal potential of the normal field
U_g	. . .	gravitational potential of the normal field
$Y_{n,m}$	. . .	spherical harmonic functions
Z	. . .	height anomaly according to Molodenskij's theory
$\mathcal{B}$	. . .	volume of the earth
$\mathcal{F}$	. . .	one-dimensional Fourier transform operator
$\mathcal{J}$	. . .	auxiliary integration kernel
$\mathcal{K}$	. . .	auxiliary integration kernel
$\mathcal{M}$	. . .	auxiliary integration kernel
$\mathcal{N}$	. . .	Newton's integration kernel
$\mathcal{P}$	. . .	Poisson's integration kernel
$\mathcal{S}$	. . .	spherical Stokes's integration kernel
$\mathcal{S}^\ell$	. . .	spheroidal Stokes's integration kernel
$\mathcal{S}^e$	. . .	ellipsoidal Stokes's integration kernel
$\mathcal{S}^\dagger$	. . .	ellipsoidal correction to spherical Stokes's kernel
$\mathbb{C}^n$	. . .	n-dimensional space of complex numbers
$\mathbb{E}^n$	. . .	n-dimensional Euclidean space
$\mathbb{L}^n$	. . .	space of real functions integrable in Lebesque sense to the power n
$\mathbb{N}^n$	. . .	n-dimensional space of integer numbers
$\mathbb{R}^n$	. . .	n-dimensional space of real numbers
α	. . .	Hörmander's coefficients
β	. . .	reduced latitude
γ	. . .	magnitude of normal gravity
γ_e	. . .	magnitude of normal gravity at equator
δg	. . .	magnitude of gravity disturbance
δA	. . .	combined direct effect on gravity

δA^a	...	direct atmospheric effect on gravity
δA^t	...	direct topographical effect on gravity
δN	...	combined primary indirect effect on geoid
δN^a	...	primary indirect atmospheric effect on geoid
δN^t	...	primary indirect topographical effect on geoid
δS	...	combined secondary indirect effect on gravity
δS^a	...	secondary indirect atmospheric effect on gravity
δS^t	...	secondary indirect topographical effect on gravity
δS^ξ	...	quasigeoid-to-geoid correction to gravity
δV	...	combined residual potential
δV^a	...	residual atmospheric potential
δV^t	...	residual topographical potential
Δg^f	...	free-air gravity anomaly
Δg^h	...	Helmert's gravity anomaly
Δg^h_ℓ	...	Helmert's reference (low-frequency) gravity anomaly
$\Delta g^{h,\ell}$	...	Helmert's residual (high-frequency) gravity anomaly
Δg^{sb}	...	simple Bouguer gravity anomaly
Δg^{cb}	...	complete Bouguer gravity anomaly
$\Delta \varrho^t$	...	anomalous topographical density
ε_g	...	ellipsoidal correction to the gravity disturbance
ε_n	...	ellipsoidal correction to the vertical gradient of normal gravity
ζ	...	auxiliary parameter
κ	...	universal gas constant
λ	...	geocentric longitude
μ	...	mean molecular weight of atmospheric masses
ξ	...	integration variable
π	...	Ludolf's number
ϱ^a	...	density of atmospheric masses

ϱ_o^a	...	density of atmospheric masses at the sea level
ϱ^t	...	density of topographical masses
ϱ_o^t	...	mean density of topographical masses
σ^a	...	condensation density of atmospheric masses
σ^{ar}	...	condensation density of the atmospheric roughness
σ^{as}	...	condensation density of the atmospheric shell
σ^t	...	condensation density of topographical masses
σ^{tr}	...	condensation density of the topographical roughness
σ^{ts}	...	condensation density of the topographical shell
τ	...	gradient of the molecular-scale temperature
ϕ	...	geodetic latitude
φ	...	geocentric latitude
ψ	...	angular distance between two points
ω	...	angular velocity of the earth rotation
Φ	...	pair of angular geodetic coordinates
Ψ	...	pair of angular ellipsoidal coordinates
Ω	...	pair of angular spherical coordinates
$\Psi_\oplus$	...	full solid angle in ellipsoidal coordinates
$\Omega_\oplus$	...	full solid angle in spherical coordinates
$\Omega_\odot$	...	spherical cap of radius ψ_o

Chapter 1

Introduction

Although gravity is by far the weakest force of nature,
its insidious and cumulative action serves to determine
the ultimate fate not only of individual astronomical objects
but of the entire cosmos ... (Paul Davies, 1994)

1.1 Geoid determination

Earth's gravity field can be described by continuous, smooth, convex surfaces of the constant potential. Among these equipotential surfaces there is one of considerable importance for geodesy and other geosciences. In 1822, Gauss was the first geodesist who defined this surface in a strict mathematical sense as a surface which everywhere intersects directions of gravity at right angles, and of which the ocean surface at rest is a part. His ideas were further developed in 1837 by Bessel who defined this equipotential surface as a reference for all geodetic works. Listing called this equipotential surface the *geoid* in 1872. Helmert then systematized the ideas of equipotential surfaces in 1884 and included this complete theory into a realm of geodesy. Using the gravity potential, the geoid is an equipotential surface with a gauge value of potential at the mean sea level. Since it is used as a vertical geodetic datum for orthometric heights, many efforts in geodesy are concentrated on its accurate determination.

The geoid can be solved for using either geometric or gravimetric approaches. In both cases, the geoid is defined by its vertical separation from the geocentric biaxial ellipsoid which conceptually was accepted in the 18th century as the earth model. The estimation of the position, size, and shape of the best fitting earth ellipsoid is another important task of geodesy which will not be discussed here any further. It is assumed that the geocentric biaxial ellipsoid is known with the best possible accuracy. Parameters of the Geodetic Reference System 1980 were used for the numerical evaluations in this dissertation [Moritz, 1984].

The *geometric geoid* is based on comparing geodetic and astronomic positions of points, which results in the estimates of astro-geodetic deflections of verticals, i.e., angles between directions of ellipsoidal normals and local gravity vectors. They can be seen as slopes of the geoid against the reference ellipsoid and when integrated, they provide the sought geoidal height. This technique was proposed first by Helmert in 1880 and is known as the astro-geodetic levelling, and its result as the astro-geodetic geoid, [e.g., Merry and Vaníček, 1974]. Recently, satellite methods of modern geodesy offer another geometric solution. Satellite-determined geodetic heights are directly differenced from orthometric heights resulting in an alternative geometric geoid.

Stokes derived in 1849 a theorem which gave the theoretical basis for the estimation of the geoid based on global gravity observations referred to the geoid (assuming no topographical and atmospheric masses above the geoid). The major advantages of the *gravimetric geoid* over the geometric one is in the existence of abundant and cheap gravity data. Its present major limitation is due to the lack of global data coverage. Fortunately, satellite dynamics can provide global long-wavelength features of the gravity field which fill gravity data gaps in inaccessible regions of the earth surface. The total geoid can then be solved for as the sum of the reference spheroid computed directly (in the spectral form) from the satellite-derived spherical harmonic coefficients, and the residual geoid based on the higher-frequency terrestrial gravity data. This approach is described in my dissertation.

1.2   Research objectives

Several topics from the theory of the accurate gravimetric geoid determination were covered by my research. The major contributions consist of the formulation of the proper scheme of gravity reduction which would, assuming the availability of suitable terrestrial gravity data, lead to the solution of the one-centimetre gravimetric geoid.

Geometric definitions, some fundamentals of the potential theory, and basic tools of mathematics and physics employed in this dissertation are given in *Chapter (2)*. Its role is to introduce elementary formulae and basic notation which are subsequently used without further explanations or definitions in the derivations throughout this dissertation. No derivations or proofs are given in this chapter.

Stokes's theorem, representing the mathematical model for the determination of the regional gravimetric geoid, is fully described in *Chapter (3)*. Due to its significance for the formulation of the correct input gravity data, a detailed description of this method is given deploying two possible geometric approximations in its formulation. It is argued that the ellipsoidal approximation gives better accuracy and must be, despite its larger theoretical and numerical complexity, employed in the final solution of the geodetic boundary-value problem. The spherical approximation is, however, used for the Helmert reduction of observed gravity data since it provides sufficient accuracy for the solution of the one-centimetre geoid. This chapter is concluded by the formulation of the Stokes theorem with the higher-degree reference field.

The core of my research is presented in *Chapter (4)*. All topographical and atmospheric effects, both on gravity potential and gravity, are derived in this chapter. In contrast to widely used planar formulations, the spherical approximation is used in all derivations. An effect of distant topographical masses is also investigated here, and spectral formulae for its numerical evaluation are presented. The proper condensation of the atmospheric masses according to Helmert's method is formulated, and atmospheric corrections, both to gravity and to geoidal heights, are derived. The

chapter is concluded by a description of downward continuation of discrete harmonic gravity data which represents the last step in the scheme of the gravity reduction.

The formulation of the Helmert residual gravity anomaly on the co-geoid for the solution of the geodetic boundary-value problem with a higher-degree reference field is presented in *Chapter (5)*. Reference topographical and atmospheric potentials on the co-geoid are derived in the first two sections of this chapter. They are subsequently used for the derivation of the Helmert reference gravity anomaly. If subtracted from the entire value of the Helmert gravity anomaly, its residual component is obtained.

Chapter (6) is devoted to computations of the Helmert residual co-geoid using the defined geodetic boundary-value problem. The appropriate form of the spherical Stokes function is introduced in the first section applying a suitable modification of its higher-degree component. Formulae for the application of the Stokes integral in the global sense, including the proper treatment of its singularity, are derived in the next two sections of this chapter. An appropriate technique to test the accuracy of the discrete Stokes integration concludes this chapter.

Numerical results for a test area in the Canadian Rocky Mountains are presented in *Chapter (7)*. This area was selected to represent the most difficult case scenario for the determination of the gravimetric geoid over Canada due to large complexity of both the topography and the earth gravity field. Series of figures and tables clearly demonstrate the importance of the gravity reductions. Input gravity and elevation data for these computations were obtained from Natural Resources Canada, Ottawa, and the U.S. National Geodetic Survey, Silver Spring.

Conclusions based on results presented in this dissertation are included in *Chapter (8)*. Recommendations for further research in the area of the determination of the regional gravimetric geoid formulated here are based on the results presented, and new gravity and other geophysical information which is becoming available every day. Theoretical derivations and their computer realizations are included in *Appendices*.

Chapter 2

General Principles

The determination of the gravimetric geoid is based on physical quantities defined in the geometric space. This chapter includes their elementary definitions. Section (2.1) defines the geometric space including necessary coordinate systems further used in theoretical derivations throughout this work. Basic geometric objects such as the earth and its two reference bodies are described here in terms of their locations, sizes, and shapes. Transformations between their parameters then conclude this section.

Definitions of spherical and ellipsoidal harmonic functions, which are heavily used in this dissertation, are included in Sec. (2.2). Partial differential equations used for their definitions are shown here, as well as their generating formulae.

Section (2.3) contains fundamentals of potential theory. Elementary quantities, such as gravitational and centrifugal accelerations based on theories of Newton and Huygens, are presented here. Important scalar quantities, called gravitational and centrifugal potentials, are derived based on applications of differential operators.

Basic quantities used to describe the earth gravity field are defined in the last section of this chapter. An approximation of the actual gravity field using the model gravity field generated by an ellipsoid of revolution is introduced, and the well-known Bruns theorem is formulated.

2.1 Geometric definitions

Let $\mathbb{E}^3$ be a three-dimensional Euclidean space with a Cartesian orthonormal right-handed coordinate system. Its origin is at the centre of earth's mass, its z-axis coincides with the mean position of the earth rotational axis, and its x-axis lies in the mean Greenwich meridian plane. The position of an arbitrary point P in $\mathbb{E}^3$ can then be defined through its radius vector $\boldsymbol{r} \in \mathbb{R}^3$

$$\boldsymbol{r} = [\ x\ \ y\ \ z\ ]^T \ . \tag{2.1}$$

A family of three curvilinear coordinate systems [Vaníček and Krakiwsky, 1986] is then defined in terms of their transformations into the Cartesian system as follows [Heiskanen and Moritz, 1967]

$$x = r\ \cos\varphi\ \cos\lambda = \sqrt{u^2 + E^2}\ \cos\beta\ \cos\lambda = (N + h)\ \cos\phi\ \cos\lambda\ , \tag{2.2}$$

$$y = r\ \cos\varphi\ \sin\lambda = \sqrt{u^2 + E^2}\ \cos\beta\ \sin\lambda = (N + h)\ \cos\phi\ \sin\lambda\ , \tag{2.3}$$

$$z = r\ \sin\varphi = u\ \sin\beta = \left(\ N\ \frac{b^2}{a^2}\ + h\ \right)\ \sin\phi\ . \tag{2.4}$$

Non-parametric *spherical coordinates* $(r, \varphi, \lambda) = (r, \Omega)$ are given by the length of the radius vector r, geocentric latitude φ, and geocentric longitude λ. One-parametric *ellipsoidal coordinates* $(u, \beta, \lambda) = (u, \Psi)$ are represented by the length of the minor semiaxis u, reduced latitude β, and geocentric longitude λ. The *linear eccentricity* E of the biaxial ellipsoid with the major semiaxis a and minor semiaxis b passing through the point P reads [ibid]

$$E = \sqrt{a^2 - b^2}\ . \tag{2.5}$$

Two-parametric *geodetic coordinates* are represented by a triplet $(h, \phi, \lambda) = (h, \Phi)$ with the geodetic latitude ϕ, geocentric longitude λ, and the geodetic height h. The ellipsoidal prime vertical radius of curvature is defined as [ibid]

$$N(\phi) = \frac{a^2}{\sqrt{a^2 \cos^2\phi + b^2 \sin^2\phi}}\ . \tag{2.6}$$

The surface of the earth can be described by an angle dependent function $r_s(\Omega)$ linked with the unknown geoidal surface $r_g(\Omega)$ by orthometric heights $H(\Omega)$ reckoned along the plumb-lines of the earth gravity field [Vaníček and Krakiwsky, 1986]. Two geometric approximations of the geoid are introduced in the sequel: an earth-centered biaxial ellipsoid $r_e(\varphi)$ and an earth-centered reference sphere of radius R. The size and shape of the *reference ellipsoid* are based on the theory of the geocentric equipotential ellipsoid. Values of the Geodetic Reference System 1980 [Moritz, 1984] are used in the numerical evaluations, see Table (7.1). The radius of the *reference sphere* is often defined as the radius of a sphere with the same volume as the reference ellipsoid [ibid]

$$ R \;=\; \left(a^2\, b \right)^{\frac{1}{3}} \; . \tag{2.7}$$

Since deviations of the reference sphere from the reference ellipsoid of revolution are relatively small, these two reference bodies are often interchanged for computational convenience. To accomplish this transformation, the following two parameters are defined: *first numerical eccentricity* [Bomford, 1971]

$$ e \;=\; \frac{E}{a} \; , \tag{2.8}$$

and *polar flattening* [ibid]

$$ f \;=\; 1 \;-\; \sqrt{1 - e^2} \; . \tag{2.9}$$

The geocentric radius of the ellipsoidal surface is [Moritz, 1990]

$$ r_e(\varphi) \;=\; a\,(1 - f\,\sin^2\varphi) \;+\; \mathcal{O}(f^2) \; . \tag{2.10}$$

To conclude this section, a transformation between geocentric and reduced latitudes reads as follows [ibid]

$$ u\,\tan\beta \;=\; \sqrt{u^2 + E^2}\,\tan\varphi \; , \tag{2.11}$$

and between the reduced and geodetic latitudes [ibid]

$$ \tan\beta \;=\; (1 - f)\,\tan\phi \; . \tag{2.12}$$

2.2 Elementary differential equations

Consider a real function $f(r, \Omega) \in \mathbb{L}^2$ defined in the external space to the sphere of radius R. Then f is called a harmonic function in this space if [Moritz, 1990]

$$\forall \, r \, > \, R \, : \, \nabla^2 \, f(r, \Omega) \, = \, 0 \, . \tag{2.13}$$

Applying the following condition

$$\lim_{r \to \infty} \, f(r, \Omega) \, = \, 0 \, , \tag{2.14}$$

a solution to the Laplace differential equation (2.13) for the function f can be found by the Fourier method in terms of its eigenfunction development [ibid]

$$\forall \, r \, > \, R \, : \, f(r, \Omega) \, = \, \sum_{n=0}^{\infty} \, g(r) \, f_n(\Omega) \, , \tag{2.15}$$

with a real function $g(r) \in \mathbb{L}^2$ [ibid]

$$\forall \, n \, \geq \, 0 \, : \, g(r) \, = \, r^{-(n+1)} \, , \tag{2.16}$$

and Laplace's surface harmonics f_n [ibid]

$$\forall \, n \, \geq \, 0 \, : \, f_n(\Omega) \, = \, \sum_{m=-n}^{n} \, F_{n,m} \, Y_{n,m}(\Omega) \, . \tag{2.17}$$

$F_{n,m}$ represents constant coefficients, and spherical harmonics are given as [ibid]

$$\forall \, m \, \leq \, n \, : \, Y_{n,m}(\Omega) \, = \, e^{im\lambda} \, P_{n,m}(\sin\varphi) \, , \quad \text{where} \, i \, = \, \sqrt{-1} \, . \tag{2.18}$$

Associated trigonometric Legendre's functions of the first kind $P_{n,m}$ are solutions y ($\forall \, n \, \geq \, m$) of the associated Legendre differential equation [Hobson, 1931]

$$\cos\varphi \, \frac{d^2y}{d\varphi^2} \, + \, \sin\varphi \, \frac{dy}{d\varphi} \, + \, \left[\, n(n+1)\cos\varphi \, - \, m^2\sec\varphi \, \right] \, y \, = \, 0 \, , \tag{2.19}$$

and usually generated from [ibid]

$$\forall \, m \, \leq \, n \, : \, P_{n,m}(\sin\varphi) \, = \, (1 - \sin^2\varphi)^{\frac{m}{2}} \, \frac{d^m}{d(\sin\varphi)^m} \, P_n(\sin\varphi) \, . \tag{2.20}$$

8

Trigonometric Legendre's polynomials represent a solution y of an equation [ibid]

$$\forall \ n \ \geq \ 0 \ : \ \sec\varphi \ \frac{d}{d\varphi} \ \left(\cos\varphi \ \frac{dy}{d\varphi} \right) \ + \ n \ (n+1) \ y \ = \ 0 \ . \tag{2.21}$$

They can be generated by the well-known Rodrigues formula [ibid]

$$\forall \ n \ \geq \ 0 \ : \ P_n(\sin\varphi) \ = \ \frac{1}{2^n \ n!} \ \frac{d^n}{d(\sin\varphi)^n} \ (\sin^2\varphi \ - \ 1)^n \ . \tag{2.22}$$

Associated Legendre's functions of the second kind $Q_{n,m}$ [Moritz, 1990]

$$\forall \ m \ \leq \ n \ \wedge \ z \ \in \ \mathbb{C} \ : \ Q_{n,m}(z) \ = \ (z^2 \ - \ 1)^{\frac{m}{2}} \ \frac{d^m}{dz^m} \ Q_n(z) \ , \tag{2.23}$$

also represent the solution to Eqn. (2.19) with polynomials Q_n [ibid]

$$\forall \ n \ \geq \ 0 \ : \ Q_n(z) \ = \ \frac{1}{2} \ P_n(z) \ \ln\frac{z+1}{z-1} \ - \ \sum_{k=1}^{n} \frac{1}{k} \ P_{k-1}(z) \ P_{n-k}(z) \ . \tag{2.24}$$

They can be used for the solution of the Laplace equation outside the ellipsoid u_e

$$\forall \ u \ > \ u_e(\phi) \ : \ \nabla^2 \ f(u, \Psi) \ = \ 0 \ . \tag{2.25}$$

Assuming again the asymptotic condition at infinity

$$\lim_{u \to \infty} \ f(u, \Psi) \ = \ 0 \ , \tag{2.26}$$

the solution of Eqn. (2.25) in terms of its eigenfunction development reads [ibid]

$$\forall \ u \ > \ u_e(\phi) \ : \ f(u, \Psi) \ = \ \sum_{n=0}^{\infty} \ f_n(u, \Psi) \ , \tag{2.27}$$

with the Laplace ellipsoidal harmonics given as [Hobson, 1931]

$$\forall \ n \ \geq \ 0 \ : \ f_n(u, \Psi) \ = \ \sum_{m=-n}^{n} \ q_{n,m}(u, b, E) \ F_{n,m} \ Y_{n,m}(\Psi) \ . \tag{2.28}$$

Polynomials $q_{n,m}$ are given by the formula [ibid]

$$\forall \ (u', b') \ \in \ \mathbb{C}^2 \ \wedge \ m \ \leq \ n \ : \ q_{n,m}(u, b, E) \ = \ \frac{Q_{n,m}(u')}{Q_{n,m}(b')} \ , \tag{2.29}$$

with two independent complex arguments

$$u' \ = \ i \ \frac{u}{E} \ \wedge \ b' \ = \ i \ \frac{b}{E} \ , \quad \text{where} \ i \ = \ \sqrt{-1} \ . \tag{2.30}$$

2.3 Fundamentals of potential theory

The magnitude of the *gravitational acceleration* generated by a body of volume $\mathcal{B}$ and density ϱ reads [Newton, 1687]

$$a_g(r, \Omega) = G \iiint_{\mathcal{B}} \varrho(r', \Omega') \, \mathcal{N}^2(r, \psi, r') \, d\mathcal{B} \,, \tag{2.31}$$

with the universal gravitational constant G, Newton's integration kernel

$$\mathcal{N}(r, \psi, r') = \frac{1}{r} \sum_{n=0}^{\infty} \left(\frac{r'}{r} \right)^n P_n(\cos \psi) \,, \tag{2.32}$$

and a spherical distance ψ between the computation and integration points

$$\cos \psi = \cos \varphi \, \cos \varphi' + \sin \varphi \, \sin \varphi' \cos (\lambda - \lambda') \,. \tag{2.33}$$

Magnitude of the *centrifugal acceleration* acting upon each particle attached to the earth rotating with a constant angular velocity ω is computed as [Huygens, 1673]

$$a_c(r, \varphi) = \omega^2 \, r \cos \varphi \,. \tag{2.34}$$

Since both gravitational and centrifugal fields are irrotational and conservative, i.e.,

$$\nabla \times \boldsymbol{a_g}(r, \Omega) = \nabla \times \boldsymbol{a_c}(r, \varphi) = 0 \,, \tag{2.35}$$

they can be described by scalar quantities called *gravitational potential*

$$W_g(r, \Omega) = G \iiint_{\mathcal{B}} \varrho(r', \Omega') \, \mathcal{N}(r, \psi, r') \, d\mathcal{B} \,, \tag{2.36}$$

and *centrifugal potential*

$$W_c(r, \varphi) = \frac{1}{2} \, \omega^2 \, r^2 \cos^2 \varphi \,. \tag{2.37}$$

Applying the Laplace differential operator to Eqns. (2.36) and (2.37), one obtains

$$\nabla^2 \, W_g(r, \Omega) = - 4\pi G \varrho(r, \Omega) \,, \tag{2.38}$$

$$\nabla^2 \, W_c(r, \varphi) = 2\omega^2 \,. \tag{2.39}$$

2.4   Earth's external gravity field

The earth's gravity field results from the superposition of the gravitational attraction of mass distribution within the earth and its atmosphere, and centrifugal acceleration caused by the earth rotation. It is fully described by the gravity potential which reads [Heiskanen and Moritz, 1967]

$$ W(r,\Omega) \; = \; \frac{GM}{r} \; \left[\; 1 - \sum_{n=2}^{\infty} \; \left(\frac{a'}{r} \right)^n \; W_n(\Omega) \right] \; + \; \frac{\omega^2 \; r^2}{3} \; [\; 1 - P_2(\sin\varphi) \;] \;\; , \quad (2.40) $$

with the radius of Brillouin's sphere a', and the geocentric gravitational constant GM. Its Laplace spherical harmonics are

$$ \forall \; n \; \geq \; 2 \; : \; W_n(\Omega) \; = \; \sum_{m=-n}^{n} \; W_{n,m} \; Y_{n,m}(\Omega) \;\; , \quad (2.41) $$

with the constant coefficients $W_{n,m}$. Applying simple linear differential operators on the gravity potential, the following formulae can be obtained [ibid]

$$ \forall \; r \; : \; \nabla \, W(r,\Omega) \; = \; \boldsymbol{g}(r,\Omega) \;\; , \quad (2.42) $$

with the gravity vector $\boldsymbol{g}$, and

$$ \forall \; r \; : \; \nabla^2 \, W(r,\Omega) \; = \; - \, 4\pi G \; \varrho(r,\Omega) \; + \; 2\omega^2 \;\; , \quad (2.43) $$

which is the well-known Poisson differential equation. The actual gravity field is often approximated by a model gravity field generated by the reference ellipsoid. It is assumed that this ellipsoid rotates at the same angular velocity ω as the real earth and its mass coincides with the mass of the real earth M. According to the Stokes-Poincaré theorem, this gravity field is fully described by four parameters a, b, M, and ω. Its gravity potential can be expressed as follows [ibid]

$$ U(r,\varphi) \; = \; \frac{GM}{r} \; \left[\; 1 - \sum_{n=1}^{\infty} \; \left(\frac{a}{r} \right)^{2n} \; U_{2n}(\varphi) \right] \; + \; \frac{\omega^2 \; r^2}{3} \; [\; 1 - P_2(\sin\varphi) \;] \;\; , \quad (2.44) $$

where zonal spherical harmonics U_n are given analytically ($\forall \; n \; \geq \; 1$)

$$ U_{2,n}(\varphi) \; = \; (-1)^{n+1} \; \frac{3 \; e^{2n}}{(2n+1) \, (2n+3)} \; \left(1 - n + 5n \; \frac{J_2}{e^2} \right) \; P_{2,n}(\sin\varphi) \;\; . \quad (2.45) $$

11

J_2 is the so-called dynamic form factor. Applying the gradient operator to the normal gravity potential, a normal gravity vector $\boldsymbol{\gamma}$ is obtained

$$\nabla\, U(r,\varphi) \;=\; \boldsymbol{\gamma}(r,\varphi) \;. \tag{2.46}$$

Poisson's differential equation for normal gravity potential in mass-free space reads

$$\forall\, r \;\geq\; r_e \;:\; \nabla^2\, U(r,\varphi) \;=\; 2w^2 \;. \tag{2.47}$$

The disturbing gravity potential is defined as the difference between the gravity potentials of the actual and model field [Vaníček and Krakiwsky, 1986]

$$T(r,\Omega) \;=\; W(r,\Omega) \;-\; U(r,\varphi) \;=\; \frac{GM}{r}\, \sum_{n=2}^{\infty}\, \left(\frac{a^{'}}{r} \right)^{n}\, T_n(\Omega)\;, \tag{2.48}$$

with even-degree coefficients given as follows

$$n \;=\; 2,\, 4,\, 6\, \dots\, :\; T_n(\Omega) \;=\; W_n(\Omega) \;-\; \left(\frac{a}{a^{'}} \right)^{n} U_n(\varphi)\;, \tag{2.49}$$

and odd-degree coefficients as follows

$$n \;=\; 3,\, 5,\, 7\, \dots\, :\; T_n(\Omega) \;=\; W_n(\Omega)\;. \tag{2.50}$$

Applying the gradient operator to Eqn. (2.48), one gets a gravity disturbance vector

$$\nabla\, T(r,\Omega) \;=\; \boldsymbol{\delta g}(r,\Omega) \;=\; \boldsymbol{g}(r,\Omega) \;-\; \boldsymbol{\gamma}(r,\varphi)\;. \tag{2.51}$$

Assuming no topographical and atmospheric masses above the geoid, then

$$\forall\, r \;\geq\; r_g \;:\; \nabla^2\, T(r,\Omega) \;=\; 0\;, \tag{2.52}$$

and the Laplace equation is satisfied. The normal gravity potential on the geoid reads

$$U(r_g,\varphi) \;\doteq\; U(r_e,\varphi) + \frac{\partial\, U(r,\varphi)}{\partial n}\bigg|_{r_e} N(\Omega) \;=\; U(r_e,\varphi) - \gamma(r_e,\varphi)\, N(\Omega)\;, \tag{2.53}$$

where N is the vertical distance between the reference ellipsoid and the geoid called geoidal height (undulation). Based on Eqn. (2.53) and the following condition

$$W(r_g,\Omega) \;=\; U(r_e,\varphi)\;, \tag{2.54}$$

the well-known Bruns formula can be derived [Bruns, 1878]

$$T(r_g,\Omega) \;=\; \gamma(r_e,\varphi)\, N(\Omega)\;. \tag{2.55}$$

12

Chapter 3

Geodetic Boundary-Value Problem

In this chapter, a mathematical model for the determination of the gravimetric geoid is formulated. It is represented by a scalar non-linear boundary-value problem with a free boundary. Its solution is the disturbing potential of the earth gravity field at the geoid which can easily be transformed, using the Bruns theorem, into the sought geoidal height.

The geodetic boundary-value problem is introduced in the first section. It consists of Laplace's differential equation for the disturbing gravity potential supplemented by the mixed boundary condition of potential theory. This boundary condition represents a link between quantities, which can be derived from observed magnitude of gravity at the topography, and unknown values of the disturbing gravity potential at the geoid.

The harmonic space outside the geoid is derived by removing the gravitational potential of all external masses from the earth's gravitational potential. This simple mathematical operation leads to the harmonic disturbing gravity potential outside the geoid. Unfortunately, the new disturbing gravity potential differs very much from the original one, and its derivation would be very difficult due to our limited knowledge about the mass distribution within the topography. An adequate compensation for this operation is usually sought. In this research, the second Helmert condensation

with the compensation potential generated by a single material layer on the geoid was deployed. The mass distribution of this layer can be selected in a variety ways. The mass-conservation scheme, when the mass of the earth is not changed, was used in this research. In any case, the existence of this layer does not violate the harmonicity of the external disturbing gravity potential.

The major advantage of this compensation consists of generating a gravitational field which is very close to the gravitational field generated by the original external topographical and atmospheric masses. Their difference represents a transformation between the actual and the new gravitational field which is now harmonic outside the geoid, and still very close to the original field. This potential difference has then a character of a residual quantity which is an important advantage for its numerical evaluations.

The solution for the new disturbing gravity potential, which is now harmonic everywhere outside the geoid, is presented in terms of Green's function for the spherical approximation of the unknown boundary surface. Gravity anomalies deployed in the formulation of the boundary condition are also formulated in this section and their derivation from the observed magnitude of gravity at the topography is explained. The second section deals with the formulation of the geodetic boundary-value problem using the higher-degree reference field. This approach is used for the combined use of terrestrial gravity observations and satellite-based global geopotential models. Major advantages of this approach are also explained in this section.

All derivations are made under these assumptions: (1) earth's body is assumed to be rigid and uniformly rotating with a constant angular velocity ω around a fixed axis passing through its centre of mass, (2) gravity data are corrected for temporal variations of gravity (such as the tidal attraction of other celestial bodies), (3) orthometric heights of the earth topography above the geoid, density distribution of topographical and atmospheric masses, and the value of the earth gravity potential on the geoid are known.

14

3.1 Formulation of the problem

Unknown values of the geoidal heights can be determined using the Bruns formula. In order to use this theorem, values of the disturbing gravity potential on the geoid must be estimated first. The solution for this unknown quantity, based on terrestrial observations of gravity, can be obtained from the differential Eqns. (2.51) and (2.52). An appropriate mathematical model is derived in this section.

Using the second Helmert condensation [Lambert 1930], a new quantity, harmonic everywhere above the geoid, is introduced [Martinec and Vaníček, 1994a]

$$\forall \; r \; : \; T^h(r,\Omega) \; = \; T(r,\Omega) \; - \; \delta V(r,\Omega) \; . \tag{3.1}$$

The superscript 'h' will denote quantities from the Helmert space derived using the second Helmert condensation. The *residual gravity potential* δV is defined as [ibid]

$$\forall \; r \; : \; \delta V(r,\Omega) \; = \; V^t(r,\Omega) \; + \; V^a(r,\Omega) \; - \; V^{ct}(r,\Omega) \; - \; V^{ca}(r,\Omega) \; , \tag{3.2}$$

where V^t and V^a are gravitational potentials of topographical and atmospheric masses above the geoid, and V^{ct} and V^{ca} are gravitational potentials of topographical and atmospheric masses condensed into a surface layer on the geoid. Unfortunately, this change of the earth gravitational potential causes a shift of all equipotential surfaces. Its effect on the geoid is according to Bruns's theorem [Wichiencharoen, 1982]

$$\delta N(\Omega) \; = \; \frac{\delta V(r_g,\Omega)}{\gamma(r_e,\varphi)} \; . \tag{3.3}$$

The shifted geoid is called a *co-geoid* (geoid in Helmert's space) $r_c(\Omega)$. The function T^h then satisfies Laplace's equation in (mass-free) space everywhere above the geoid

$$\forall \; r \; > \; r_g \; : \; \nabla^2 \, T^h(r,\Omega) \; = \; 0 \; , \tag{3.4}$$

and the following boundary condition (with the geoid being the boundary)

$$r \; = \; r_g \; : \; T^h(r,\Omega) \; = \; W(r,\Omega) \; - \; U(r,\varphi) \; - \; \delta V(r,\Omega) \; . \tag{3.5}$$

These two equations, together with the asymptotic condition at infinity

$$\lim_{r \to \infty} T^h(r,\Omega) = 0 , \qquad (3.6)$$

form a boundary-value problem with the boundary condition defined on the unknown (free) boundary surface. A formulation of this boundary condition in terms of gravity observations on the topography will be attempted next.

The observed magnitude of gravity on the topography r_s can be expressed as

$$r = r_s : g(r,\Omega) = \Big| \operatorname{grad} \Big[T^h(r,\Omega) + U(r,\varphi) + \delta V(r,\Omega) \Big] \Big| . \qquad (3.7)$$

The linear form of Eqn. (3.7) is derived using the binomial theorem [Martinec, 1998]

$$g(r,\Omega) \doteq \gamma(r,\varphi) + \frac{\operatorname{grad} U(r,\varphi)}{\gamma(r,\varphi)} \cdot \operatorname{grad} \Big[T^h(r,\Omega) + \delta V(r,\Omega) \Big] , \qquad (3.8)$$

with an admissible relative error of 10^{-7} introduced by neglecting non-linear terms, and a scalar product of two vectors $\{\cdot\}$. A partial derivative of the disturbing potential can be expressed as follows [Rektorys, 1995]

$$\frac{\partial T^h(r,\Omega)}{\partial n} = - \mid \operatorname{grad} T^h(r,\Omega) \mid \cos \Big[\operatorname{grad} T^h(r,\Omega), \operatorname{grad} U(r,\varphi) \Big] , \qquad (3.9)$$

and similarly in case of the residual potential

$$\frac{\partial \, \delta V(r,\Omega)}{\partial n} = - \mid \operatorname{grad} \delta V(r,\Omega) \mid \cos \Big[\operatorname{grad} \delta V(r,\Omega), \operatorname{grad} U(r,\varphi) \Big] . \qquad (3.10)$$

Both directional derivatives are taken along the direction of the normal gravity vector which coincides with the ellipsoidal normal n. Equation (3.8) then reads

$$r = r_s : g(r,\Omega) \doteq \gamma(r,\varphi) - \frac{\partial T^h(r,\Omega)}{\partial n} \bigg|_r - \frac{\partial \, \delta V(r,\Omega)}{\partial n} \bigg|_r , \qquad (3.11)$$

and can be rewritten using the gravity disturbance, see Eqn. (2.51),

$$r = r_s : \delta g(r,\Omega) \doteq - \frac{\partial T^h(r,\Omega)}{\partial n} \bigg|_r - \frac{\partial \, \delta V(r,\Omega)}{\partial n} \bigg|_r . \qquad (3.12)$$

16

Since the evaluation of normal gravity on the topography would require the knowledge of (usually unknown) geodetic heights, the gravity disturbance is transformed into a more available gravity anomaly (with the telluroid r_t) as follows [Vaníček et al., 1999]

$$\Delta g(r_s, \Omega) \;=\; \delta g(r_s, \Omega) \;+\; \gamma(r_s, \varphi) \;-\; \gamma(r_t, \varphi) \;=\; \delta g(r_s, \Omega) \;+\; \delta\gamma(r_s, \varphi) \;. \quad (3.13)$$

The transformation consists of adding a new quantity $\delta\gamma$ to the gravity disturbance which accounts for the vertical displacement of the actual equipotential surface with respect to the normal equipotential surface at a point on the topography [ibid]

$$r = r_s \;:\; \delta\gamma(r, \varphi) \;=\; |\operatorname{grad}\, \gamma(r, \varphi)|\, Z(r, \Omega) \;\doteq\; \left. \frac{\partial\gamma(r, \varphi)}{\partial n} \right|_r Z(r, \Omega) \;=$$

$$= \frac{T(r, \Omega)}{\gamma(r_t, \varphi)} \left. \frac{\partial\gamma(r, \varphi)}{\partial n} \right|_r = \frac{T^h(r, \Omega)}{\gamma(r_t, \varphi)} \left. \frac{\partial\gamma(r, \varphi)}{\partial n} \right|_r + \frac{\delta V(r, \Omega)}{\gamma(r_t, \varphi)} \left. \frac{\partial\gamma(r, \varphi)}{\partial n} \right|_r \;. \quad (3.14)$$

The vertical displacement Z is the so-called height anomaly in Molodenskij's theory. Equation (3.12) can be then reformulated into a form

$$r \;=\; r_s \;:\; \Delta g(r, \Omega) \;\doteq\; - \left. \frac{\partial T^h(r, \Omega)}{\partial n} \right|_r - \left. \frac{\partial\, \delta V(r, \Omega)}{\partial n} \right|_r + \delta\gamma(r, \Omega) \;. \quad (3.15)$$

Normal gravity on the reference ellipsoid can be computed using the Somigliana-Pizzetti closed formula [Pizzetti, 1911; Somigliana, 1929]

$$\gamma(r_e, \varphi) \;\doteq\; \gamma(\phi) \;=\; \gamma_e\, \frac{1 + k\,\sin^2\phi}{(1 - e^2\sin^2\phi)^{\frac{1}{2}}} \;, \quad (3.16)$$

where γ_e is the magnitude of normal gravity at the ellipsoidal equator, and k is a constant of the normal gravity formula. Its upward continuation from the reference ellipsoid to the telluroid is derived by expanding Eqn. (3.16) into a Taylor series

$$\gamma(r_t, \varphi) \;=\; \gamma(r_e, \varphi) \;+\; \left. \frac{\partial\gamma(r, \varphi)}{\partial n} \right|_{r_e} H^N(\Omega) +$$

$$+ \frac{1}{2} \left. \frac{\partial^2\gamma(r, \varphi)}{\partial n^2} \right|_{r_e} \left[\, H^N(\Omega)\,\right]^2 \;+\; \frac{1}{6} \left. \frac{\partial^3\gamma(r, \varphi)}{\partial n^3} \right|_{r_e} \left[\, H^N(\Omega)\,\right]^3 \;+\; \ldots \quad (3.17)$$

17

Since the orthometric heights are usually used in practice, a difference between the orthometric and normal heights must be evaluated [Heiskanen and Moritz, 1967]

$$H^N(\Omega) \; - \; H(\Omega) \; \doteq \; H(\Omega) \; \frac{\Delta g^{sb}(\Omega)}{\gamma(r_e, \varphi)} \quad . \tag{3.18}$$

The simple Bouguer gravity anomaly (for the mean topographical density) is [ibid]

$$\Delta g^{sb}(\Omega) \; = \; g(r_s, \Omega) \; - \; \gamma(r_t, \varphi) \; - \; 2\pi\varrho_o^t \, GH(\Omega) \; . \tag{3.19}$$

Substituting Eqn. (3.18) into Eqn. (3.17), one gets after neglecting non-linear terms in the Taylor series the following expression

$$\gamma(r_t, \varphi) \; \doteq \; \gamma(r_e, \varphi) \; + \; \frac{\partial \gamma(r, \varphi)}{\partial n} \bigg|_{r_e} H(\Omega) \left[1 \; + \; \frac{\Delta g^{sb}(\Omega)}{\gamma(r_e, \varphi)} \right] . \tag{3.20}$$

A linear term of the Taylor expansion is sometimes taken only into the account for the evaluation of $\gamma(r_t, \varphi)$. However, this simplification does not give accurate enough results, and a higher order approximation is required [Vaníček and Martinec, 1994]. At least the latitude and the altitude effects have to be considered.

Realizing that the free-air gravity anomaly reads [ibid]

$$\Delta g^f(\Omega) \; = \; g(r_s, \Omega) \; - \; \gamma(r_e, \varphi) \; - \; \frac{\partial \gamma(r, \varphi)}{\partial n} \bigg|_{r_e} H(\Omega) \; , \tag{3.21}$$

then Eqn. (3.15) can be rewritten as follows

$$\Delta g^f(\Omega) \; - \; \frac{\partial \gamma(r, \varphi)}{\partial n} \bigg|_{r_e} H(\Omega) \frac{\Delta g^{sb}(\Omega)}{\gamma(r_e, \varphi)} \; - \; \frac{\partial \gamma(r, \varphi)}{\partial n} \bigg|_{r_e} \frac{\delta V(r_s, \Omega)}{\gamma(r_t, \varphi)} \; \doteq$$

$$\doteq \; \frac{\partial \gamma(r, \varphi)}{\partial n} \bigg|_{r_s} \frac{T^h(r_s, \Omega)}{\gamma(r_t, \varphi)} \; - \; \frac{\partial T^h(r, \Omega)}{\partial n} \bigg|_{r_s} \; - \; \frac{\partial \, \delta V(r, \Omega)}{\partial n} \bigg|_{r_s} \; . \tag{3.22}$$

Two spherical approximations can be deployed in the last equation. First, the normal derivative of T^h is replaced by the radial derivative [Vaníček et al., 1999]

$$\frac{\partial T^h(r, \Omega)}{\partial n} \; = \; \frac{\partial T^h(r, \Omega)}{\partial r} \; - \; \varepsilon_g(T^h) \; , \tag{3.23}$$

where the *ellipsoidal correction to the gravity disturbance* is [ibid]

$$\varepsilon_g(T^h) \;=\; \frac{f}{R}\,\sin 2\varphi\,\left.\frac{\partial\,T^h(r_s,\Omega)}{\partial\varphi}\right|_\varphi \;+\; \mathcal{O}(f^2)\,. \tag{3.24}$$

Second, the vertical gradient of normal gravity is approximated as [ibid]

$$\frac{1}{\gamma(r,\varphi)}\,\frac{\partial\gamma(r,\varphi)}{\partial n} \;\doteq\; -\frac{2}{a}\left(1 \;+\; m \;+\; f\cos 2\varphi \;-\; \frac{f}{3}\right) \;\doteq\; -\frac{2}{R}\,, \tag{3.25}$$

where m is the geodetic parameter defined as [Torge, 1989]

$$m \;=\; \frac{a\,\omega^2}{\gamma_e}\,. \tag{3.26}$$

Substituting these two approximations into Eqn. (3.22), the spherical form of Eqn. (3.7) can be derived and written in terms of the *Helmert gravity anomaly* Δg^h

$$r \;=\; r_s \;:\; \Delta g^h(r,\Omega) \;=\; \Delta g^f(\Omega) \;+\; \delta S^t(r,\Omega) \;+\; \delta S^a(r,\Omega) \;+$$

$$+\; \delta A^t(r,\Omega) \;+\; \delta A^a(r,\Omega) \;+\; \delta S^\xi(r,\Omega) \;\doteq$$

$$\doteq\; -\frac{2}{R}\,T^h(r,\Omega) \;-\; \varepsilon_n(T^h) \;-\; \left.\frac{\partial T^h(r,\Omega)}{\partial r}\right|_r \;+\; \varepsilon_g(T^h)\,. \tag{3.27}$$

Here, the *secondary indirect topographical effect on gravity* is [Vaníček et al., 1999]

$$\delta S^t(r_s,\Omega) \;=\; \frac{2}{R}\,\delta V^t(r_s,\Omega)\,, \tag{3.28}$$

and the *secondary indirect atmospheric effect on gravity* [ibid]

$$\delta S^a(r_s,\Omega) \;=\; \frac{2}{R}\,\delta V^a(r_s,\Omega)\,. \tag{3.29}$$

The *direct topographical effect on gravity* is [Martinec and Vaníček, 1994b]

$$\delta A^t(r_s,\Omega) \;=\; \left.\frac{\partial\,\delta V^t(r,\Omega)}{\partial r}\right|_{r_s}\,, \tag{3.30}$$

and the *direct atmospheric effect on gravity* [ibid]

$$\delta A^a(r_s,\Omega) \;=\; \left.\frac{\partial\,\delta V^a(r,\Omega)}{\partial r}\right|_{r_s}\,. \tag{3.31}$$

Finally, the *geoid-to-quasigeoid correction* is [Vaníček et al., 1999]

$$\delta S^{\xi}(r_s, \Omega) = \frac{2}{R} H(\Omega) \Delta g^{sb}(\Omega) . \tag{3.32}$$

A small ellipsoidal correction can be written as [ibid]

$$\varepsilon_n(T^h) = \frac{2}{R} \left(m + f \cos 2\varphi - \frac{f}{3} \right) T^h(r_s, \Omega) . \tag{3.33}$$

The last step consists of the *downward continuation* of the Helmert gravity anomaly, defined in Eqn. (3.27), from the topography to the geoid in Helmert's space [ibid]

$$\Delta g^h(r_c, \Omega) = \Delta g^h(r_s, \Omega) + D\Delta g^h(\Omega) , \tag{3.34}$$

where $D\Delta g^h$ is the downward continuation term, see Sec. (4.6). The solution for T^h is then unique and stable if Δg^h on the co-geoid do not contain first-degree (forbidden) harmonics [Martinec, 1998]

$$\forall \, m = -1, \, 0, \, 1 \, : \, \iint_{\Omega_\oplus} \Delta g^h(r_c, \Omega') \, Y^*_{1,m}(\Omega') \, d\Omega' = 0 . \tag{3.35}$$

Here, the asterisk denotes the complex conjugate of the spherical harmonic function. Generally, observed and reduced values of gravity do not satisfy this condition and three new unknown coefficients α are usually introduced [Hörmander, 1976]

$$r = r_c \, : \, \Delta g^h(r, \Omega) + \sum_{m=-1}^{1} \alpha_{1,m} \, Y_{1,m}(\Omega) \doteq$$

$$\doteq -\frac{2}{R} T^h(r, \Omega) - \varepsilon_n(T^h) - \left. \frac{\partial T^h(r, \Omega)}{\partial r} \right|_r + \varepsilon_g(T^h) . \tag{3.36}$$

Neglecting the small ellipsoidal corrections in the boundary condition, the solution is given by the spherical Stokes integral [Stokes, 1849]

$$r = r_c \, : \, T^h(r, \Omega) \doteq \frac{R}{4\pi} \iint_{\Omega_\oplus} \Delta g^h(r, \Omega') \, \mathcal{S}(\psi) \, d\Omega' , \tag{3.37}$$

where $\mathcal{S}$ stands for the homogeneous *spherical Stokes function* [ibid]

$$\mathcal{S}(\psi) = 1 + \csc\frac{\psi}{2} - 6\sin\frac{\psi}{2} - 5\cos\psi - 3\cos\psi \, \ln\left(\sin\frac{\psi}{2} + \sin^2\frac{\psi}{2} \right) . \tag{3.38}$$

Ellipsoidal corrections are usually evaluated from the previous knowledge of T^h derived from any global geopotential model. The alternative solution is represented by an iterative approach [Cruz, 1985]. Unfortunately, its convergence has not been proved yet. The solution using Green's function was derived by [Martinec, 1998]

$$r \ = \ r_c \ : \ T^h(r, \Omega) \ \doteq \ \frac{e^2 R}{4\pi} \ \left[\ e^{-2} \ \iint_{\Omega_\oplus} \Delta g^h(r, \Omega^{'}) \ \mathcal{S}(\psi) \ d\Omega^{'} \ + \right.$$

$$\left. + \ 3 \ \sin^2 \varphi \ \iint_{\Omega_\oplus} \Delta g^h(r, \Omega^{'}) \ d\Omega^{'} \ - \ \iint_{\Omega_\oplus} \Delta g^h(r, \Omega^{'}) \ \mathcal{S}^{\dagger}(\psi) \ d\Omega^{'} \ \right] \ . \tag{3.39}$$

The *ellipsoidal correction to the spherical Stokes function* was derived in a spectral form as [ibid]

$$\mathcal{S}^{\dagger}(\psi) \ = \ 4\pi \ \sum_{n=2}^{\infty} \ \sum_{m=-n}^{n} \ \left[\ \frac{a_{n+2,m}}{n-1} \ Y_{n+2,m}(\Omega) \ Y_{n,m}^{*}(\Omega^{'}) \ + \right.$$

$$\left. + \ \frac{b_{n,m}}{n-1} \ Y_{n,m}(\Omega) \ Y_{n,m}^{*}(\Omega^{'}) \ + \ \frac{c_{n,m}}{n+1} \ Y_{n,m}(\Omega) \ Y_{n,m}^{*}(\Omega^{'}) \ \right] \ . \tag{3.40}$$

Algebraic coefficients were derived $\forall \ n \ \geq \ 2 \ , \ m \ \leq \ n$ as follows [ibid]

$$a_{n,m} \ = \ \frac{n+1}{(n-1) \ (2n-1)} \ \left\{ \ \frac{[(n-1)^2 - m^2] \ (n^2 - m^2)}{(2n-3) \ (2n+1)} \ \right\}^{\frac{1}{2}} , \tag{3.41}$$

$$b_{n,m} \ = \ \frac{3}{n-1} \ \left[\ \frac{(n+1)^2 - m^2}{(2n-1) \ (2n+3)} \ - \ \frac{n}{2n-1} \ \right] , \tag{3.42}$$

$$c_{n,m} \ = \ \frac{n}{(1-n) \ (2n+3)} \ \left\{ \ \frac{[(n+1)^2 - m^2] \ [(n+2)^2 - m^2]}{(2n+1) \ (2n+5)} \ \right\}^{\frac{1}{2}} . \tag{3.43}$$

This solution was formulated while neglecting the terms of the order e^4 which causes an admissible absolute error of 2 mm in geoidal heights. The spatial representation of Eqn. (3.40) expressed in terms of a finite combination of elementary analytical functions was also derived [ibid] and it was concluded that the singularity of the correcting integration kernel is weaker than the singularity of the original function.

Equation (3.36) was also formulated for the reference ellipsoid [Martinec, 1998]

$$u = b : \Delta g^h(u, \Psi) \doteq - \frac{2}{u} \; T^h(u, \Psi) \; - \; \frac{\partial T^h(u, \Psi)}{\partial u} \bigg|_u \; , \tag{3.44}$$

where two small quantities correcting for the vertical gradient of normal gravity and the change of the directional derivative of T^h are neglected. The ellipsoidal coordinate u is identified with the minor semiaxis of the reference ellipsoid b. Its solution is [ibid]

$$T^h(b, \Psi) \doteq \frac{\beta_{0,0}}{4\pi} \iint_{\Psi_\oplus} \Delta g^h(b, \Psi') \, d\Psi' +$$

$$+ \frac{b}{4\pi} \iint_{\Psi_\oplus} \Delta g^h(b, \Psi') \left[\mathcal{S}(\psi) - e^2 \; \mathcal{S}^e(\Psi, \Psi') \right] \, d\Psi' \; , \tag{3.45}$$

where $\mathcal{S}^e$ stands for the anisotropic *ellipsoidal Stokes function* [ibid]

$$\mathcal{S}^e(\Psi, \Psi') = 4\pi \sum_{n=2}^{\infty} \sum_{m=-n}^{n} \beta_{n,m} \, Y_{n,m}(\Psi) \, Y_{n,m}^*(\Psi') \; . \tag{3.46}$$

This function was derived while neglecting the terms of the order e^4 which causes again an absolute error of 2 mm in geoidal heights. Parameters β are [ibid]

$$n = m = 0 : \beta_{n,m} = - Q_{n,m}(b') \left[\frac{dQ_{n,m}(b')}{du} + \frac{2}{b} \, Q_{n,m}(b') \right]^{-1} , \tag{3.47}$$

$$\forall \, n \geq 2 \, , \, m \leq n \, : \, \beta_{n,m} = \frac{1}{(n-1)^2} \left[\frac{(n+1)^2 - m^2}{2n+3} - (n+1) \right] \; . \tag{3.48}$$

Both the spherical and ellipsoidal Stokes functions have the same degree of singularity for $\psi = 0$, namely ψ^{-1}. The spatial representation of Eqn. (3.46) expressed in terms of the finite combination of elementary analytical functions was also derived [ibid].

Applying the Bruns formula on the value in Eqn. (3.37), the co-geoid reads

$$N^h(\Omega) = \frac{T^h(r_c, \Omega)}{\gamma(r_e, \varphi)} \; , \tag{3.49}$$

and the geoid is using the *primary indirect topographical and atmospheric effects*

$$N(\Omega) = N^h(\Omega) + \delta N(\Omega) = N^h(\Omega) + \delta N^t(\Omega) + \delta N^a(\Omega) =$$

$$= \frac{T^h(r_c, \Omega)}{\gamma(r_e, \varphi)} + \frac{\delta V^t(r_c, \Omega)}{\gamma(r_e, \varphi)} + \frac{\delta V^a(r_c, \Omega)}{\gamma(r_e, \varphi)} \; . \tag{3.50}$$

22

3.2 Generalized Stokes-Helmert scheme

Stokes-Helmert's approach has recently been reformulated by Vaníček and Sjøberg [1991] taking gravity potential generated by a higher-degree spheroid as a reference. The major idea of this approach is to use the low-frequency potential of the satellite-based global equipotential model to compute the so-called reference spheroid which is subsequently refined by the residual geoid based on higher-frequency terrestrial gravity data. The cut-off frequency between low- and high-frequency components is chosen to be approximately at degree 20. This selection is based on two assumptions. First, terrestrial gravity data do not contribute significantly to low-frequency features of the gravity field. Second, higher frequencies of the global models are burdened by high noise, and their amplitudes are significantly attenuated.

The geoidal height can be computed using Eqn. (3.50) as a sum of the geoid in the Helmert space and the combined primary indirect effects. Based on the spectral decomposition of the gravity data, the geoid can be written as a sum of the *reference spheroid* and the *residual geoid*

$$N(\Omega) \; = \; N_\ell(\Omega) \; + \; N^\ell(\Omega) \; . \tag{3.51}$$

The solution of the reference spheroid is given by Bruns's theorem

$$N_\ell(\Omega) \; = \; \frac{T_\ell(r_g, \Omega)}{\gamma(r_e, \varphi)} \; . \tag{3.52}$$

Gravity potentials of the actual and normal fields were introduced in their spectral form in Sec. (2.4). The low-frequency coefficients of the actual gravity potential are taken from a global geopotential model. Assuming the same mass of the earth and the reference geocentric ellipsoid, the reference disturbing gravity potential can be derived in spectral domain as [Najafi, 1996]

$$T_\ell(r_g, \Omega) \; = \; \frac{GM}{r_g} \; \sum_{n=2}^{\ell} \left(\frac{a'}{r_g} \right)^n T_n(\Omega) \; , \tag{3.53}$$

23

with the cut-off frequency ℓ. Even-degree Laplace's coefficients are given as follows

$$\forall \, n \, = \, 2, \, 4, \, 6 \, \ldots \, \ell \, : \, T_n(\Omega) \, = \, W_n(\Omega) \, - \, \left(\frac{a}{a'} \right)^n J_n \, P_n(\sin \varphi) \, , \qquad (3.54)$$

and the odd-degree coefficients are as follows

$$\forall \, n \, = \, 3, \, 5, \, 7 \, \ldots \, \ell - 1 \, : \, T_n(\Omega) \, = \, W_n(\Omega) \, . \qquad (3.55)$$

This finite series can be employed everywhere outside the topographical surface r_s due to the finite values of the spherical harmonic coefficients T_n . A computation scheme for the determination of the reference spheroid in Helmert's space (for the ellipsoidal approximation of the geoid) was derived by [Najafi, 1996], and is not discussed here any further.

The residual geoid is solved for in the Helmert space. The solution of the Helmert residual geoid is based on the geodetic boundary-value problem and properly reduced terrestrial gravity data [Martinec, 1998]

$$\forall \, r \, > \, r_c \, : \, \nabla^2 \, T^{h,\ell}(r, \Omega) \, = \, 0 \, , \qquad (3.56)$$

with the boundary condition given as follows

$$r \, = \, r_c \, : \, \Delta g^{h,\ell}(r, \Omega) \, + \, \sum_{m=-1}^{1} \, \alpha_{1,m} \, Y_{1,m}(\Omega) \, \doteq$$

$$\doteq \, - \frac{2}{R} \, T^{h,\ell}(r, \Omega) \, - \, \varepsilon_n(T^{h,\ell}) \, - \, \left. \frac{\partial T^{h,\ell}(r, \Omega)}{\partial r} \right|_r \, + \, \varepsilon_g(T^{h,\ell}) \, , \qquad (3.57)$$

and the asymptotic condition at infinity

$$\lim_{r \to \infty} \, T^{h,\ell}(r, \Omega) \, = \, 0 \, . \qquad (3.58)$$

Its solution is given by the (spheroidal) Stokes integral

$$r \, = \, r_c \, : \, T^{h,\ell}(r, \Omega) \, \doteq \, \frac{R}{4\pi} \, \iint_{\Omega_\oplus} \Delta g^{h,\ell}(r, \Omega') \, \mathcal{S}^\ell(\psi) \, d\Omega' \, . \qquad (3.59)$$

The *spheroidal Stokes function* is defined as [Vaníček and Kleusberg, 1987]

$$\mathcal{S}^{\ell}(\psi) \;=\; \mathcal{S}(\psi) \;-\; \sum_{n=2}^{\ell} \frac{2n+1}{n-1} \, P_n(\cos\psi) \;. \tag{3.60}$$

Finally, the Helmert residual geoid is computed using Bruns's theorem

$$N^{h,\ell}(\Omega) \;=\; \frac{T^{h,\ell}(r_c,\Omega)}{\gamma(r_e,\varphi)} \;\;, \tag{3.61}$$

which is transformed to the real space using the residual primary indirect effects

$$N^{\ell}(\Omega) \;=\; N^{h,\ell}(\Omega) \;+\; \frac{\delta V^{\ell}(r_c,\Omega)}{\gamma(r_e,\varphi)} \;\;. \tag{3.62}$$

The proper derivation of the Helmert residual gravity anomaly $\Delta g^{h,\ell}$ on the Helmert geoid is the crucial problem of this approach, and is discussed in the next two chapters.

The major advantage of the geoidal solution based on the spectral decomposition described above is the efficient use of available gravity data. Using the pure satellite-derived global gravity data for the reference spheroid and the terrestrial data for the residual geoid, an efficient technique for the geoid determination is formulated.

Although the approach of using a combination of the terrestrial and satellite-derived gravity data is presented for the spheroidal Stokes function only, other approximations can also be employed. Removal of the low-frequency component from the integration kernel is in every case a necessity since the kernel should be blind to possible leakage of low frequencies from the terrestrial gravity data. Derivation of the modified spheroidal Stokes function, including its numerical evaluation, is given in *Chapter (6)*.

Chapter 4

Helmert's Reduction of Gravity

Gravity data required for the rigorous solution of the geodetic boundary-value problem are derived in this chapter. The Helmert second method of condensation [Helmert, 1884; Lambert 1930], based on replacing the gravitational potential of topographical and atmospheric masses by the gravitational potential of a surface material layer on the geoid, is used for the gravity reduction, see Fig. (7.1) [Vaníček et al., 1999].

Sections (4.1) and (4.2) contain the derivations of topographical effects both on gravity potential and gravity. Based on the spherical approximation of the geoid and constant density of topographical masses, formulae suitable for their numerical evaluation are derived in these two sections. Effects of the anomalous topographical density studied recently by [Huang et al., 1999] are not included here.

Section (4.3) explains the formulation of the density distribution of atmospheric masses, and the following two sections (4.4) and (4.5), contain formulae for numerical evaluations of atmospheric effects on gravity potential and gravity. Once again, all formulations are based on the spherical approximation of the geoid.

The problem of the discrete downward continuation of gravity from the topography to the geoid is briefly explained in the last section (4.6). Although it is not a part of the main investigation, it represents the last but not least important step in the entire scheme of gravity reduction, as explained in the previous chapter.

4.1 Topographical effect on potential

The residual gravity potential, which was introduced during the "helmertization" of the earth gravity field outside the geoid, can be defined as the sum of the residual topographical potential and residual atmospheric potential. The first term, called also an indirect topographical effect on the earth gravity potential, is the difference of the gravitational potential of the topographical masses V^t and the gravitational potential of the condensed topographical layer V^{ct}. Introducing the spatial form of Newton's kernel, see Eqn. (2.32),

$$\mathcal{N}(r,\psi,r^{'}) = \left(r^2 + r^{'2} - 2\,r\,r^{'}\cos\psi \right)^{-\frac{1}{2}} , \tag{4.1}$$

the gravitational potential of the topographical masses can be computed using the volume integral [Martinec and Vaníček, 1994b]

$$V^t(r,\Omega) = G \iint_{\Omega_\oplus} \int_{\xi=r_g(\Omega^{'})}^{r_s(\Omega^{'})} \varrho^t(\xi,\Omega^{'})\,\mathcal{N}(r,\psi,\xi)\,\xi^2\,d\xi\,d\Omega^{'} , \tag{4.2}$$

where ϱ^t is the density of topographical masses. The potential of the topographical condensation layer is then defined using the surface integral [ibid]

$$V^{ct}(r,\Omega) = G \iint_{\Omega_\oplus} \sigma^t(r_g,\Omega^{'})\,\mathcal{N}[\,r,\psi,r_g(\Omega^{'})\,]\,r_g^{\,2}(\Omega^{'})\,d\Omega^{'} , \tag{4.3}$$

where σ^t is the surface density of the topographical condensation layer. Both V^t and V^{ct} can be simplified using the approximation of the geoid r_g by the reference sphere of radius R, and using a simplified model for the density of the topographical masses $\varrho^t(\xi,\Omega^{'}) \approx \varrho^t(\Omega^{'})$. The spherical approximation causes an error in the geoidal height of 30 mm at most [Martinec, 1993]. Equation (4.2) can then be written as

$$V^t(r,\Omega) = G \iint_{\Omega_\oplus} \varrho^t(\Omega^{'}) \int_{\xi=R}^{R+H(\Omega^{'})} \mathcal{N}(r,\psi,\xi)\,\xi^2\,d\xi\,d\Omega^{'} , \tag{4.4}$$

and similarly Eqn. (4.3) gives

$$V^{ct}(r,\Omega) = GR^2 \iint_{\Omega_\oplus} \sigma^t(\Omega^{'})\,\mathcal{N}(r,\psi,R)\,d\Omega^{'} . \tag{4.5}$$

There are many options for the definition of the condensation density σ^t. In this dissertation, the mass-conservation scheme is deployed only. Its major disadvantage consists of introducing the first-degree terms into the potential of the earth gravity field. This can be accounted for by introducing additional unknowns in the fundamental gravimetric equation (3.36). The surface density has a form [Wichiencharoen, 1982]

$$\sigma^t(\Omega') = \frac{\varrho^t(\Omega')}{R^2} \int_{\xi=R}^{R+H(\Omega')} \xi^2 \; d\xi = \varrho^t(\Omega') \left[H(\Omega') + \frac{H^2(\Omega')}{R} + \frac{H^3(\Omega')}{3R^2} \right] \; . \quad (4.6)$$

Both the volume (4.4) and surface (4.5) integrals have a singularity at the computation point. To avoid their evaluation for $\psi = 0$, a simple mathematical trick is introduced. The volume integral can numerically be split as

$$V^t(r,\Omega) \;=\; V^{ts}(r,\Omega) \;+\; V^{tr}(r,\Omega) \; , \quad (4.7)$$

with the gravitational potential of the spherical topographical shell of thickness H

$$V^{ts}(r,\Omega) \;=\; G \iint_{\Omega_\oplus} \varrho^t(\Omega') \int_{\xi=R}^{R+H(\Omega)} \mathcal{N}(r,\psi,\xi) \; \xi^2 \; d\xi \; d\Omega' \; , \quad (4.8)$$

and the gravitational potential of the topographical roughness (terrain)

$$V^{tr}(r,\Omega) \;=\; G \iint_{\Omega_\oplus} \varrho^t(\Omega') \int_{\xi=R+H(\Omega)}^{R+H(\Omega')} \mathcal{N}(r,\psi,\xi) \; \xi^2 \; d\xi \; d\Omega' \; . \quad (4.9)$$

Similarly, the gravitational potential of the condensed topography is split as

$$V^{ct}(r,\Omega) \;=\; V^{cts}(r,\Omega) \;+\; V^{ctr}(r,\Omega) \; , \quad (4.10)$$

with the gravitational potential of the condensed spherical topographical shell

$$V^{cts}(r,\Omega) \;=\; GR^2 \iint_{\Omega_\oplus} \sigma^{ts}(\Omega') \, \mathcal{N}(r,\psi,R) \; d\Omega' \; , \quad (4.11)$$

and the potential of the condensed topographical roughness (condensed terrain)

$$V^{ctr}(r,\Omega) \;=\; GR^2 \iint_{\Omega_\oplus} \sigma^{tr}(\Omega') \, \mathcal{N}(r,\psi,R) \; d\Omega' \; . \quad (4.12)$$

28

The condensation density in Eqn. (4.11) is defined as

$$\sigma^{ts}(\Omega') = \frac{\varrho^t(\Omega')}{R^2} \int_{\xi=R}^{R+H(\Omega)} \xi^2 \, d\xi = \varrho^t(\Omega') \left[H(\Omega) + \frac{H^2(\Omega)}{R} + \frac{H^3(\Omega)}{3R^2} \right] , \quad (4.13)$$

and the same quantity in Eqn. (4.12) as

$$\sigma^{tr}(\Omega') = \frac{\varrho^t(\Omega')}{R^2} \int_{\xi=R+H(\Omega)}^{R+H(\Omega')} \xi^2 \, d\xi =$$

$$= \varrho^t(\Omega') \left[H(\Omega') - H(\Omega) + \frac{H^2(\Omega') - H^2(\Omega)}{R} + \frac{H^3(\Omega') - H^3(\Omega)}{3R^2} \right] . \quad (4.14)$$

A good knowledge of the topographical density ϱ^t is required for the correct evaluation of all these integrals. For computational convenience, the topographical density can be replaced by the sum [Martinec, 1993; Huang et al., 1999]

$$\varrho^t(\Omega') = \varrho_o^t + \Delta\varrho^t(\Omega') , \quad (4.15)$$

with the mean topographical density $\varrho_o^t = 2,670$ kg m^{-3}, and a term $\Delta\varrho^t$ modelling the departures of actual density values from this global mean. Magnitudes of this anomalous density vary approximately within a range of $\pm$ 10% of the global mean.

Assuming a constant topographical density ϱ_o^t only, the potential of the spherical topographical shell evaluated at the point on the topography

$$V^{ts}(R+H, \Omega) = 4\pi\varrho_o^t \, GR^2 \, \frac{H(\Omega)}{R+H(\Omega)} \left[1 + \frac{H(\Omega)}{R} + \frac{H^2(\Omega)}{3R^2} \right] , \quad (4.16)$$

and the same potential on the geoid

$$V^{ts}(R, \Omega) = 4\pi\varrho_o^t \, GH(\Omega) \left[R + \frac{H(\Omega)}{2} \right] . \quad (4.17)$$

The potential of the condensed spherical topographical shell on the topography is

$$V^{cts}(R+H, \Omega) = 4\pi GR^2 \, \frac{\sigma^t(\Omega)}{R+H(\Omega)} , \quad (4.18)$$

and the same term computed on the geoid

$$V^{cts}(R, \Omega) = 4\pi GR \, \sigma^t(\Omega) . \quad (4.19)$$

29

The potential of the topographical roughness can be evaluated in its general form, for the point on a geocentric radius r, as follows

$$V^{tr}(r, \Omega) = G \iint_{\Omega_{\oplus}} \varrho^t(\Omega') \, \mathcal{M}(r, \psi, \xi) \bigg|_{\xi=R+H(\Omega)}^{R+H(\Omega')} d\Omega' . \qquad (4.20)$$

The integration kernel $\mathcal{M}$ is derived as [Gradshteyn and Ryzhik, 1980]

$$\mathcal{M}(r, \psi, \xi) = \int_{\xi} \mathcal{N}(r, \psi, \xi) \, \xi^2 \, d\xi = \frac{\xi + 3 \, r \cos \psi}{2 \, \mathcal{N}(r, \psi, \xi)} +$$

$$+ \frac{r^2}{2} \, (3 \cos^2 \psi - 1) \, \ln \bigg| \xi - r \cos \psi + \mathcal{N}^{-1}(r, \psi, \xi) \bigg| + C_m , \qquad (4.21)$$

where C_m is an integration constant. Because potentials of the actual and condensed spherical topographical shells evaluated on the topography cancel each other

$$V^{ts}(R + H, \Omega) - V^{cts}(R + H, \Omega) = 0 , \qquad (4.22)$$

the residual topographical potential on the topography reads

$$\delta V^t(R + H, \Omega) = V^{tr}(R + H, \Omega) - V^{ctr}(R + H, \Omega) . \qquad (4.23)$$

The same term evaluated on the geoid is

$$\delta V^t(R, \Omega) = V^{ts}(R, \Omega) - V^{cts}(R, \Omega) + V^{tr}(R, \Omega) - V^{ctr}(R, \Omega) . \qquad (4.24)$$

where the term corresponding to Eqn. (4.22) is equal to

$$V^{ts}(R, \Omega) - V^{cts}(R, \Omega) = - 2\pi \varrho_o^t \, G H^2(\Omega) \left[1 + \frac{2H(\Omega)}{3R} \right] . \qquad (4.25)$$

Next, formulae suitable for numerical evaluations of potentials associated with the topographical roughness and condensed topographical roughness are derived. To evaluate these two quantities, the global integration over functional values of the orthometric height has to be carried out. The discrete numerical representation of orthometric heights over limited regions is given in a form of digital elevation models.

Furthermore, its global representation is known in spherical harmonics. Numerical techniques used for the evaluation of the aforementioned integrals reflect the character of the available data. The entire integration domain $\Omega_\oplus$, representing the surface of the earth, can be split into a spherical cap $\Omega_\odot$ and its remainder $\Omega_\oplus - \Omega_\odot$. In the first domain, called the *near zone*, a summation over discrete elevation values is used. In the second domain, called the *distant zone*, a spectral technique [Molodenskij et al., 1960] is employed. To obtain the residual topographical potential on the topography, see Eqn. (4.23), the following integrals must be evaluated

$$\delta V^t(R+H,\Omega) \;=\; G \; \iint_{\Omega_\oplus} \varrho^t(\Omega') \, \mathcal{M}(R+H,\psi,\xi) \, \Bigg|_{\xi=R+H(\Omega)}^{R+H(\Omega')} \, d\Omega' \;-$$

$$- \, GR^2 \iint_{\Omega_\oplus} \sigma^{tr}(\Omega') \, \mathcal{N}(R+H,\psi,R) \, d\Omega' \;. \tag{4.26}$$

The contribution of the near zone to the residual topographical potential evaluated on the topography can be computed as

$$\delta V^t_\odot(R+H,\Omega) \;=\; G \, \sum_{i=1}^{j-1} \varrho^t(\Omega_i) \, \mathcal{M}(R+H,\psi_i,\xi) \, \Bigg|_{\xi=R+H(\Omega)}^{R+H(\Omega_i)} \, \Delta\Omega_i \;-$$

$$- \, GR^2 \sum_{i=1}^{j-1} \sigma^{tr}(\Omega_i) \, \mathcal{N}(R+H,\psi_i,R) \, \Delta\Omega_i \;, \tag{4.27}$$

where j is the number of data within the spherical cap, and $\Delta\Omega_i$ is the area of the i-th geographical cell. The contribution of the distant zone to the residual topographical potential on the topography is computed using a constant topographical density

$$\delta V^t_{\oplus-\odot}(R+H,\Omega) \;=\; G \, \varrho^t_o \, \iint_{\Omega_\oplus-\Omega_\odot} \mathcal{M}(R+H,\psi,\xi) \, \Bigg|_{\xi=R+H(\Omega)}^{R+H(\Omega')} \, d\Omega' \;-$$

$$- \, GR^2 \iint_{\Omega_\oplus-\Omega_\odot} \sigma^{tr}(\Omega') \, \mathcal{N}(R+H,\psi,R) \, d\Omega' \;, \tag{4.28}$$

and an appropriate formula which can be used for its numerical evaluation must be derived. The integration kernel $\mathcal{M}$ is expanded into a power series, see Apx. (A.1).

Taking a linear and quadratic term of this series into the account only, a convolutive form of the first integral in Eqn. (4.28) reads

$$
V^{tr}_{\oplus-\odot}(R+H,\Omega) = G \, \varrho^t_o \, \frac{R+H(\Omega)}{2} \, \iint_{\Omega_\oplus-\Omega_\odot} \left[\, H(\Omega') - H(\Omega) \, \right] \, \mathcal{M}_1(\psi) \, d\Omega' \; +
$$

$$
+ \, \frac{3}{4} \, G \, \varrho^t_o \, \iint_{\Omega_\oplus-\Omega_\odot} \left[\, H(\Omega') - H(\Omega) \, \right]^2 \mathcal{M}_2(\psi) \, d\Omega' \; + \; \mathcal{O}(H^3) \,, \tag{4.29}
$$

with following auxiliary integration kernels

$$
\mathcal{M}_1(\psi) \; = \; \frac{2 \, + \, (2 \, - \, 2\cos\psi)^{\frac{1}{2}}}{1 \, - \, \cos\psi \, + \, (2-2\cos\psi)^{\frac{1}{2}}} \;\; , \tag{4.30}
$$

$$
\mathcal{M}_2(\psi) \; = \; \frac{3 \, - \, 4\cos\psi \, + \, \cos^2\psi \, + \, 2\,(1-\cos\psi)\,(2-2\cos\psi)^{\frac{1}{2}}}{(2 \, - \, 2\cos\psi)^{\frac{1}{2}} \left[\, 1 \, - \, \cos\psi \, + \, (2-2\cos\psi)^{\frac{1}{2}} \, \right]^2} \;\; . \tag{4.31}
$$

Applying the same approach to the second integral in Eqn. (4.28), the following formula can be derived in a form

$$
V^{ctr}_{\oplus-\odot}(R+H,\Omega) = G R^2 \, \varrho^t_o \, \iint_{\Omega_\oplus-\Omega_\odot} \left[\, H(\Omega') - H(\Omega) \, \right] \, \mathcal{N}(R+H,\psi,R) \, d\Omega' \; +
$$

$$
+ \, GR \, \varrho^t_o \, \iint_{\Omega_\oplus-\Omega_\odot} \left[\, H^2(\Omega') - H^2(\Omega) \, \right] \, \mathcal{N}(R+H,\psi,R) \, d\Omega' \; + \; \mathcal{O}(H^3) \,. \tag{4.32}
$$

Using the spectral approach [Molodenskij et al., 1960], the potential of the topographical roughness in the distant zone can be evaluated as

$$
V^{tr}_{\oplus-\odot}(R+H,\Omega) \; = \; \pi G \, \varrho^t_o \, \left[\, R+H(\Omega) \, \right] \sum_{n=0}^{\infty} \, p_n(\psi,\psi_o) \, H_n(\Omega) \; -
$$

$$
- \, 2\pi G \, \varrho^t_o \, H(\Omega) \sum_{n=0}^{\infty} \, q_n(\psi,\psi_o) \, H_n(\Omega) \; +
$$

$$
+ \, \pi G \, \varrho^t_o \, \sum_{n=0}^{\infty} \, r_n(\psi,\psi_o) \, H^2_n(\Omega) \; + \; \mathcal{O}(H^3_n) \,. \tag{4.33}
$$

Similarly, the potential of the condensed topographical roughness in a distant zone is

$$V^{ctr}_{\oplus-\odot}(R+H,\Omega) = 2\pi G R^2 \, \varrho_o^t \, \sum_{n=0}^{\infty} \, s_n(R+H,\psi,\psi_o) \, H_n(\Omega) +$$

$$+ 2\pi G R \, \varrho_o^t \, \sum_{n=0}^{\infty} \, s_n(R+H,\psi,\psi_o) \, H_n^2(\Omega) \; + \; \mathcal{O}(H_n^3) \; . \tag{4.34}$$

The truncation coefficients in Eqns. (4.33) and (4.34) read as follows ($\forall \, n \geq 0$)

$$p_n(\psi,\psi_o) = \int_{\psi=\psi_o}^{\pi} \mathcal{M}_1(\psi) \, [\, P_n(\cos\psi) - 1 \,] \, \sin\psi \, d\psi \; , \tag{4.35}$$

$$q_n(\psi,\psi_o) = \int_{\psi=\psi_o}^{\pi} \mathcal{M}_2(\psi) \, P_n(\cos\psi) \, \sin\psi \, d\psi \; , \tag{4.36}$$

$$r_n(\psi,\psi_o) = \int_{\psi=\psi_o}^{\pi} \mathcal{M}_2(\psi) \, [\, P_n(\cos\psi) + 1 \,] \, \sin\psi \, d\psi \; , \tag{4.37}$$

$$s_n(R+H,\psi,\psi_o) = \int_{\psi=\psi_o}^{\pi} \mathcal{N}(R+H,\psi,R) \, [\, P_n(\cos\psi) - 1 \,] \, \sin\psi \, d\psi \; . \tag{4.38}$$

Adding the difference of the quantities (4.33) and (4.34) to the value computed in Eqn. (4.27), the residual topographical potential on the topography can be estimated.

The potential of the topographical roughness in the near zone on the geoid is

$$\delta V^{tr}_{\odot}(R,\Omega) = G \, \sum_{i=1}^{j-1} \, \varrho^t(\Omega_i) \, \mathcal{M}(R,\psi_i,\xi) \, \Big|_{\xi=R+H(\Omega)}^{R+H(\Omega_i)} \Delta\Omega_i -$$

$$- G R^2 \, \sum_{i=1}^{j-1} \, \sigma^{tr}(\Omega_i) \, \mathcal{N}(R,\psi_i,R) \, \Delta\Omega_i \; . \tag{4.39}$$

The contribution of the distant zone has the following form

$$\delta V^{tr}_{\oplus-\odot}(R,\Omega) = G \, \varrho_o^t \, \iint_{\Omega_{\oplus}-\Omega_{\odot}} \mathcal{M}(R,\psi,\xi) \, \Big|_{\xi=R+H(\Omega)}^{R+H(\Omega')} d\Omega' -$$

$$- G R^2 \, \iint_{\Omega_{\oplus}-\Omega_{\odot}} \sigma^{tr}(\Omega') \, \mathcal{N}(R,\psi,R) \, d\Omega' \; . \tag{4.40}$$

33

Expanding the integration kernel $\mathcal{M}$ into a series truncated in a quadratic term, see Apx. (A.2), the convolutive form of the first integral in Eqn. (4.40) reads

$$V_{\oplus-\odot}^{tr}(R,\Omega) = \frac{G}{4} R \, \varrho_o^t \iint_{\Omega_{\oplus}-\Omega_{\odot}} \left[H(\Omega') - H(\Omega) \right] \mathcal{H}_1(\eta,\psi) \, d\Omega' +$$

$$+ \frac{G}{8} \varrho_o^t \iint_{\Omega_{\oplus}-\Omega_{\odot}} \left[H^2(\Omega') - H^2(\Omega) \right] \mathcal{H}_2(\eta,\psi) \, d\Omega' -$$

$$- \frac{G}{8} \varrho_o^t \iint_{\Omega_{\oplus}-\Omega_{\odot}} \left[H(\Omega') - H(\Omega) \right]^2 \mathcal{H}_3(\eta,\psi) \, d\Omega' + \mathcal{O}(H^3) . \qquad (4.41)$$

Auxiliary integration kernels required for its numerical evaluation are

$$\mathcal{H}_1(\eta,\psi) = 3 \, (2 - 2\cos\psi)^{\frac{1}{2}} \, (1 + \cos\psi) +$$

$$+ (3\cos^2\psi - 1) \, \frac{2 + (2 - 2\cos\psi)^{\frac{1}{2}}}{\eta - \cos\psi + (1 + \eta^2 - 2\eta\cos\psi)^{\frac{1}{2}}} , \qquad (4.42)$$

$$\mathcal{H}_2(\eta,\psi) = \frac{5 + 3\cos^2\psi}{(2 - 2\cos\psi)^{\frac{1}{2}}} +$$

$$+ \frac{(3\cos^2\psi - 1) \, (1 + \cos\psi)}{(2 - 2\cos\psi)^{\frac{1}{2}} \left[\eta - \cos\psi + (1 + \eta^2 - 2\eta\cos\psi)^{\frac{1}{2}} \right]} , \qquad (4.43)$$

$$\mathcal{H}_3(\eta,\psi) = (3\cos^2\psi - 1) \, \frac{3 - \cos\psi + 2 \, (2 - 2\cos\psi)^{\frac{1}{2}}}{\left[\eta - \cos\psi + (1 + \eta^2 - 2\eta\cos\psi)^{\frac{1}{2}} \right]^2} . \qquad (4.44)$$

They are functions of the spherical distance between the computation and integration points ψ, and the dimensionless parameter

$$\eta(\Omega) = \frac{R + H(\Omega)}{R} = 1 + \frac{H(\Omega)}{R} \qquad (4.45)$$

only. With respect to the magnitude of the parameter $\eta \leq 1.3 \times 10^{-3}$, the integration kernels (4.42), (4.43), and (4.44) were derived neglecting η^3 and higher order terms.

34

Having obtained the convolution integral, it can be now expressed in spectral form

$$V_{\oplus-\odot}^{tr}(R,\Omega) = \pi G R \, \varrho_o^t \sum_{n=0}^{\infty} a_n(\eta,\psi,\psi_o) \, H_n(\Omega) +$$

$$+ \pi G \, \varrho_o^t \sum_{n=0}^{\infty} b_n(\eta,\psi,\psi_o) \, H_n^2(\Omega) +$$

$$+ 2\pi G \, \varrho_o^t \, H(\Omega) \sum_{n=0}^{\infty} c_n(\eta,\psi,\psi_o) \, H_n(\Omega) -$$

$$- \pi G \, \varrho_o^t \sum_{n=0}^{\infty} d_n(\eta,\psi,\psi_o) \, H_n^2(\Omega) \, + \, \mathcal{O}(H_n^3) \, . \tag{4.46}$$

Truncation coefficients are defined as one-dimensional convolution integrals of the auxiliary integration kernels and Legendre's polynomials ($\forall \, n \geq 0$)

$$a_n(\eta,\psi,\psi_o) = \int_{\psi=\psi_o}^{\pi} \mathcal{H}_1(\eta,\psi) \, \left[\, P_n(\cos\psi) - 1 \, \right] \, \sin\psi \, d\psi \, , \tag{4.47}$$

$$b_n(\eta,\psi,\psi_o) = \int_{\psi=\psi_o}^{\pi} \mathcal{H}_2(\eta,\psi) \, \left[\, P_n(\cos\psi) - 1 \, \right] \, \sin\psi \, d\psi \, , \tag{4.48}$$

$$c_n(\eta,\psi,\psi_o) = \int_{\psi=\psi_o}^{\pi} \mathcal{H}_3(\eta,\psi) \, P_n(\cos\psi) \, \sin\psi \, d\psi \, , \tag{4.49}$$

$$d_n(\eta,\psi,\psi_o) = \int_{\psi=\psi_o}^{\pi} \mathcal{H}_3(\eta,\psi) \, \left[\, P_n(\cos\psi) + 1 \, \right] \, \sin\psi \, d\psi \, . \tag{4.50}$$

All of them are again functions of the spherical distance ψ and the parameter η only.

In practice, these coefficients are evaluated in a form of tables for selected reference heights. During computations, the heights of computation points are used to find the appropriate kernel values. The second integral in Eqn. (4.40) can be rewritten

$$V_{\oplus-\odot}^{ctr}(R,\Omega) = G R^2 \, \varrho_o^t \iint_{\Omega_\oplus-\Omega_\odot} \left[\, H(\Omega') - H(\Omega) \, \right] \, \mathcal{N}(R,\psi,R) \, d\Omega' +$$

$$+ \, G R \, \varrho_o^t \iint_{\Omega_\oplus-\Omega_\odot} \left[\, H^2(\Omega') - H^2(\Omega) \, \right] \, \mathcal{N}(R,\psi,R) \, d\Omega' \, + \, \mathcal{O}(H^3) \, . \tag{4.51}$$

35

The spectral approach then yields the following formula

$$V_{\oplus-\odot}^{ctr}(R,\Omega) = 2\pi G R^2 \varrho_o^t \sum_{n=0}^{\infty} e_n(\psi,\psi_o) H_n(\Omega) +$$

$$+ 2\pi G R \varrho_o^t \sum_{n=0}^{\infty} e_n(\psi,\psi_o) H_n^2(\Omega) + \mathcal{O}(H_n^3) , \qquad (4.52)$$

with the following truncation coefficient ($\forall n \geq 0$)

$$e_n(\psi,\psi_o) = \int_{\psi=\psi_o}^{\pi} \mathcal{N}(R,\psi,R) [P_n(\cos\psi) - 1] \sin\psi \, d\psi . \qquad (4.53)$$

Zonal coefficients for the spherical harmonic representation of H can be computed from the global elevation model such as TUG87 [Wieser, 1987]

$$\forall n = 0 \ldots 180 : H_n(\Omega) = \sum_{m=-n}^{n} H_{n,m} Y_{n,m}(\Omega) , \qquad (4.54)$$

and the same coefficients for squared heights H^2

$$\forall n = 0 \ldots 90 : H_n^2(\Omega) = \sum_{m=-n}^{n} H_{n,m}^2 Y_{n,m}(\Omega) . \qquad (4.55)$$

4.2 Topographical effect on gravity

The residual topographical potential δV^t is the tool for the transformation of the real gravity anomaly into the Helmert space. Its effect on gravity can be evaluated as its negative vertical derivative. Changing its sign, the direct topographical effect on gravity on the topography is obtained as follows [Martinec and Vaníček, 1994b]

$$\delta A^t(R+H,\Omega) = \frac{\partial}{\partial r} \left[V^t(r,\Omega) - V^{ct}(r,\Omega) \right] \Big|_{r=R+H} =$$

$$= A^t(R+H,\Omega) - A^{ct}(R+H,\Omega) . \qquad (4.56)$$

Evaluating the radial derivative in Eqn. (4.56), the term A^t is split into the attraction of the spherical topographical shell, see Eqn. (4.16),

$$A^{ts}(R+H,\Omega) = -4\pi\varrho_o^t G \left[\frac{R}{R+H(\Omega)} \right]^2 \left[H(\Omega) + \frac{H^2(\Omega)}{R} + \frac{H^3(\Omega)}{3R^2} \right] , \quad (4.57)$$

36

and the attraction of the topographical roughness, see Eqn. (4.9),

$$A^{tr}(R+H,\Omega) \;=\; G \; \iint_{\Omega_{\oplus}} \varrho^{t}(\Omega') \, \mathcal{K}(R+H,\psi,\xi) \, \bigg|_{\substack{R+H(\Omega') \\ \xi=R+H(\Omega)}} \, d\Omega' \; . \qquad (4.58)$$

The integration kernel $\mathcal{K}$ for the point of geocentric radius r is the following primitive function [Gradshteyn and Ryzhik, 1980], see Eqn. (4.21),

$$\mathcal{K}(r,\psi,\xi) \;=\; \frac{\partial}{\partial r} \, \mathcal{M}(r,\psi,\xi) \, \bigg|_{r} \;=\;$$

$$=\; \Big[(\xi^2 \,+\, 3 \, r^2) \cos\psi \,+\, r \, \xi \, (1 \,-\, 6\cos^2\psi) \Big] \, \mathcal{N}(r,\psi,\xi) \,+\,$$

$$+\, r \, (3\cos^2\psi \,-\, 1) \, \ln \Big| \, \xi \,-\, r\cos\psi \,+\, \mathcal{N}^{-1}(r,\psi,\xi) \, \Big| \,+\, C_k \; , \qquad (4.59)$$

where C_k is an integration constant. Using the same approach as above, the attraction of the condensed spherical topographical shell is

$$A^{cts}(R+H,\Omega) \;=\; -\, 4\pi G \, \sigma^{ts}(\Omega) \, \left[\frac{R}{R+H(\Omega)} \right]^2 \; . \qquad (4.60)$$

The next term represents the attraction of the condensed topographical roughness

$$A^{ctr}(R+H,\Omega) \;=\; GR^2 \iint_{\Omega_{\oplus}} \sigma^{tr}(\Omega') \, \mathcal{J}(R+H,\psi,R) \, d\Omega' \; , \qquad (4.61)$$

with the surface density being already defined in Eqn. (4.13). The integration kernel $\mathcal{J}$ for the point of geocentric radius r has the following form

$$\mathcal{J}(r,\psi,R) \;=\; \frac{\partial}{\partial r} \, \mathcal{N}(r,\psi,R) \, \bigg|_{r} \;=\; (\, R\cos\psi \,-\, r \,) \, \mathcal{N}^3(r,\psi,R) \; . \qquad (4.62)$$

All terms which contribute to the direct topographical effect on gravity are now defined. Its entire value is

$$\delta A^{t}(R+H,\Omega) \;=\; A^{ts}(R+H,\Omega) \,+\, A^{tr}(R+H,\Omega) \,-$$

$$-\, A^{cts}(R+H,\Omega) \,-\, A^{ctr}(R+H,\Omega) \; . \qquad (4.63)$$

37

Using the mass-conservation condensation scheme, we have

$$A^{ts}(R+H,\Omega) \;-\; A^{cts}(R+H,\Omega) \;=\; 0 \;, \tag{4.64}$$

and the direct topographical effect on gravity reduces to the difference

$$\delta A^{t}(R+H,\Omega) \;=\; A^{tr}(R+H,\Omega) \;-\; A^{ctr}(R+H,\Omega) \;. \tag{4.65}$$

The terms on the right-hand side of the last equation, representing the gravitational effects of both the actual and condensed terrain, are called the *terrain and condensed terrain effects on gravity*. Looking closer at the first term, it can be realized that it is nothing else but the so-called terrain correction to gravity [Heiskanen and Moritz, 1967]. This correction is included in the complete Bouguer gravity anomaly [ibid]

$$\Delta g^{cb}(R+H,\Omega) \;=\; \Delta g^{f}(R+H,\Omega) \;-\; 2\pi\varrho^{t}_{o}\,GH(\Omega) \;+\; A^{tr}(R+H,\Omega) \;, \tag{4.66}$$

which are usually used as the starting data for the gravimetric geoid computations. The condensed terrain effect is then the only term to be evaluated. Introducing the following approximation for the surface density, see Eqn. (4.14),

$$\sigma^{tr}(\Omega') \;=\; \varrho^{t}(\Omega')\,\Big[\,H(\Omega')-H(\Omega)\,\Big] \;+\; \mathcal{O}(H^2) \;, \tag{4.67}$$

Equation (4.61) can be written in the following form

$$A^{ctr}(R+H,\Omega) \doteq GR^2 \iint_{\Omega_\oplus} \varrho^{t}(\Omega')\,\Big[\,H(\Omega')-H(\Omega)\,\Big]\,\mathcal{J}(R+H,\psi,R)\,d\Omega'. \tag{4.68}$$

Formulae for the numerical evaluation of the direct topographical effect can now be derived. Recalling Eqns. (4.58) and (4.61), the direct topographical effect can be written as the difference of the following two global integrals

$$\delta A^{t}(R+H,\Omega) \;=\; G\,\iint_{\Omega_\oplus} \varrho^{t}(\Omega')\,\mathcal{K}(R+H,\psi,\xi)\,\Bigg|_{\xi=R+H(\Omega)}^{R+H(\Omega')}\,d\Omega' \;-$$

$$-\;GR^2\,\iint_{\Omega_\oplus}\sigma^{tr}(\Omega')\,\mathcal{J}(R+H,\psi,R)\,d\Omega' \;. \tag{4.69}$$

The contribution of the near zone is obtained as the sum over discrete values within a spherical cap $\Omega_\odot$

$$\delta A_\odot^t (R + H, \Omega) \;=\; G \sum_{i=1}^{j-1} \varrho^t(\Omega_i)\, \mathcal{K}(R + H, \psi_i, \xi) \Bigg|_{\xi = R + H(\Omega)}^{R + H(\Omega_i)} \Delta\Omega_i \;-$$

$$- \, GR^2 \sum_{i=1}^{j-1} \sigma^{tr}(\Omega_i)\, \mathcal{J}(R + H, \psi_i, R)\, \Delta\Omega_i \;. \tag{4.70}$$

The contribution of the distant zone to the attraction of the topographical roughness, defined by the first integral in Eqn. (4.69), can be derived using the truncated power series as follows, see Apx. (A.3),

$$A_{\oplus - \odot}^{tr}(R + H, \Omega) \;=\; G\, \varrho_o^t \iint_{\Omega_\oplus - \Omega_\odot} \Big[H(\Omega') - H(\Omega) \Big]\, \mathcal{K}_1(\psi)\, d\Omega' \;+$$

$$+ \, \frac{G\, \varrho_o^t}{R + H(\Omega)} \iint_{\Omega_\oplus - \Omega_\odot} \Big[H(\Omega') - H(\Omega) \Big]^2 \mathcal{K}_2(\psi)\, d\Omega' \;+\; \mathcal{O}(H^3) \;. \tag{4.71}$$

The first auxiliary integration kernel is

$$\mathcal{K}_1(\psi) \;=\; -\, \frac{1}{2\,(2\, -\, 2\cos\psi)^{\frac{1}{2}}} \;, \tag{4.72}$$

and the second one is

$$\mathcal{K}_2(\psi) \;=\; -\, \frac{3 - 10\cos\psi + 3\cos^2\psi - 2\,(3\cos\psi - 1)\,(2 - 2\cos\psi)^{\frac{1}{2}}}{8\,(2\, -\, 2\cos\psi)^{\frac{1}{2}} \Big[\, 1\, -\, \cos\psi\, +\, (2 - 2\cos\psi)^{\frac{1}{2}} \,\Big]^2} \;. \tag{4.73}$$

Both are functions of the spherical distance ψ only.

Similarly, the contribution of the distant zone to the attraction of the condensed topographical roughness, defined by the second integral in Eqn. (4.69), is derived as

$$A_{\oplus - \odot}^{ctr}(R + H, \Omega) \;=\; GR^2\, \varrho_o^t \iint_{\Omega_\oplus - \Omega_\odot} \Big[H(\Omega') - H(\Omega) \Big]\, \mathcal{J}(R + H, \psi, R)\, d\Omega' \;+$$

$$+ \, GR\, \varrho_o^t \iint_{\Omega_\oplus - \Omega_\odot} \Big[H^2(\Omega') - H^2(\Omega) \Big]\, \mathcal{J}(R + H, \psi, R)\, d\Omega' \;+\; \mathcal{O}(H^3) \;. \tag{4.74}$$

39

Applying again the spectral approach, the attraction of the topographical roughness in the distant zone can be written as follows

$$
A^{tr}_{\oplus-\odot}(R+H,\Omega) = \pi G \, \varrho^t_o \sum_{n=0}^{\infty} t_n(\psi,\psi_o) \, H_n(\Omega) -
$$

$$
- 2\pi G \, \varrho^t_o \, \frac{H(\Omega)}{R+H(\Omega)} \sum_{n=0}^{\infty} u_n(\psi,\psi_o) \, H_n(\Omega) +
$$

$$
+ \pi G \, \varrho^t_o \, \frac{1}{R+H(\Omega)} \sum_{n=0}^{\infty} v_n(\psi,\psi_o) \, H^2_n(\Omega) + \mathcal{O}(H^3_n) , \tag{4.75}
$$

and its counterpart for the condensed topographical roughness

$$
A^{ctr}_{\oplus-\odot}(R+H,\Omega) = 2\pi G R^2 \, \varrho^t_o \sum_{n=0}^{\infty} w_n(R+H,\psi,\psi_o) \, H_n(\Omega) +
$$

$$
+ 2\pi G R \, \varrho^t_o \sum_{n=0}^{\infty} w_n(R+H,\psi,\psi_o) \, H^2_n(\Omega) + \mathcal{O}(H^3_n) . \tag{4.76}
$$

Truncation coefficients in Eqns. (4.75) and (4.76) are given as follows ($\forall \, n \geq 0$)

$$
t_n(\psi,\psi_o) = \int_{\psi=\psi_o}^{\pi} \mathcal{K}_1(\psi) \, [\, P_n(\cos\psi) - 1 \,] \, \sin\psi \, d\psi , \tag{4.77}
$$

$$
u_n(\psi,\psi_o) = \int_{\psi=\psi_o}^{\pi} \mathcal{K}_2(\psi) \, P_n(\cos\psi) \, \sin\psi \, d\psi , \tag{4.78}
$$

$$
v_n(\psi,\psi_o) = \int_{\psi=\psi_o}^{\pi} \mathcal{K}_2(\psi) \, [\, P_n(\cos\psi) + 1 \,] \, \sin\psi \, d\psi , \tag{4.79}
$$

$$
w_n(R+H,\psi,\psi_o) = \int_{\psi=\psi_o}^{\pi} \mathcal{J}(R+H,\psi,R) \, [\, P_n(\cos\psi) - 1 \,] \, \sin\psi \, d\psi . \tag{4.80}
$$

4.3   Atmospheric density function

The atmospheric density ϱ^a as a function of position (r, Ω) holds the important role in the numerical evaluation of all atmospheric effects. Among several existing atmospheric models, one of the most frequently used is [United States Standard Atmosphere, 1976]

$$\varrho^a(H) \; = \; \frac{\mu \; P(H)}{\kappa \; T(H)} \; , \tag{4.81}$$

with the universal gas constant κ [N m mol^{-1} K^{-1}] (constant), mean molecular weight of the atmospheric masses μ [kg mol^{-1}] at the sea level (constant), atmospheric pressure P [N m^{-2}], and molecular-scale temperature of the atmosphere T [K], see Table (7.2). For the estimation of the height-dependent parameters, i.e., atmospheric pressure and temperature, atmospheric masses between the topography and the height of 86 kilometres are divided into seven layers, within each the molecular-scale temperature can be modelled by a linear function of altitude [ibid]

$$\forall \; i \; = \; 1 \; \ldots \; 7 \; : \; T(H) \; = \; T_i \; + \; \tau_i \; (H - H_i) \; , \tag{4.82}$$

where T_i is the reference (initial) value of the molecular-scale temperature for the i-th layer, τ_i is the molecular-scale temperature gradient for the i-th layer, and H_i is the reference (initial) orthometric height for the i-th layer, see Table (7.3). The atmospheric pressure P is computed using one of the following two equations [ibid]

$$\forall \; i \; \in \; \{ \; 1, 3, 4, 6, 7 \; \} \; : \; P(H) \; = \; P_i \; \left[\frac{T_i}{T_i \; + \; \tau_i \; (H \; - \; H_i)} \right]^{\frac{g\mu}{\kappa\tau_i}} \; , \tag{4.83}$$

for the molecular-scale temperature gradient τ_i being not equal to zero, and

$$\forall \; i \; \in \; \{ \; 2, 5 \; \} \; : \; P(H) \; = \; P_i \; \exp \left[\frac{- \; g \; \mu \; (H \; - \; H_i)}{\kappa \; T_i} \right] \; , \tag{4.84}$$

for the molecular-scale temperature gradient τ_i being equal to zero. P_i in both these equations stands for the reference pressure for the i-th layer, and g is the "reference value" of gravity at the sea level, i.e., $g = g(r_g, \Omega)$, see Table (7.2).

41

Due to complexity of the above expressions, suitable approximations are usually sought using, e.g., a polynomial function [Anderson et. al, 1975]

$$\varrho^a(H) \;=\; \varrho_o^a \;+\; \alpha\,H \;+\; \beta\,H^2 \;+\; \ldots \;\; , \tag{4.85}$$

an exponential function [Ecker and Mittermayer, 1969]

$$\varrho^a(H) \;=\; \varrho_o^a \;\exp\left(-\,\alpha\,H\right), \tag{4.86}$$

or another model with the positive constant ν based on the required fit of model and actual values of atmospheric density [Sjøberg, 1993]

$$\forall\,\nu \;\in\; \mathbb{N} \;\; \wedge \;\; \nu \;>\; 2 \;:\; \varrho^a(H) \;=\; \varrho_o^a\;\left(\frac{R}{R\,+\,H}\right)^{\nu} . \tag{4.87}$$

Having investigated possible approximations, it was found that the second degree polynomial function gives acceptable results for heights up to 9 kilometres which is very important for numerical investigations. Absolute values of the relative error are smaller than 5×10^{-3} everywhere, which is negligible on the accuracy level of one centimetre geoid. The atmospheric density function can then be written as

$$\forall\,H \;<\; 9\;km \;:\; \varrho^a(H) \;=\; \varrho_o^a \;+\; \alpha\,H \;+\; \beta\,H^2 \;, \tag{4.88}$$

where ϱ_o^a is the value of the sea-level density, α is the linear coefficient, and β is the quadratic coefficient. Estimated values of the coefficients can be found in Table (7.4). The atmospheric density of the spherical shell above 9 kilometres can be divided into k spherical sub-shells of a unique thickness. The atmospheric density ϱ^a within each sub-shell can be approximated either by a linear or even a constant function.

4.4   Atmospheric effect on potential

The residual atmospheric potential is defined as the difference of the gravitational potential of the atmospheric masses and the gravitational potential of the condensed

atmospheric layer. The gravitational potential of the actual atmospheric masses V^a can be computed using Newton's volume integral

$$V^a(r,\Omega) \;=\; G \; \iint_{\Omega_\oplus} \int_{\xi=r_s(\Omega')}^{r_a} \varrho^a(\xi,\Omega') \, \mathcal{N}(r,\psi,\xi) \, \xi^2 \; d\xi \; d\Omega' \;, \qquad (4.89)$$

where ϱ^a is the density of the atmospheric masses, and r_a is the upper limit of the atmosphere where density becomes negligible. The gravitational potential of the atmospheric condensation layer V^{ac} is estimated using Newton's surface integral

$$V^{ac}(r,\Omega) \;=\; G \; \iint_{\Omega_\oplus} \sigma^a(r_g,\Omega') \, \mathcal{N}[\, r,\psi,r_g(\Omega') \,] \, r_g^{\,2}(\Omega') \, d\Omega' \;, \qquad (4.90)$$

where σ^a is the surface density of the atmospheric condensation layer. Both V^a and V^{ac} can be further simplified using the spherical approximation of the geoid ($r_g = R$), and using the laterally homogeneous model for the atmospheric mass density distribution, $\varrho^a(r)$. Under these assumptions, Eqn. (4.89) can be rewritten as

$$V^a(r,\Omega) \;=\; G \; \iint_{\Omega_\oplus} \int_{\xi=R+H(\Omega')}^{R+H^a} \varrho^a(\xi) \, \mathcal{N}(r,\psi,\xi) \, \xi^2 \; d\xi \; d\Omega' \;, \qquad (4.91)$$

and similarly Eqn. (4.90)

$$V^{ac}(r,\Omega) \;=\; GR^2 \; \iint_{\Omega_\oplus} \sigma^a(\Omega') \, \mathcal{N}(r,\psi,R) \, d\Omega' \;. \qquad (4.92)$$

Using the mass-conservation condensation, the surface density σ^a has a form

$$\sigma^a(\Omega') \;=\; \frac{1}{R^2} \int_{\xi=R+H(\Omega')}^{R+H^a} \varrho^a(\xi) \, \xi^2 \; d\xi \;, \qquad (4.93)$$

which also represents the straight column averaging. Similar to the topographical effects, the potential of the real atmosphere V^a can be decomposed into two parts

$$V^a(r,\Omega) \;=\; V^{as}(r,\Omega) \;+\; V^{ar}(r,\Omega) \;. \qquad (4.94)$$

V^{as} is the gravitational potential of the atmospheric shell with the lower boundary being at the point of interest at the topography, and the upper boundary H^a at some particular height with negligible atmospheric density (usually the height of 50

43

kilometres is used rendering the effect of the residual atmosphere negligible). V^{ar} is the gravitational potential of the part of the atmosphere between the topography and the lower boundary of the spherical shell. This atmospheric roughness has the maximum thickness equal to about 9 kilometres. The same treatment can be applied to the gravitational potential of the condensed atmospheric masses V^{ac} which is just a counterpart of V^a in the Helmert space:

$$V^{ac}(r,\Omega) \;=\; V^{cas}(r,\Omega) \;+\; V^{car}(r,\Omega) \,. \tag{4.95}$$

The gravitational potential of the spherical atmospheric shell is evaluated as a sum over potentials of k individual sub-shells

$$V^{as}(r,\Omega) \;=\; G \sum_{i=1}^{k} \left[\varrho_i^a \iint_{\Omega_\oplus} \int_{\xi=r_i}^{r_i+\Delta r} \mathcal{N}(r,\psi,\xi)\, \xi^2 \, d\xi \, d\Omega' \right] \,, \tag{4.96}$$

where ϱ_i^a is a constant atmospheric density within the i-th sub-shell with the lower boundary r_i and thickness Δr (unique thickness of 100 metres was used for numerical evaluations, i.e., $n = 410$). The integral in Eqn. (4.96) can be evaluated for a point of radius r as

$$V^{as}(r,\Omega) \;=\; 2\pi G \sum_{i=1}^{k} \varrho_i^a \left[(r_i + \Delta r)^2 \;-\; r_i^2 \right] \,. \tag{4.97}$$

The atmospheric roughness represents a more challenging numerical problem. While one of the bounds in the integral is a regular spherical surface, the other one is the topography known either as a discrete numerical function (elevations in the form of digital elevation models) or as a series of spherical harmonic functions. In the first case, an analytical solution in the spatial form for the gravitational potential does not exist and some numerical approximations must be deployed. The potential V^{ar} can theoretically be evaluated as

$$V^{ar}(r,\Omega) \;=\; G \iint_{\Omega_\oplus} \int_{\xi=R+H(\Omega')}^{R+H(\Omega)} \varrho^a(\xi)\, \mathcal{N}(r,\psi,\xi)\, \xi^2 \, d\xi \, d\Omega' \,, \tag{4.98}$$

with the atmospheric density ϱ^a modelled as follows, cf. Eqn. (4.88),

$$\varrho^a(\xi) \;=\; \varrho_o^a \;+\; \alpha\,(\xi - R) \;+\; \beta\,(\xi - R)^2 \,. \tag{4.99}$$

44

Substituting this model for the atmospheric density into Eqn. (4.98), the potential of the atmospheric roughness reads

$$V^{ar}(r, \Omega) = \frac{G}{2} \left[\varrho_o^a - \alpha R + \beta R^2 \right] \iint_{\Omega_\oplus} \mathcal{N}_1 \left[R + H(\Omega), \psi, R + H(\Omega') \right] d\Omega' +$$

$$+ \frac{G}{6} \left[\alpha - 2\beta R \right] \iint_{\Omega_\oplus} \mathcal{N}_2 \left[R + H(\Omega), \psi, R + H(\Omega') \right] d\Omega' +$$

$$+ \frac{G}{24} \beta \iint_{\Omega_\oplus} \mathcal{N}_3 \left[R + H(\Omega), \psi, R + H(\Omega') \right] d\Omega' , \qquad (4.100)$$

where the auxiliary integration kernels can be derived as, see Apx. (A.4),

$$\mathcal{N}_1 \left[R + H(\Omega), \psi, R + H(\Omega') \right] = \int_{\xi = R + H(\Omega')}^{R + H(\Omega)} \mathcal{N}(r, \psi, \xi) \, \xi^2 \, d\xi , \qquad (4.101)$$

$$\mathcal{N}_2 \left[R + H(\Omega), \psi, R + H(\Omega') \right] = \int_{\xi = R + H(\Omega')}^{R + H(\Omega)} \mathcal{N}(r, \psi, \xi) \, \xi^3 \, d\xi , \qquad (4.102)$$

$$\mathcal{N}_3 \left[R + H(\Omega), \psi, R + H(\Omega') \right] = \int_{\xi = R + H(\Omega')}^{R + H(\Omega)} \mathcal{N}(r, \psi, \xi) \, \xi^4 \, d\xi . \qquad (4.103)$$

Similarly, the gravitational potential of the condensed spherical atmospheric shell is computed as the sum of gravitational potentials of n condensed sub-shells

$$V^{cas}(r, \Omega) = GR^2 \sum_{i=1}^{k} \left[\sigma_i^{as} \iint_{\Omega_\oplus} \mathcal{N}(r, \psi, R) \, d\Omega' \right] , \qquad (4.104)$$

with the surface density σ_i^a being defined as, cf. Eqn. (4.13),

$$\sigma_i^{as} = \frac{\varrho_i^a}{R^2} \int_{\xi = r_i}^{r_i + \Delta r} \xi^2 \, d\xi . \qquad (4.105)$$

Having evaluated the integral in Eqn. (4.104), the following equation is obtained

$$V^{cas}(r, \Omega) = 4\pi G \frac{R^2}{R + H(\Omega)} \sum_{i=1}^{k} \sigma_i^{as} , \qquad (4.106)$$

with the condensation density equal to, see Eqn. (4.105),

$$\sigma_i^{as} = \frac{\varrho_i^a}{3 R^2} \left[(r_i + \Delta r)^3 - r_i^3 \right] . \qquad (4.107)$$

45

The potential of the condensed atmospheric roughness is expressed as follows

$$V^{car}(r, \Omega) \;=\; GR^2 \; \iint_{\Omega_\oplus} \; \sigma^{ar}(\Omega') \, \mathcal{N}(r, \psi, R) \; d\Omega' \;, \qquad (4.108)$$

with the surface density defined as follows

$$\sigma^{ar}(\Omega') \;=\; \frac{1}{R^2} \; \int_{\xi=R+H(\Omega')}^{R+H(\Omega)} \; \varrho^a(\xi) \; \xi^2 \; d\xi \;. \qquad (4.109)$$

Having defined the individual terms for the evaluation of the residual atmospheric potential, its entire value is written as

$$\delta V^a(r, \Omega) \;=\; V^{as}(r, \Omega) \;+\; V^{ar}(r, \Omega) \;-\; V^{cas}(r, \Omega) \;-\; V^{car}(r, \Omega) \;, \qquad (4.110)$$

where the radius r is equal either to $R + H$ (for the surface potential required for the derivation of the secondary indirect atmospheric effect), or to R (for the geoidal potential required for the derivation of the primary indirect atmospheric effect).

There is a direct parallelism between the quantities derived for the topographical and atmospheric masses. Both residual potentials and their effects on gravity have the same role in the process of the second Helmert condensation. However, formulae for their evaluation have to be derived independently due to the different geometric properties of masses involved in the computations.

4.5   Atmospheric effect on gravity

The direct atmospheric effect on gravity is defined as the radial derivative of the atmospheric residual potential at the point on the topography. Since the gravitation of the atmospheric shell is equal to zero [MacMillan, 1930], only three more terms have to be evaluated. The derivation of the potential of the spherical atmospheric shell on its lower boundary is justified, however, since this quantity is required for the theoretical evaluation of the secondary indirect atmospheric effect on gravity. The gravitation of the atmospheric roughness can be evaluated as the radial derivative of

the appropriate potential for $r_s = R + H(\Omega)$, see Eqn. (4.100),

$$A^{ar}(r_s,\Omega) = G \iint_{\Omega_\oplus} \frac{\partial}{\partial r} \left[\int_{\xi=R+H(\Omega')}^{R+H(\Omega)} \varrho^a(\xi) \, \mathcal{N}(r,\psi,\xi) \, \xi^2 \, d\xi \right]_{r=r_s} d\Omega' \, . \quad (4.111)$$

Using the atmospheric density from Eqn. (4.99), Eqn. (4.111) can be rewritten

$$A^{ar}(r_s,\Omega) = \frac{G}{2} \left(\varrho_o^a - \alpha R + \beta R^2 \right) \iint_{\Omega_\oplus} \mathcal{J}_1 \left[R + H(\Omega), \psi, R + H(\Omega') \right] d\Omega' +$$

$$+ \frac{G}{6} \left(\alpha - 2\beta R \right) \iint_{\Omega_\oplus} \mathcal{J}_2 \left[R + H(\Omega), \psi, R + H(\Omega') \right] d\Omega' +$$

$$+ \frac{G}{24} \beta \iint_{\Omega_\oplus} \mathcal{J}_3 \left[R + H(\Omega), \psi, R + H(\Omega') \right] d\Omega' \, . \quad (4.112)$$

Auxiliary integration kernels from this equation can be derived as, see Apx. (A.5),

$$\mathcal{J}_1 \left[R + H(\Omega), \psi, R + H(\Omega') \right] = \frac{\partial}{\partial r} \int_{\xi=R+H(\Omega')}^{R+H(\Omega)} \mathcal{N}(r,\psi,\xi) \, \xi^2 \, d\xi \bigg|_{r=r_s} , \quad (4.113)$$

$$\mathcal{J}_2 \left[R + H(\Omega), \psi, R + H(\Omega') \right] = \frac{\partial}{\partial r} \int_{\xi=R+H(\Omega')}^{R+H(\Omega)} \mathcal{N}(r,\psi,\xi) \, \xi^3 \, d\xi \bigg|_{r=r_s} , \quad (4.114)$$

$$\mathcal{J}_3 \left[R + H(\Omega), \psi, R + H(\Omega') \right] = \frac{\partial}{\partial r} \int_{\xi=R+H(\Omega')}^{R+H(\Omega)} \mathcal{N}(r,\psi,\xi) \, \xi^4 \, d\xi \bigg|_{r=r_s} . \quad (4.115)$$

The effect of the condensed atmospheric shell on gravity is, see Eqn. (4.106),

$$A^{cas}(R + H, \Omega) = -4\pi G \left[\frac{R}{R + H(\Omega)} \right]^2 \sum_{i=1}^{k} \sigma_i^{as} , \quad (4.116)$$

with the value of the surface atmospheric density, see Eqn. (4.107), being

$$\sigma_i^{as} = \left(\varrho_o^a - \alpha R + \beta R^2 \right) \frac{r_s^3(\Omega) - r_s^3(\Omega')}{3R^2} +$$

$$+ \left(\alpha - 2\beta R \right) \frac{r_s^4(\Omega) - r_s^4(\Omega')}{4R^2} + \beta \frac{r_s^5(\Omega) - r_s^5(\Omega')}{5R^2} \, . \quad (4.117)$$

47

The effect of the condensed atmospheric roughness on gravity is based on Eqn. (4.108), and can be written as follows

$$A^{car}(R+H,\Omega) \; = \; GR^2 \; \iint_{\Omega_\oplus} \; \sigma^{ar}(\Omega') \, \mathcal{J}(R+H,\psi,R) \, d\Omega' \; . \qquad (4.118)$$

The surface atmospheric density σ^{ar} has already been defined in Eqn. (4.109). The entire direct atmospheric effect on gravity is finally obtained as the sum

$$\delta A^a(R+H,\Omega) = A^{ar}(R+H,\Omega) - A^{cas}(R+H,\Omega) - A^{car}(R+H,\Omega) \; . \quad (4.119)$$

Looking closer at this formula, the first-order effect is represented by the spherical shell A^{cas}, and the second-order effect is represented by the difference

$$\delta A^{ar}(R+H,\Omega) \; = \; A^{ar}(R+H,\Omega) \; - \; A^{car}(R+H,\Omega) \; . \qquad (4.120)$$

This quantity could be called a *terrain correction to the direct atmospheric effect on gravity* because it originates in the roughness of the topography (terrain). Due to the magnitude of the atmospheric density, its values are small when compared to the topographical terrain correction.

Theoretically, all integrals should once again be evaluated over the full spatial angle. Since the magnitude of all atmospheric effects is significantly lower compared to the topographical effects, no attempt was made to evaluate effects of distant zones. If necessary, a spectral method and some global elevation model could be used for its effect on the atmospheric terrain correction.

4.6   Downward continuation of gravity

The last step in the gravity reduction consists of the downward continuation of gravity data from the topography to the co-geoid. Its role was briefly explained in Sec. (3.1) where basic formulations were also introduced. The proper formulation of the entire problem is now in place.

Using the second Helmert condensation, harmonic gravity data are derived on the topography. However, for the solution of the Stokes problem their values on the co-geoid are required. The mathematical formulation of the problem is based on the first boundary-value problem of potential theory which consists of the Laplace equation

$$\forall \, r \, > \, r_c \, : \, \nabla^2 \, \Big[\, r \, \Delta g^h(r, \Omega) \, \Big] \; = \; 0 \; , \tag{4.121}$$

with the following boundary condition defined on the co-geoid, see Eqn. (3.57),

$$\forall \, r \, = \, r_c \, : \, r \, \Delta g^h(r, \Omega) \; = \; - \, 2 \, T^h(r, \Omega) \; - \; r \, \left. \frac{\partial T^h(r, \Omega)}{\partial r} \right|_r \; , \tag{4.122}$$

and the asymptotic condition at infinity

$$\lim_{r \, \to \, \infty} \, \Delta g^h(r, \Omega) \; = \; 0 \; . \tag{4.123}$$

This problem solves for functional values of Δg^h everywhere outside the co-geoid and is sometimes called the upward continuation of a harmonic function. Its solution is given by the Poisson integral [Kellogg, 1929]

$$\forall \, r \, \geq \, r_c \, : \, r \, \Delta g^h(r, \Omega) \; \doteq \; \frac{1}{4\pi} \, \iint_{\Omega_\oplus} r_c \, \Delta g^h(r_c, \Omega') \, \mathcal{P}(r, \psi, r_c) \, d\Omega' \; , \tag{4.124}$$

with the Poisson kernel defined as follows [ibid]

$$\mathcal{P}(r, \psi, r_c) \; = \; r_c \, \Big(\, r^2 \, - \, r_c^2 \, \Big) \, \mathcal{N}^3(r, \psi, r_c) \; , \tag{4.125}$$

which has, using the spherical approximation ($r_c = R$), the following spectral form

$$\mathcal{P}(r, \psi, R) \; = \; \sum_{n=0}^{\infty} \, (2n + 1) \, \left(\frac{R}{r} \right)^{n+1} \, P_n(\cos \psi) \; . \tag{4.126}$$

Obviously, the inverse of this problem is the downward continuation of gravity.

Chapter 5

Helmert's Residual Gravity

Terrestrial gravity data, due to their incomplete distribution, cannot be used for computing the low-frequency features of the gravity field. A method for combining the satellite-derived and terrestrial gravity data was briefly introduced in Sec. (3.2). The major topic of this chapter is the derivation of the Helmert residual gravity anomaly on the co-geoid which is used for the solution of the generalized Stokes-Helmert problem.

In the first section, the reference part of the residual topographical potential on the co-geoid is derived in the spectral domain and the spherical harmonic representation of the global topography. Its counterpart for the residual atmospheric potential is formulated in the second section using a simplified model of the atmospheric density function. The spectral method and spherical harmonic representation of the global topography are also deployed in these derivations.

Based on these two potentials, the reference components of all topographical and atmospheric effects on gravity are derived in the last section. They are subsequently used for the derivation of the Helmert residual gravity anomaly on the co-geoid which could be used for the determination of the Helmert residual co-geoid. The residual primary indirect effects, required for the transformation of the Helmert residual co-geoid into the real space, are included at the end of this section.

5.1 Reference topographical potentials

The gravitational potential of the actual topographical masses on the co-geoid, see Eqn. (4.4), can be written in the spectral form as follows

$$V^t(r_c, \Omega) \; = \; G \, \varrho_o^t \, r_c \, \sum_{n=0}^{\infty} \iint_{\Omega_\oplus} P_n(\cos \psi) \int_{\xi=R}^{R+H(\Omega')} \left(\frac{\xi}{r_c} \right)^{n+2} d\xi \, d\Omega' \; , \quad (5.1)$$

with Newton's kernel, see Eqn. (4.1),

$$\mathcal{N}(r_c, \psi, \xi) \; = \; \frac{1}{r_c} \sum_{n=0}^{\infty} \left(\frac{\xi}{r_c} \right)^{n} P_n(\cos \psi) \; . \quad (5.2)$$

Equation (5.1) can be rewritten as [Vaníček et al., 1995]

$$V^t(r_c, \Omega) \; = \; GR^2 \, \varrho_o^t \, \sum_{n=0}^{\infty} \left(\frac{R}{r_c} \right)^{n+1} \frac{1}{n+3} \; \times$$

$$\sum_{k=1}^{n+3} \binom{n+3}{k} \iint_{\Omega_\oplus} \left[\frac{H(\Omega')}{R} \right]^{k} P_n(\cos \psi) \, d\Omega' \; . \quad (5.3)$$

Assuming the mass-conservation condensation of topographical masses, see Eqn. (4.6), the spectral form of the gravitational potential of the condensed topography, see Eqn. (4.5), can be written as

$$V^{ct}(r_c, \Omega) \; = \; GR \, \sum_{n=0}^{\infty} \left(\frac{R}{r_c} \right)^{n+1} \iint_{\Omega_\oplus} \sigma^t(\Omega') \, P_n(\cos \psi) \, d\Omega' \; . \quad (5.4)$$

The residual topographical potential can be obtained by differencing [ibid]

$$\delta V^t(r_c, \Omega) = GR^2 \, \varrho_o^t \, \sum_{n=0}^{\infty} \left(\frac{R}{r_c} \right)^{n+1} \left\{ \frac{1}{n+3} \sum_{k=1}^{n+3} \binom{n+3}{k} \iint_{\Omega_\oplus} \zeta^k(\Omega') \times \right.$$

$$\left. P_n(\cos \psi) \, d\Omega' - \iint_{\Omega_\oplus} \zeta(\Omega') \left[1 + \zeta(\Omega') + \frac{\zeta^2(\Omega')}{3} \right] P_n(\cos \psi) \, d\Omega' \right\} \; , \quad (5.5)$$

with the unitless parameter ζ defined as follows

$$\zeta(\Omega') \; = \; \frac{H(\Omega')}{R} \; . \quad (5.6)$$

51

Investigating the behavior of the summation over k, it can be shown that this series converges very fast and only the first three terms need to be used [Vaníček et al., 1995]. After few algebraic operations, the following formula can be derived [ibid]

$$\delta V^t(r_c, \Omega) \doteq GR^2 \, \varrho_o^t \, \sum_{n=1}^{\infty} \frac{n}{2} \left(\frac{R}{r_c} \right)^{n+1} \left\{ \iint_{\Omega_{\oplus}} \zeta^2(\Omega') \times \right.$$

$$\left. P_n(\cos\psi) \, d\Omega' \; + \; \frac{n+3}{3} \iint_{\Omega_{\oplus}} \zeta^3(\Omega') \, P_n(\cos\psi) \, d\Omega' \right\} . \tag{5.7}$$

Its reference (low-frequency) part then reads

$$\delta V_{\ell}^t(r_c, \Omega) \doteq 2\pi G \, \varrho_o^t \, \sum_{n=1}^{\ell} \frac{n}{2n+1} \left(\frac{R}{r_c} \right)^{n+1} H_n^2(\Omega) \; +$$

$$2\pi G \, \frac{\varrho_o^t}{3R} \, \sum_{n=1}^{\ell} \frac{n \, (n+3)}{2n+1} \left(\frac{R}{r_c} \right)^{n+1} H_n^3(\Omega) \, , \tag{5.8}$$

which can be written as

$$\delta V_{\ell}^t(r_c, \Omega) \; = \; \frac{GM}{a'} \, \sum_{n=1}^{\ell} \left(\frac{a'}{r_c} \right)^{n+1} \delta V_n^t(\Omega) \, . \tag{5.9}$$

The coefficients of this spherical harmonic series are given as follows ($\forall \, n = 1 \, \ldots \, \ell$)

$$\delta V_n^t(\Omega) \doteq \frac{2\pi}{M} \, \varrho_o^t \, \frac{n}{2n+1} \left(\frac{R}{a'} \right)^n \left[R \, H_n^2(\Omega) \; + \; (n+3) \, \frac{H_n^3(\Omega)}{3} \right] . \tag{5.10}$$

Zonal coefficients for the spherical harmonic representation of squared heights H^2 can be computed from the global elevation model using Eqn. (4.55), and the same for cubed heights H^3

$$\forall \, n \; = \; 0 \, \ldots \, \ell \; : \; H_n^3(\Omega) \; = \; \sum_{m=-n}^{n} H_{n,m}^3 \, Y_{n,m}(\Omega) \, . \tag{5.11}$$

Equation (5.9) should be evaluated on the co-geoid. Since this surface is unknown, an appropriate approximation has to be introduced. The vertical separation of the co-geoid above the geoid is about 2 metres at most. Therefore the co-geoid can also be approximated by the reference ellipsoid, see Eqn. (2.10),

$$r_c(\Omega) \doteq r_e(\varphi) \; = \; a' \, (1 - f \, \sin^2 \varphi) \; + \; \mathcal{O}(f^2) \, . \tag{5.12}$$

Then the radial term in Eqn. (5.9) changes into [Vaníček et al., 1995]

$$\forall\, n \;=\; 1 \;\ldots\; \ell \;:\; \left(\frac{a'}{r_c} \right)^{n+1} \;\doteq\; 1 \;+\; (n+1)\, f \;\sin^2\varphi\;.$$ (5.13)

Hence, the ellipsoidal approximation of Eqn. (5.9) is

$$\delta V_\ell^t(r_c,\Omega) \;=\; \frac{GM}{a'} \; \sum_{n=1}^{\ell} \; \Big[\; 1 \;+\; (n+1)\, f\; \sin^2\varphi \;\Big] \; \delta V_n^t(\Omega)\;.$$ (5.14)

5.2 Reference atmospheric potentials

The laterally-symmetrical atmospheric density model, see Eqn. (4.87),

$$\forall\, \nu \;>\; 2 \;:\; \varrho^a(\xi) \;=\; \varrho_o^a \; \left(\frac{R}{R+\xi} \right)^\nu \;,$$ (5.15)

and the mass-conservation condensation density selected as follows

$$\sigma^a(\Omega) \;=\; \frac{1}{R^2} \; \int_{\xi=R+H(\Omega)}^{R+H^a} \; \varrho^a(\xi)\, \xi^2 \; d\xi\;,$$ (5.16)

are employed in following derivations. To keep the new formulae consistent with previous derivations, the same upper limit of the atmosphere is used. This upper boundary could eventually be put equal to infinity. The use of the finite value yields, however, identical results. The potential of atmospheric masses V^a can be rewritten in the spectral form as follows

$$V^a(r_c,\Omega) = G \sum_{n=0}^{\infty} \; r_c^{-n-1} \iint_{\Omega_\oplus} P_n(\cos\psi) \int_{\xi=R+H(\Omega')}^{R+H^a} \varrho^a(\xi)\, \xi^{n+2} \; d\xi \; d\Omega'\;.$$ (5.17)

The integral over ξ is evaluated using the model density from Eqn. (5.15)

$$\int_{\xi=R+H(\Omega')}^{R+H^a} \varrho^a(\xi)\, \xi^{n+2} \; d\xi \;=\; \varrho_o^a \; \int_{\xi=R+H(\Omega')}^{R+H^a} \xi^{n+2} \left(\frac{R}{\xi} \right)^\nu \; d\xi\;,$$ (5.18)

and then substituted into Eqn. (5.17)

$$V^a(r_c,\Omega) = GR^\nu \varrho_o^a \sum_{n=0}^{\infty} \; r_c^{-n-1} \iint_{\Omega_\oplus} \left\{ \frac{\xi^{n-\nu+3}}{n-\nu+3} \right\}_{\xi=R+H(\Omega')}^{R+H^a} P_n(\cos\psi) \; d\Omega'\;.$$ (5.19)

For the numerical evaluation of the potential V^a, the binomial theorem can be used

$$\left\{ \frac{\xi^{n-\nu+3}}{n-\nu+3} \right\}_{\xi=R+H(\Omega')}^{R+H^a} = \left\{ \frac{(R+\xi)^{n-\nu+3}}{n-\nu+3} \right\}_{\xi=H(\Omega')}^{H^a} =$$

$$= \frac{R^{n-\nu+3}}{n-\nu+3} \sum_{k=1}^{n-\nu+3} \binom{n-\nu+3}{k} \left\{ \left(\frac{H^a}{R} \right)^k - \left[\frac{H(\Omega')}{R} \right]^k \right\} . \quad (5.20)$$

This series converges fast, and only its first three terms have to be taken into account.

For the evaluation of the potential V^{ca}, the condensation density must be evaluated first. It can be written

$$\sigma^a(\Omega') = \frac{\varrho_o^a}{R^2} \int_{\xi=R+H(\Omega')}^{R+H^a} \left(\frac{R}{\xi} \right)^\nu \xi^2 \, d\xi . \quad (5.21)$$

The gravitational potential V^{ca} of the condensed atmosphere then reads

$$V^{ca}(r_c, \Omega) \doteq \frac{G\varrho_o^a}{R^{1-\nu}} \sum_{n=0}^\infty \left(\frac{R}{r_c} \right)^{n+1} \iint_{\Omega_\oplus} \left\{ \frac{\xi^{3-\nu}}{3-\nu} \right\}_{\xi=R+H(\Omega')}^{R+H^a} P_n(\cos\psi) \, d\Omega' . \quad (5.22)$$

For the numerical evaluation, the binomial theorem is used once again

$$\sigma^a(\Omega') = \varrho_o^a \frac{R}{3-\nu} \sum_{k=1}^{3-\nu} \binom{3-\nu}{k} \left\{ \left(\frac{H^a}{R} \right)^k - \left[\frac{H(\Omega')}{R} \right]^k \right\} . \quad (5.23)$$

The residual potential is then obtained as the difference of the potential V^a and V^{ca}

$$\delta V_\ell^a(r_c, \Omega) \doteq GR^2 \varrho_o^a \sum_{n=1}^\ell \frac{n}{2} \left(\frac{R}{r_c} \right)^{n+1} \iint_{\Omega_\oplus} \left\{ \frac{(H^a)^2 - H(\Omega')^2}{R^2} + \right.$$

$$\left. + (n-2\nu+3) \frac{(H^a)^3 - H(\Omega')^3}{3R^3} \right\} P_n(\cos\psi) \, d\Omega' , \quad (5.24)$$

which can be written as

$$\delta V_\ell^a(r_c, \Omega) \doteq -2\pi G \varrho_o^a \sum_{n=1}^\ell \frac{n}{2n+1} \left(\frac{R}{r_c} \right)^{n+1} H_n^2(\Omega) -$$

$$- 2\pi G \frac{\varrho_o^a}{3R} \sum_{n=1}^\ell \frac{n(n-2\nu+3)}{2n+1} \left(\frac{R}{r_c} \right)^{n+1} H_n^3(\Omega) . \quad (5.25)$$

54

Introducing the following form

$$\delta V_{\ell}^a(r_c, \Omega) = \frac{GM}{a'} \sum_{n=1}^{\ell} \left(\frac{a'}{r_c} \right)^{n+1} \delta V_n^a(\Omega) , \qquad (5.26)$$

the coefficients of this spherical harmonic series are given as follows ($\forall n = 1 \ \ldots \ \ell$)

$$\delta V_n^a(\Omega) \doteq - 2\pi \frac{\varrho_o^a}{M} \frac{n}{2n+1} \left(\frac{R}{a'} \right)^n \left[R H_n^2(\Omega) + (n - 2\nu + 3) \frac{H_n^3(\Omega)}{3} \right] . \quad (5.27)$$

The ellipsoidal approximation of the combined residual potential then reads

$$\delta V_{\ell}(r_c, \Omega) = \frac{GM}{a'} \sum_{n=1}^{\ell} \left(\frac{a'}{r_c} \right)^{n+1} \left[\delta V_n^t(\Omega) + \delta V_n^a(\Omega) \right] \doteq$$

$$\doteq \frac{GM}{a'} \sum_{n=1}^{\ell} \left[1 + (n+1) f \sin^2 \varphi \right] \delta V_n(\Omega) , \qquad (5.28)$$

with coefficients of the spherical harmonic series

$$\forall n = 1 \ \ldots \ \ell : \ \delta V_n(\Omega) \doteq 2\pi \frac{R}{M} \left(\varrho_o^t - \varrho_o^a \right) \frac{n}{2n+1} \left(\frac{R}{a'} \right)^n H_n^2(\Omega) +$$

$$+ \frac{2\pi}{3M} \frac{n}{2n+1} \left[(n+3) \left(\varrho_o^t - \varrho_o^a \right) + 2\nu \ \varrho_o^a \right] \left(\frac{R}{a'} \right)^n H_n^3(\Omega) . \qquad (5.29)$$

5.3 Helmert's residual gravity anomaly

In this section, the derivation of Helmert's residual gravity anomaly is summarized. Surface values of the Helmert gravity anomaly were defined in Eqn. (3.27) as

$$\Delta g^h(r_s, \Omega) \doteq \Delta g^f(\Omega) + \delta A(r_s, \Omega) + \delta S(r_s, \Omega) + \delta S^{\xi}(r_s, \Omega) , \qquad (5.30)$$

with the free-air gravity anomaly Δg^f given by Eqn. (3.21). The values of the Helmert gravity anomaly on the co-geoid can be obtained using the downward continuation of gravity, see Eqn. (3.34),

$$\Delta g^h(r_c, \Omega) = \Delta g^h(r_s, \Omega) + D\Delta g^h(\Omega) . \qquad (5.31)$$

The Helmert residual gravity anomaly then reads

$$\Delta g^{h,\ell}(r_c, \Omega) \;=\; \Delta g^h(r_c, \Omega) \;-\; \Delta g^h_\ell(r_c, \Omega) \;, \tag{5.32}$$

with the reference part defined as follows

$$\Delta g^h_\ell(r_c, \Omega) \;\doteq\; \Delta g^f_\ell(r_c, \Omega) \;+\; \delta A_\ell(r_c, \Omega) \;+\; \delta S_\ell(r_c, \Omega) \;+\; \delta S^\xi_\ell(r_c, \Omega) \;. \tag{5.33}$$

The reference free-air gravity anomaly can be obtained as follows

$$\Delta g^f_\ell(r_c, \Omega) \;=\; \frac{GM}{r_c^2} \sum_{n=2}^{\ell} (n-1) \left(\frac{a'}{r_c} \right)^n T_n(\Omega) \;. \tag{5.34}$$

The reference combined direct effect on gravity reads

$$\delta A_\ell(r_c, \Omega) \;=\; -\frac{GM}{r_c^2} \sum_{n=1}^{\ell} (n+1) \left(\frac{a'}{r_c} \right)^n \delta V_n(\Omega) \;, \tag{5.35}$$

and the reference combined secondary indirect effect on gravity is

$$\delta S_\ell(r_c, \Omega) \;=\; -2 \frac{GM}{r_c^2} \sum_{n=1}^{\ell} \left(\frac{a'}{r_c} \right)^n \delta V_n(\Omega) \;. \tag{5.36}$$

The reference quasigeoid-to-geoid correction is defined as

$$\delta S^\xi_\ell(r_c, \Omega) = 2 \frac{GM}{r_c^3} H(\Omega) \sum_{n=1}^{\ell} (n-1) \left(\frac{a'}{r_c} \right)^n T_n(\Omega) - 4\pi G \, \varrho^t_o \, \frac{H^2(\Omega)}{R} \;. \tag{5.37}$$

The reference component of Helmert's gravity anomaly is then equal to

$$\Delta g^h_\ell(r_c, \Omega) \;=\; \frac{GM}{r_c^2} \sum_{n=1}^{\ell} \left(\frac{a'}{r_c} \right)^n g^h_n(\Omega) \;-\; 4\pi G \, \varrho^t_o \, \frac{H^2(\Omega)}{R} \;, \tag{5.38}$$

with the coefficients of the spherical harmonic series given as follows

$$\forall \, n \; \geq \; 1 \; : \; g^h_n(\Omega) \;\doteq\; (n-1) \, T_n(\Omega) \left[1 + \frac{2H(\Omega)}{R} \right] - (n+3) \, \delta V_n(\Omega) \;. \tag{5.39}$$

The residual primary indirect topographical effect on the geoid, required for the transformation of the Helmert residual geoid into the real space, can be computed

$$\delta N^{t,\ell}(\Omega) \;=\; \frac{\delta V^t(r_c, \Omega) \;-\; \delta V^t_\ell(r_c, \Omega)}{\gamma(r_e, \varphi)} \;, \tag{5.40}$$

and the residual primary indirect atmospheric effect on the geoid

$$\delta N^{a,\ell}(\Omega) \;=\; \frac{\delta V^a(r_c, \Omega) \;-\; \delta V^a_\ell(r_c, \Omega)}{\gamma(r_e, \varphi)} \;. \tag{5.41}$$

Chapter 6

Helmert's Residual Geoid

Converting the original free boundary-value problem to the problem with some fixed boundary, the unknown values of the disturbing gravity potential can be determined uniquely. An appropriate form of the Stokes integration kernel depends on the shape of the boundary surface. The modified spheroidal Stokes kernel (spherical Stokes's kernel degenerates into the spheroidal one when residual gravity data are deployed) is used in this chapter for the evaluation of the Helmert residual geoid.

There are several problems with the numerical evaluation of the Stokes integration which have to be first accounted for. The most serious one is the lack of global coverage of suitable surface gravity data which does not allow for a global integration. The solution is usually sought over some limited integration domain and the effect of the neglected distant gravity data is accounted for by using global models, see Fig. (7.2).

There are different approaches to the evaluation of the Stokes integral over the limited domain, and different treatments of the singularity of the Stokes kernel for spherical distance equal to zero. Generally, the solution can be obtained either using the discrete numerical integration or converting the convolution integral from the space domain into the frequency domain, and back again. The discrete numerical integration is used in this chapter only.

6.1   Modified spheroidal Stokes's function

To account for the incomplete gravity data coverage, the integration domain for the Stokes integral is divided into the near zone $\Omega_{\odot}$ (spherical cap of radius ψ_o) and the distant zone $\Omega_{\oplus} - \Omega_{\odot}$, where the omitted gravity data effect is taken into account using a global gravity model. Because of significant differences between available geopotential models [Najafi, 1996], one should try to keep the contribution of the distant zone as small as possible. This can be done by modifying the integration kernel.

Several modifications for the original spherical Stokes function have been derived. For instance, a modification introduced by [Vaníček and Sjöberg, 1991] gives the following *modified spheroidal Stokes function* [ibid]

$$\mathcal{S}^{\ell}(\psi, \psi_o) \; = \; \mathcal{S}^{\ell}(\psi) \; - \; \sum_{n=2}^{\ell} \frac{2n+1}{2} \; t_n(\psi_o) \; P_n(\cos \psi) \; . \tag{6.1}$$

Substituting the spheroidal Stokes function $\mathcal{S}^{\ell}$ from Eqn. (3.62), one gets

$$\mathcal{S}^{\ell}(\psi, \psi_o) \; = \; \mathcal{S}(\psi) - \sum_{n=2}^{\ell} \frac{2n+1}{n-1} \; P_n(\cos \psi) - \sum_{n=2}^{\ell} \frac{2n+1}{2} \; t_n(\psi_o) \; P_n(\cos \psi) \; . \tag{6.2}$$

Searching for the minimum effect of the distant zone, it can be shown that

$$\forall \, t_n \; \in \; \mathrm{I\!R}^n \; : \; \min_{t_n} \left\{ \iint_{\Omega_{\oplus} - \Omega_{\odot}} \Delta g^{\ell}(r_c, \Omega^{'}) \; S^{\ell}(\psi, \psi_o) \; d\Omega^{'} \right\} \; =$$

$$= \; \min_{t_n} \left\{ \iint_{\Omega_{\oplus} - \Omega_{\odot}} \left[\, S^{\ell}(\psi, \psi_o) \, \right]^2 d\Omega^{'} \right\} \; , \tag{6.3}$$

and the modification coefficients t_n can then be solved for using the following system of linear equations [ibid]

$$\forall \, m \; \leq \; \ell \; : \; \sum_{n=2}^{\ell} \frac{2n+1}{2} \; R_{n,m}(\psi_o) \; t_n(\psi_o) \; = \; Q_m^{\ell}(\psi_o) \; . \tag{6.4}$$

The coefficients $R_{n,m}(\psi_o)$ were introduced by [Paul, 1973]

$$\forall \, m \; \leq \; n \; : \; R_{n,m}(\psi_o) \; = \; \int_{\psi=\psi_o}^{\pi} P_n(\cos \psi) \; P_m(\cos \psi) \; \sin \psi \; d\psi \; . \tag{6.5}$$

Molodenskij's truncation coefficients for the spheroidal Stokes function in Eqn. (6.4) can be evaluated as [Molodenskij et al., 1960]

$$\forall \; m \; \leq \; \ell \; : \; Q^\ell_m(\psi_o) \; = \; \int_{\psi=\psi_o}^{\pi} \; \mathcal{S}^\ell(\psi) \; P_m(\cos \psi) \; \sin \psi \; d\psi \; . \tag{6.6}$$

6.2 Contribution of the near zone

The Helmert residual geoid, see Eqn. (3.51), can be written as

$$N^{h,\ell}(\Omega) \; = \; N^{h,\ell}_\odot(\Omega) \; + \; N^{h,\ell}_{\oplus-\odot}(\Omega) \; . \tag{6.7}$$

The contribution of the near zone to Helmert's residual geoid reads

$$N^{h,\ell}_\odot(\Omega) \; = \; \frac{R}{4\pi\gamma(r_e,\varphi)} \; \iint_{\Omega_\odot} \Delta g^{h,\ell}(r_c,\Omega') \; \mathcal{S}^\ell(\psi,\psi_o) \; d\Omega' \; . \tag{6.8}$$

This integral is weakly singular for the spherical distance $\psi = 0°$. A classical method for treating a removable singularity consists of adding and subtracting a value of the gravity anomaly at the singular point to obtain

$$N^{h,\ell}_\odot(\Omega) \; = \; \frac{R}{4\pi\gamma(r_e,\varphi)} \; \iint_{\Omega_\odot} \left[\; \Delta g^{h,\ell}(r_c,\Omega') - \Delta g^{h,\ell}(r_c,\Omega) \; \right] \; \mathcal{S}^\ell(\psi,\psi_o) \; d\Omega' \; +$$

$$+ \; \frac{R}{4\pi\gamma(r_e,\varphi)} \; \Delta g^{h,\ell}(r_c,\Omega) \; \iint_{\Omega_\odot} \mathcal{S}^\ell(\psi,\psi_o) \; d\Omega' \; . \tag{6.9}$$

The second integral in Eqn. (6.9) can be evaluated analytically. It can be written as a sum [Martinec, 1993]

$$\int_{\psi=0}^{\psi_o} \mathcal{S}^\ell(\psi,\psi_o) \; d\Omega' \; = \; \int_{\psi=0}^{\psi_o} \; \mathcal{S}(\psi) \; \sin \psi \; d\psi \; -$$

$$- \; \sum_{n=2}^{\ell} \frac{2n+1}{n-1} \int_{\psi=0}^{\psi_o} \; P_n(\cos \psi) \; \sin \psi \; d\psi \; -$$

$$- \; \sum_{n=2}^{\ell} \frac{2n+1}{2} \; t_n(\psi_o) \int_{\psi=0}^{\psi_o} \; P_n(\cos \psi) \; \sin \psi \; d\psi \; . \tag{6.10}$$

The solution of this integral is attempted in terms of quantities which were already defined. The zero-degree truncation coefficient is given as [Molodenskij et al., 1960]

$$Q_0(\psi_o) = -4w + 5w^2 + 6w^3 - 7w^4 + 6w^2(1-w^2) \ln(w+w^2) , \quad (6.11)$$

with the following parameter

$$w = \sin\frac{\psi_o}{2} , \quad (6.12)$$

and the Paul function [Paul, 1973]

$$\forall\; n \;\geq\; 2 \;:\; R_{n,0}(\psi_o) \;=\; \frac{P_{n+1}(\cos\psi_o) \;-\; P_{n-1}(\cos\psi_o)}{2n+1} \quad . \quad (6.13)$$

The integral on the left-hand side of Eqn. (6.10) is then derived as [Martinec, 1993]

$$\int_{\psi=0}^{\psi_o} \mathcal{S}^\ell(\psi,\psi_o)\, d\Omega' = -Q_0^\ell(\psi_o) + \sum_{n=2}^{\ell} \frac{2n+1}{2}\, t_n(\psi_o)\, R_{n,0}(\psi_o) - t_0(\psi_o) . \quad (6.14)$$

The singularity contribution to the geoidal height is then given by [ibid]

$$N_s^{h,\ell}(\Omega) = \frac{R\,\Delta g^{h,\ell}(r_c,\Omega)}{4\pi\gamma(r_e,\varphi)} \left[2\pi \int_{\psi=0}^{\psi_o} \mathcal{S}^\ell(\psi,\psi_o)\, d\Omega' \right] =$$

$$= -\frac{R\,\Delta g^{h,\ell}(r_c,\Omega)}{2\,\gamma(r_e,\varphi)} \left[Q_0^\ell(\psi_o) - \sum_{n=2}^{\ell} \frac{2n+1}{2}\, t_n(\psi_o)\, R_{n,0}(\psi_o) + t_0(\psi_o) \right] . \quad (6.15)$$

The contribution of the rest of the cap can be evaluated by the discrete summation over mean values of gravity anomalies within the cap [Heiskanen and Moritz, 1967]

$$N_\odot^{h,\ell}(\Omega) = \frac{R}{4\pi\gamma(r_e,\varphi)} \iint_{\Omega_\odot} \left[\Delta g^{h,\ell}(r_c,\Omega') - \Delta g^{h,\ell}(r_c,\Omega) \right] \mathcal{S}^\ell(\psi,\psi_o)\, d\Omega' =$$

$$= \frac{R}{4\pi\gamma(r_e,\varphi)} \sum_{k}^{j-1} \left\{ \iint_{\Omega_k} \left[\Delta g^{h,\ell}(r_c,\Omega') - \Delta g^{h,\ell}(r_c,\Omega) \right] \mathcal{S}^\ell(\psi,\psi_o)\, d\Omega' \right\} =$$

$$= \frac{R}{4\pi\gamma(r_e,\varphi)} \sum_{k}^{j-1} \left[\overline{\Delta g^{h,\ell}}(r_c,\Omega_k) - \overline{\Delta g^{h,\ell}}(r_c,\Omega) \right] \mathcal{S}^\ell(\psi_k,\psi_o)\, \Delta\Omega_k . \quad (6.16)$$

According to the mean value theorem, the integration was replaced by the summation over $(j-1)$ cells within the spherical cap of the product of discrete mean values of gravity anomalies [Vaníček and Krakiwsky, 1986]

$$\overline{\Delta g^{h,\ell}}(r_c, \Omega_k) \;=\; \frac{1}{\Delta \Omega_k} \iint_{\Omega_k} \Delta g^{h,\ell}(r_c, \Omega') \, d\Omega' \; , \tag{6.17}$$

with point values of the modified spheroidal Stokes function defined for a spherical distance ψ_k. This unknown value is approximated by a spherical distance between the integration point and the centre of the k-th cell. $\Delta \Omega_k$ is the area of the k-th cell. A regular geographical grid is usually used in numerical evaluations.

An alternative approach to the discrete numerical integration is represented by the solution in the spectral domain which is based on the convolution theorem. The discrete one-dimensional Fourier transform applied to mean gravity data within the spherical cap $\Omega_\odot$ can be written ($\forall \, \varphi = \varphi_k$) as follows [Schwarz et al., 1990]

$$N_\odot^\ell(\Omega) \doteq \frac{R}{4\pi\gamma(r_e, \varphi)} \, \mathcal{F}^{-1} \left\{ \sum_{k=1}^{j} \mathcal{F}\left[\overline{\Delta g^\ell}(\Omega_k) \, \cos\varphi_k \right] \mathcal{F}\left[\mathcal{S}^\ell(\psi_k, \psi_o) \right] \right\} \; , \tag{6.18}$$

where $\mathcal{F}$ and $\mathcal{F}^{-1}$ stand for the one-dimensional Fourier transform operator and its inverse, respectively. When applied correctly to the same gravity data, both the spatial and spectral method produce identical solutions for geoidal heights. Concerning their numerical efficiency, it has been argued for a long time that the discrete Fourier transform is computationally superior to the discrete numerical integration. Due to the latest developments in the discrete numerical integration (due to the independence of the Stokes kernel on longitude, and the symmetry along the central meridian, only half of the kernel values are computed for each parallel) [Huang and Vaníček, 1999], both methods use comparable amount of time. Moreover, the simplicity of the spatial integration might be important for computer realization.

6.3 Contribution of the distant zone

The influence of the distant zone on the Stokes integration has been derived by several authors. An approach derived by [Molodenskij et al., 1960] which uses the so-called Molodenskij coefficients (weights) to account for the influence of distant gravity data is used here. These coefficients for the original Stokes function read as follows

$$\forall n \geq 2 \ : \ Q_n(\psi_o) \ = \ \int_{\psi=\psi_o}^{\pi} \ \mathcal{S}(\psi) \ P_n(\cos \psi) \ \sin \psi \ d\psi \ . \tag{6.19}$$

Molodenskij coefficients for the modified spheroidal Stokes function are expressed analogously as

$$\forall n \geq 2 \ : \ \tilde{Q}_n^{\ell}(\psi_o) \ = \ \int_{\psi=\psi_o}^{\pi} \ \mathcal{S}^{\ell}(\psi, \psi_o) \ P_n(\cos \psi) \ \sin \psi \ d\psi \ . \tag{6.20}$$

The truncation coefficients $Q_n(\psi_o)$ and $\tilde{Q}_n^{\ell}(\psi_o)$ are related through [Martinec, 1993]

$$\forall n \geq 2 \ : \ \tilde{Q}_n^{\ell}(\psi_o) \ = \ Q_n^{\ell}(\psi_o) \ - \ \sum_{n=2}^{\ell} \frac{2n+1}{2} \ t_n(\psi_o) \ R_{n,m}(\psi_o) \ =$$

$$= \ Q_n(\psi_o) \ - \ \sum_{n=2}^{\ell} \frac{2n+1}{n-1} \ R_{n,m}(\psi_o) \ - \ \sum_{n=2}^{\ell} \frac{2n+1}{2} \ t_n(\psi_o) \ R_{n,m}(\psi_o) \ . \tag{6.21}$$

Minimizing the norm (6.3) in the least-squares sense with respect to the truncation coefficients results in the following normal equations

$$\forall n \leq \ell \ : \ \tilde{Q}_n^{\ell}(\psi_o) \ = \ 0 \ , \tag{6.22}$$

and the contribution of the distant zone to the geoidal height can be evaluated using

$$N_{\oplus-\odot}^{h,\ell}(\Omega) \ = \ \frac{R}{2} \ \sum_{n=\ell+1}^{120} \ (n-1) \ \tilde{Q}_n^{\ell}(\psi_o) \ T_n^{h}(\Omega) \ , \tag{6.23}$$

with the spherical harmonic coefficients of the Helmert disturbing gravity potential T_n^{h} usually replaced by the coefficients T_n taken from a global geopotential model. The maximum degree equal to 120 is usually used for numerical evaluations rendering the effect of higher-degree terms smaller a one millimetre [Martinec, 1993].

The Stokes integral for the Helmert residual geoid can be written as a sum

$$N^{h,\ell}(\Omega) \; = \; N^{h,\ell}_{\odot}(\Omega) \; + \; N^{h,\ell}_{s}(\Omega) \; + \; N^{h,\ell}_{\oplus-\odot}(\Omega) \; =$$

$$= \; \frac{R}{4\pi\gamma(r_e,\varphi)} \; \sum_{k}^{j-1} \; \Big[\; \overline{\Delta g^{h,\ell}}(r_c,\Omega_k) - \overline{\Delta g^{h,\ell}}(r_c,\Omega) \; \Big] \; \mathcal{S}^{\ell}(\psi_k,\psi_o) \; \Delta\Omega_k \; -$$

$$- \; \frac{R \; \Delta g^{h,\ell}(r_c,\Omega)}{2 \; \gamma(r_e,\varphi)} \; \Big[\; \tilde{Q}^{\ell}_0(\psi_o) + t_0(\psi_o) \; \Big] + \frac{R}{2} \sum_{n=\ell+1}^{120} \; (n-1) \; \tilde{Q}^{\ell}_n(\psi_o) \; T^{h}_n(\Omega) \; , \quad (6.24)$$

where the epicentre contribution was reformulated into a simplified form.

6.4 Accuracy of Stokes's integration

Over the Canadian territory, mean gravity data on a $5'$ regular grid, prepared by the Geodetic Survey Division of Natural Resources Canada, are usually used for the determination of the residual gravimetric geoid. The corresponding Nyquist frequency for the spectral representation of the gravity field is equal to 2160. A simple procedure was developed to test the numerical accuracy of the discrete Stokes integration described above. Since available global models contain coefficients only up to degree and order 360, synthetic higher-degree coefficients had to be generated. An approach developed at the Curtin University of Technology, Perth, is used here.

Coefficients of the latest global model EGM96 [Lemoine et al., 1996] correspond to the spherical harmonic expansion of the gravity potential on the sphere of fixed radius a. To generate the synthetic higher-degree coefficients, a Kaula-kind decaying degree variance is most easily obtained by rescaling the given coefficients to a smaller sphere of radius b and their "recycling" for the higher-degree coefficients using a factor of $(b/a)^{n-360}$. This scaling factor can be changed in order to increase or decrease the power of the higher frequencies. Increasing the value of b will increase the power of the generated higher frequencies and vice-versa. In terms of mathematics, the potential

of the earth gravity field up to degree 2160 can be computed as follows

$$W(r, \Omega) = \frac{GM}{r} \sum_{n=2}^{2160} \left(\frac{b}{r} \right)^n W_n(\Omega) , \qquad (6.25)$$

with the low-degree coefficients taken from the model

$$2 \leq n \leq 360 \quad \wedge \quad m \leq n : W_n(\Omega) = \left(\frac{a}{b} \right)^n W_{n,m}(\Omega) , \qquad (6.26)$$

and the higher-degree coefficients are generated as follows

$$361 \leq n \leq 2160 \quad \wedge \quad m \leq n : W_n(\Omega) = \left(\frac{b}{a} \right)^{n-360} W_{360,m}(\Omega) . \qquad (6.27)$$

$W_{n,m}$ stands for the spherical harmonic coefficients of the global geopotential model, i.e., EGM96. In such a way, gravity potential for any point in space can be computed using the scaled EGM96 coefficients of degrees 2 to 360, and the generated coefficients of degrees 361 to 2160 which are simply the scaled EGM96 coefficients of degree 360.

Such a synthetic geopotential model is then used to generate the geoid and gravity data up to degree $n = 2160$. The higher-degree gravity data of degree 21 to 2160 are obtained by subtracting the reference gravity data of maximum degree 20. The accuracy of the discrete numerical integration is assessed as the difference of two geoidal solutions: first generated using directly the spectral form with the geopotential coefficients, and the second one as the sum of the reference spheroid of degree 20 and the residual geoid computed in the way described in this chapter from discrete gravity values obtained from the spectral form with the geopotential coefficients. This difference should theoretically be equal to zero everywhere. The actual values are used as indicators of the accuracy of the Stokes integrator. The scheme is in Fig. (7.3).

64

Chapter 7

Numerical Results

Computed results based on some of the formulae derived in this dissertation are presented in both graphical and tabular form. Figures provide information about spatial behaviour of individual quantities and can be used, in combination with tabulated statistical values, to assess their significance in view of the accurate geoid. The area used for numerical tests is bounded by parallels of 43° and 60° northern latitude, and by meridians of 224° and 258° eastern longitude. Due to the selected size of the spherical cap (radius of 6° is used in Stokes's integration), appropriate effects in the geoidal space were evaluated over a smaller area bounded by parallels of 49° and 54° northern latitude, and by meridians of 236° and 246° eastern longitude. All gravity data within the integration domain were available for each computation point.

Two topographical models were used for numerical evaluations: mean elevations (smooth) on the 5′ regular grid, see Fig. (7.4), and point elevations on the 30 × 60″ regular grid, which were provided by Natural Resources Canada, and the U.S. National Geodetic Survey, respectively. Global elevation model TUG87 was also employed, see Fig. (7.5). It contains the spherical harmonic representation of the global topography to the degree and order 180. The coefficients for the power of the global topography up to degree and order 90 were also available for the evaluation of the effects due to the distant topographical masses.

The latest combined geopotential model EGM96 [Lemoine et al., 1996] was used in computations, see Fig. (7.6). It contains fully-normalized, unitless spherical harmonic coefficients and their standard deviations, for a gravitational model complete from degree 2 order 0, to degree and order 360. The synthetic higher-degree gravitational fields, mentioned in *Chapter (6)*, were generated from this model.

The first series of figures and tables represents values of *topographical effects* defined both in gravity and geoidal space obtained as described in *Chapter (4)*. Contributions of the near zone, represented by a spherical cap with radius of 3°, to the terrain, condensed terrain, direct topographical, and secondary indirect topographical effect on gravity computed on the topography can be found in Figs. (7.7) – (7.10). The Newton integrals were computed using the 30" × 60" point elevations within a 1° × 1° rectangle centered at the computation point. The 5′ × 5′ mean elevations were used for the integration over the remainder of the spherical cap. The effects on gravity at the topographical surface are represented by their 5' mean values computed from the fifty 30" × 60" point values. This approach was selected with respect to the available elevation data and very long computational times.

The corresponding effects of the distant topographical masses, described also in *Chapter (4)*, can be found in Figs. (7.11) – (7.14). Their combined effects in geoidal space, estimated using the Poisson and Stokes integration, are shown in Figs. (7.15) – (7.22). Point values of the primary indirect topographical effect are in Figs. (7.23) and (7.24). Basic statistical values including arithmetic means and standard deviations for individual topographical effects in gravity space can be found in Tables (7.5) and (7.6), and in geoidal space in Tables (7.7) and (7.8). Both the figures and the tabulated values correspond with the expected behaviour of the topographical effects: the topographical masses within the near zone generate a high-frequency gravity field and the distant topographical masses are responsible for an attenuated low-frequency gravitational field. This is a consequence of Newton's law of gravitation. Looking at the effects in gravity space, one may consider the distant zone effects to be less critical

for the geoid computations. Their contribution to the geoid is important, however, due to the smoothing effect of the Stokes integration where not only the magnitude but also the frequency content of the gravity data plays an important role.

Atmospheric effects represent a second group of results. The derived coefficients of the second degree polynomial function used to approximate the actual density distribution of atmospheric masses for heights up to 9 kilometres are included in Table (7.4). The direct atmospheric effect on gravity is in Fig. (7.25). Its spherical part can be seen in Fig. (7.26) and the corresponding atmospheric terrain correction can be found in Fig. (7.27). The corresponding effect in geoidal space is shown in Fig. (7.28). Basic statistical values for individual atmospheric effects both in gravity and geoidal space are in Tables (7.9) and (7.10). Atmospheric effects on gravity represent mean values evaluated using discrete numerical integration over a spherical cap with radius of 3°. Applying the second Helmert condensation on the atmospheric masses, the last step in the reduction of gravity data conformal to the Stokes-Helmert theory was completed. The derived gravity data can further be downward continued to the geoid using the inverse Poisson integration. We succeeded, within available accuracy, to derive gravity data which corresponds to the harmonic disturbing gravity potential. The use of the boundary-value problem of one kind or another is then possible and theoretically fully justified.

Results for the *numerical accuracy of the Stokes integration* using higher-degree synthetic fields are included at the end of this chapter. The first two figures compare degree variances of two generated synthetic fields against the high-frequency global potential model GPM98B [Wenzel, 1998] which is defined up to degree 1800, see Figs. (7.29) and (7.30). Figures (7.31) and (7.32) represent the geoid of degree 2160 based on the first synthetic field and its corresponding statistics. Figures (7.33) and (7.34) then show the same results for the second synthetic field. Extreme values of these results can be found in Table (7.11). These values represent numerical errors of the discrete Stokes integration when applied on errorless 5' mean values of gravity.

Parameter	Symbol	Magnitude	Dimension
Major semiaxis	a	6378137	m
Geocentric gravitational constant	GM	3986005×10^8	$m^3\ s^{-2}$
Dynamic form factor	J_2	$108263\ \times 10^{-8}$	
Angular velocity	ω	7292115×10^{-11}	s^{-1}

Table 7.1: Constants of the Geodetic Reference System 1980

Parameter	Symbol	Magnitude	Dimension
Universal gas constant	κ	8314.32	$N\ m\ kmol^{-1}\ K^{-1}$
Mean molecular weight	μ	28.9644	$kg\ kmol^{-1}$
Sea-level air pressure	P	101325	$N\ m^{-2}$
Sea-level air temperature	T	288.15	K
Sea-level gravity	g	9.80665	$m\ s^{-2}$

Table 7.2: Constants of the United States Standard Atmosphere 1976

Subscript	Height [km]	Gradient [K km^{-1}]
1	00 - 11	$-$ 6.5
2	11 - 20	$+$ 0.0
3	20 - 32	$+$ 1.0
4	32 - 48	$+$ 2.8
5	48 - 51	$+$ 0.0
6	51 - 71	$-$ 2.8
7	71 - 86	$-$ 2.0

Table 7.3: Temperature gradients of linearly-segmented height profile

Parameter	Magnitude	Dimension
Density at the sea level	$+$ 1.2227	kg m^{-3}
Linear coefficient	$-$ 1.1436 $\times$ 10^{-4}	kg m^{-4}
Quadratic coefficient	$+$ 3.4057 $\times$ 10^{-9}	kg m^{-5}

Table 7.4: Derived model of atmospheric density function

Parameter	Minimum	Maximum	Mean value	Std deviation
Terrain effect	− 1.468	+ 48.029	+ 1.681	± 3.537
Condensed terrain effect	− 25.136	+ 92.776	+ 0.954	± 4.915
Direct effect	− 44.747	+ 45.150	+ 0.729	± 4.167
Secondary indirect effect	− 0.017	+ 0.002	− 0.000	± 0.001

Table 7.5: Topographical effects on gravity - near zone (mGal)

Parameter	Minimum	Maximum	Mean value	Std deviation
Terrain effect	− 43.993	+ 290.519	+ 55.599	± 65.062
Condensed terrain effect	− 44.062	+ 292.130	+ 55.655	± 65.243
Direct effect	− 1.613	+ 0.351	− 0.056	± 0.220
Secondary indirect effect	− 0.266	+ 0.290	− 0.005	± 0.047

Table 7.6: Topographical effects on gravity - distant zone (mGal)

Parameter	Minimum	Maximum	Mean value	Std deviation
Terrain effect	+ 0.298	+ 2.695	+ 1.696	± 0.519
Condensed terrain effect	+ 0.140	+ 2.012	+ 1.080	± 0.366
Direct effect	+ 0.158	+ 1.163	+ 0.616	± 0.187
Secondary indirect effect	− 0.001	+ 0.000	− 0.001	± 0.000
Primary indirect effect	− 1.397	+ 0.000	− 0.104	± 0.142

Table 7.7: Topographical effects on geoid - near zone (m)

Parameter	Minimum	Maximum	Mean value	Std deviation
Terrain effect	+ 12.951	+ 50.682	+ 39.949	± 6.681
Condensed terrain effect	+ 12.949	+ 50.814	+ 40.021	± 6.706
Direct effect	− 0.136	+ 0.002	− 0.073	± 0.028
Secondary indirect effect	− 0.014	+ 0.011	− 0.002	± 0.006
Primary indirect effect	− 0.295	+ 1.096	+ 0.053	± 0.141

Table 7.8: Topographical effects on geoid - distant zone (m)

71

Parameter	Minimum	Maximum	Mean value	Std deviation
Spherical direct effect	+ 0.559	+ 0.870	+ 0.799	± 0.057
Terrain correction	− 0.042	+ 0.012	− 0.001	± 0.003
Secondary indirect effect	− 0.002	− 0.001	− 0.002	± 0.000

Table 7.9: Atmospheric effects on gravity (mGal)

Parameter	Minimum	Maximum	Mean value	Std deviation
Direct effect	+ 0.278	+ 0.304	+ 0.285	± 0.004
Secondary indirect effect	− 0.000	+ 0.000	− 0.000	± 0.000
Primary indirect effect	− 0.006	− 0.006	− 0.006	± 0.000

Table 7.10: Atmospheric effects on geoid (m)

Model	Minimum	Maximum	Mean value	Std deviation
Field A	− 0.017	+ 0.026	+ 0.003	± 0.008
Field B	− 0.030	+ 0.039	+ 0.003	± 0.010

Table 7.11: Accuracy of Stokes's integration (m)
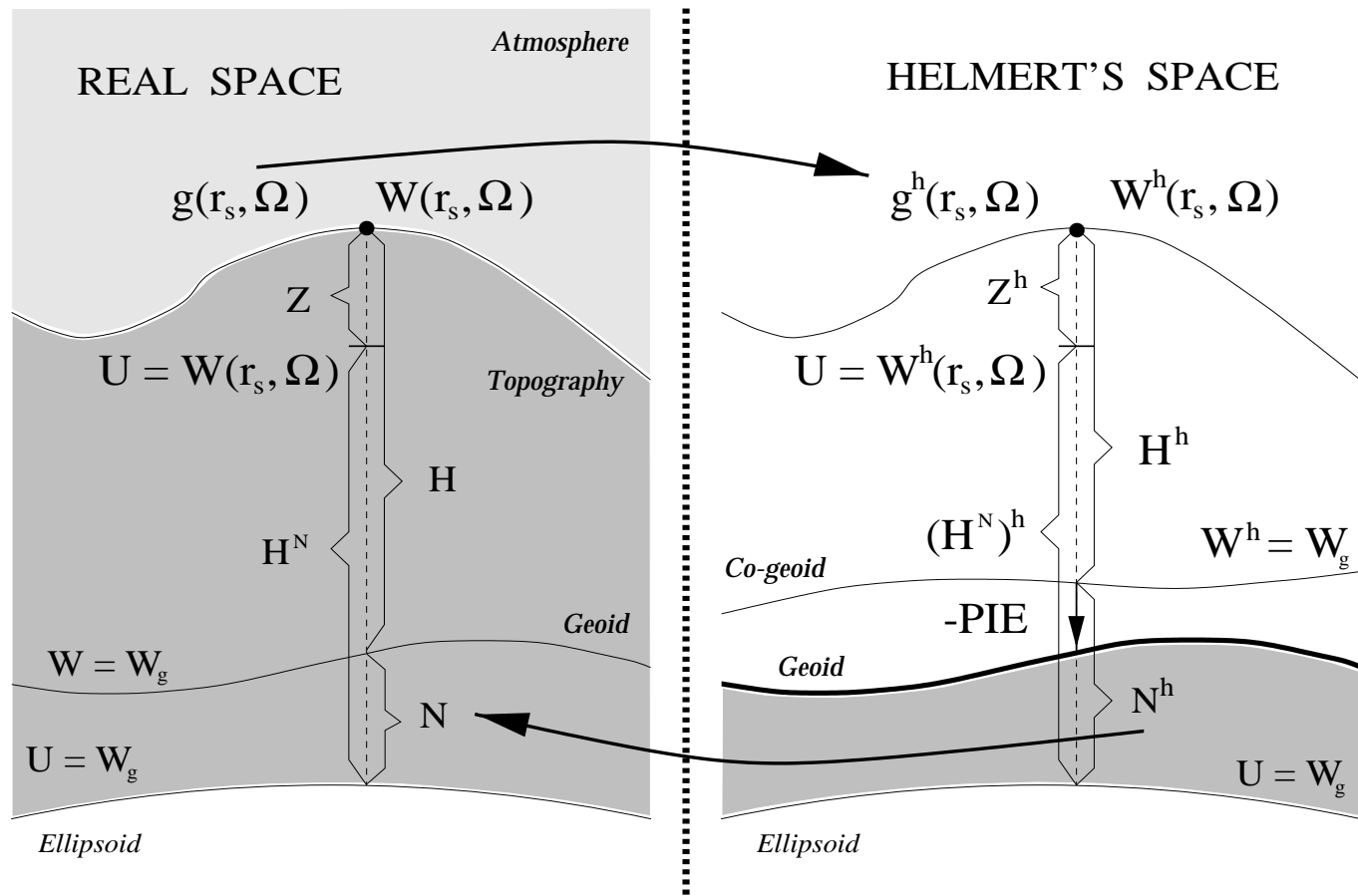
Figure 7.1: Scheme of second Helmert's condensation
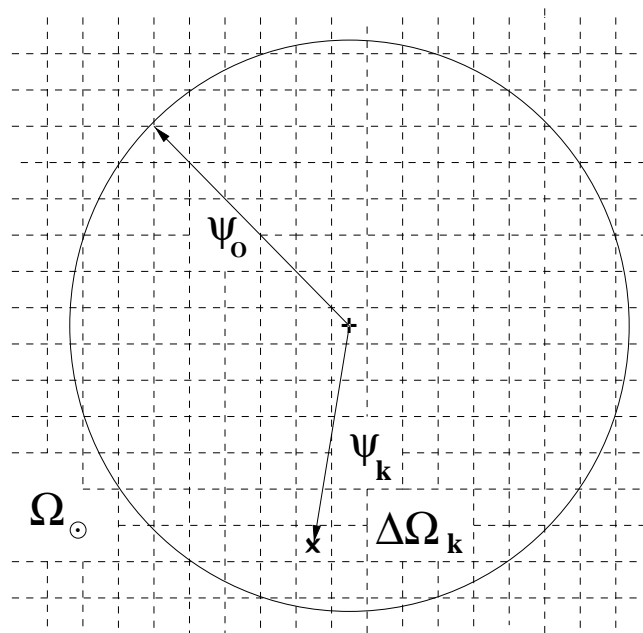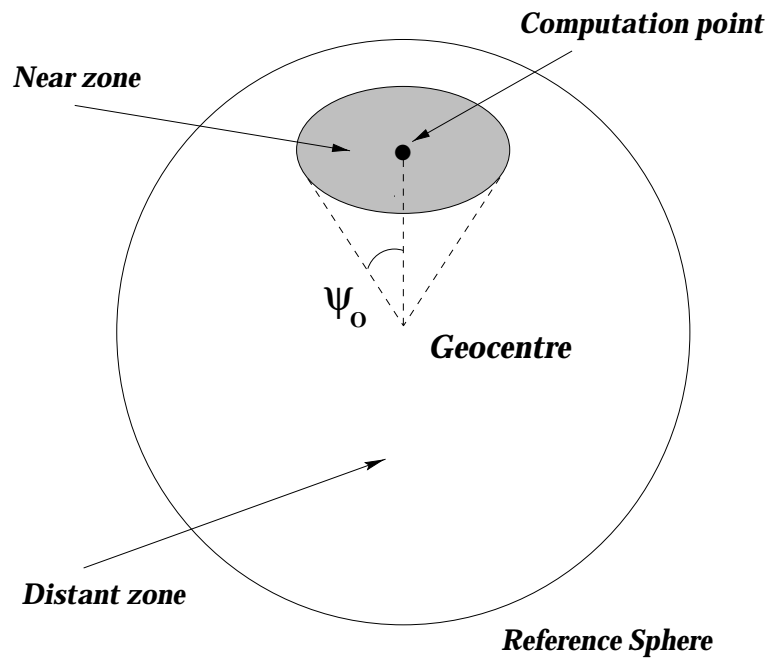
Figure 7.2: Integration subdomains for Stokes's integration

Scheme of the Testing Procedure
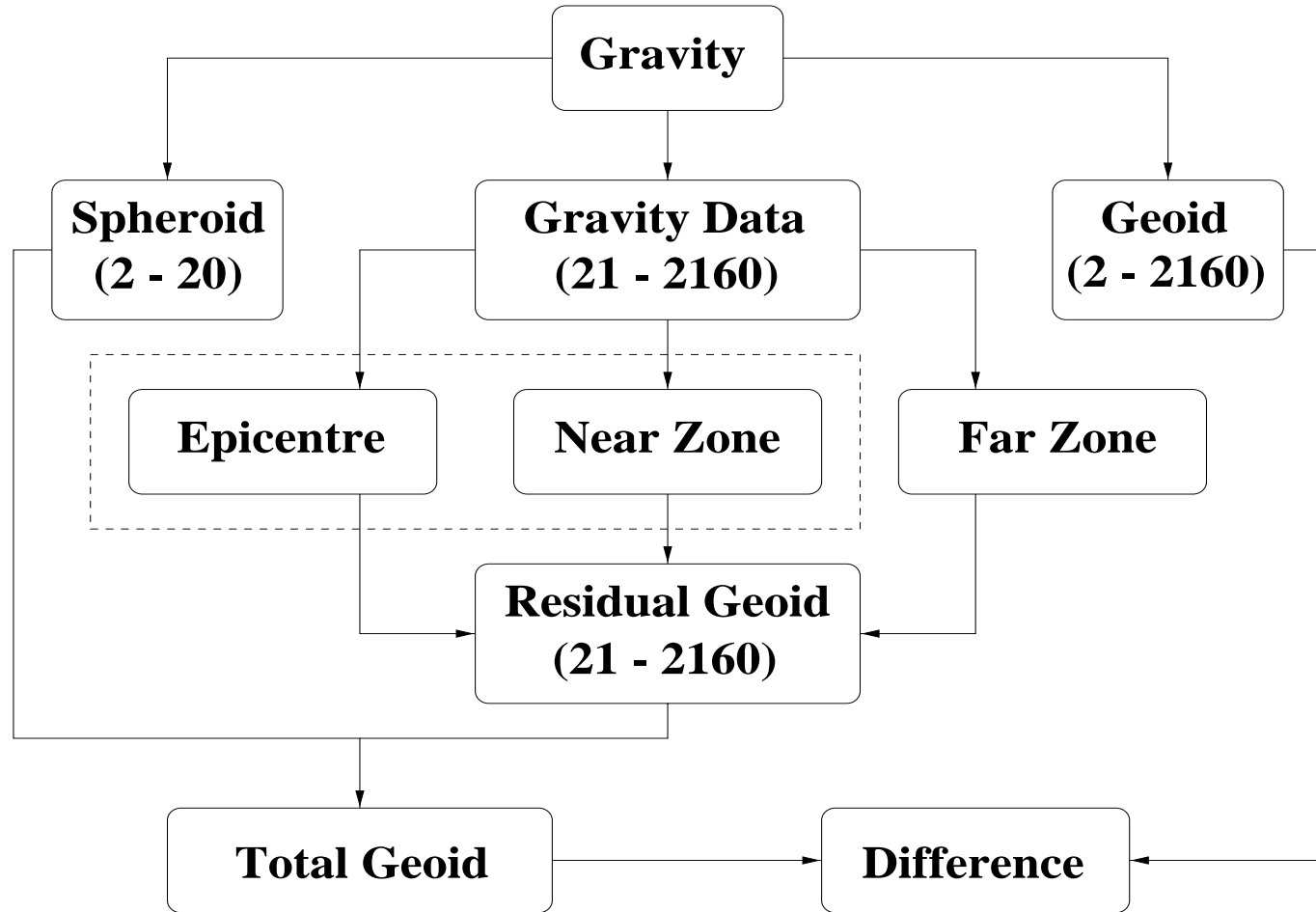
Figure 7.3: Testing procedure for Stokes's integration
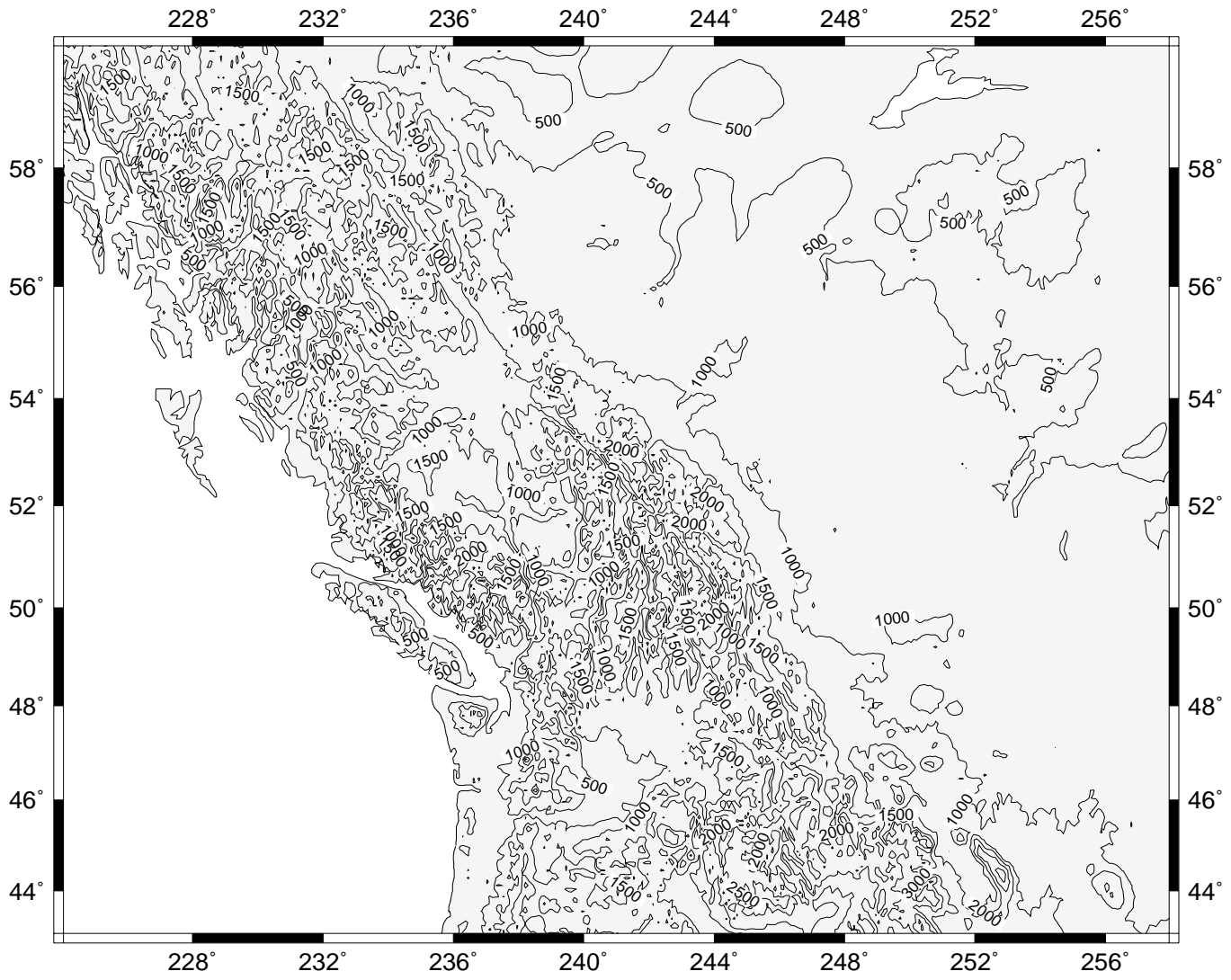
Figure 7.4: Discrete 5' mean elevation data (m)

Figure 7.5: Global elevation model TUG87 (m)

77
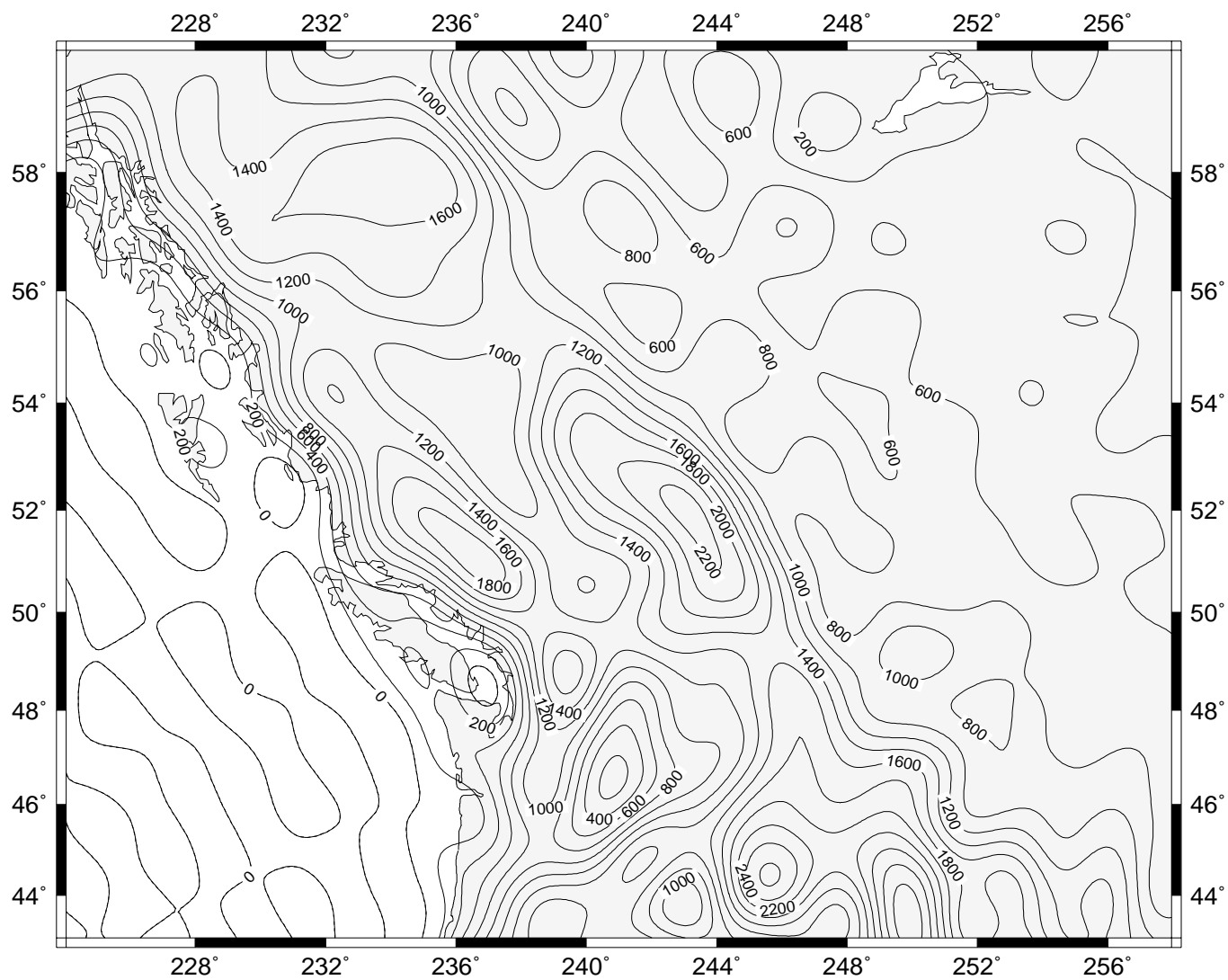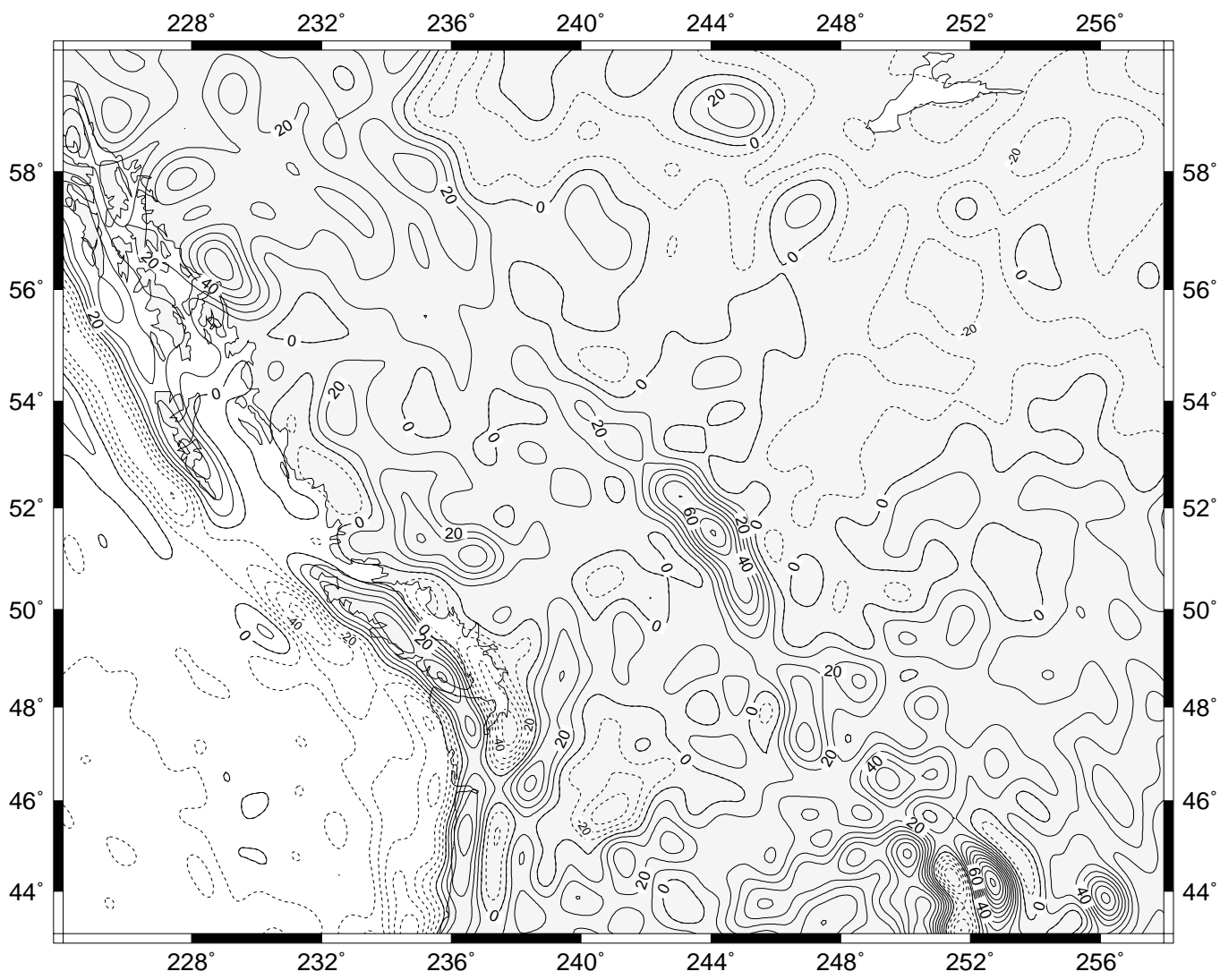
Figure 7.6: Global gravity field EGM96 (mGal)

78
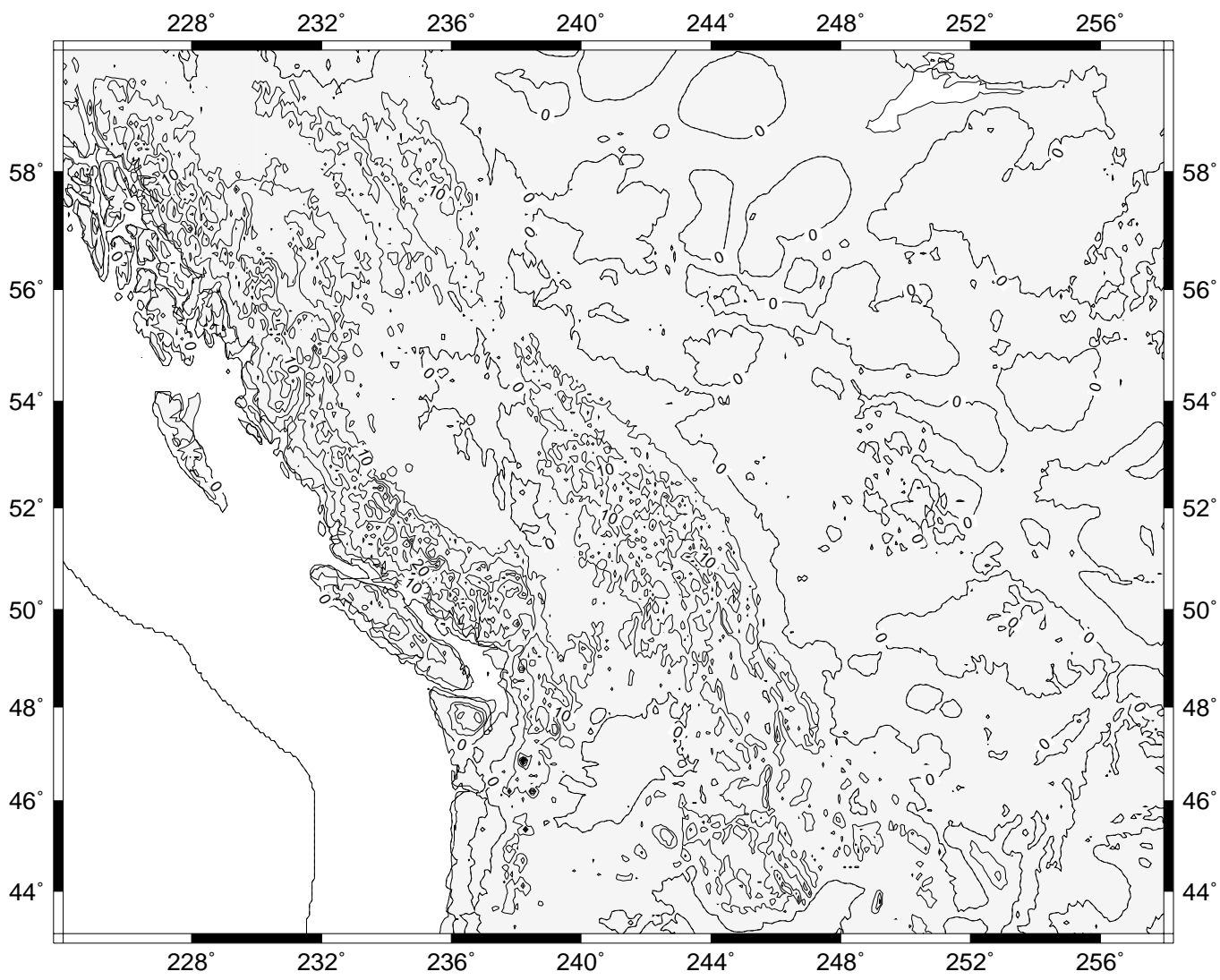
Figure 7.7: Terrain effect on gravity - near zone (mGal)

Figure 7.8: Condensed terrain effect on gravity - near zone (mGal)
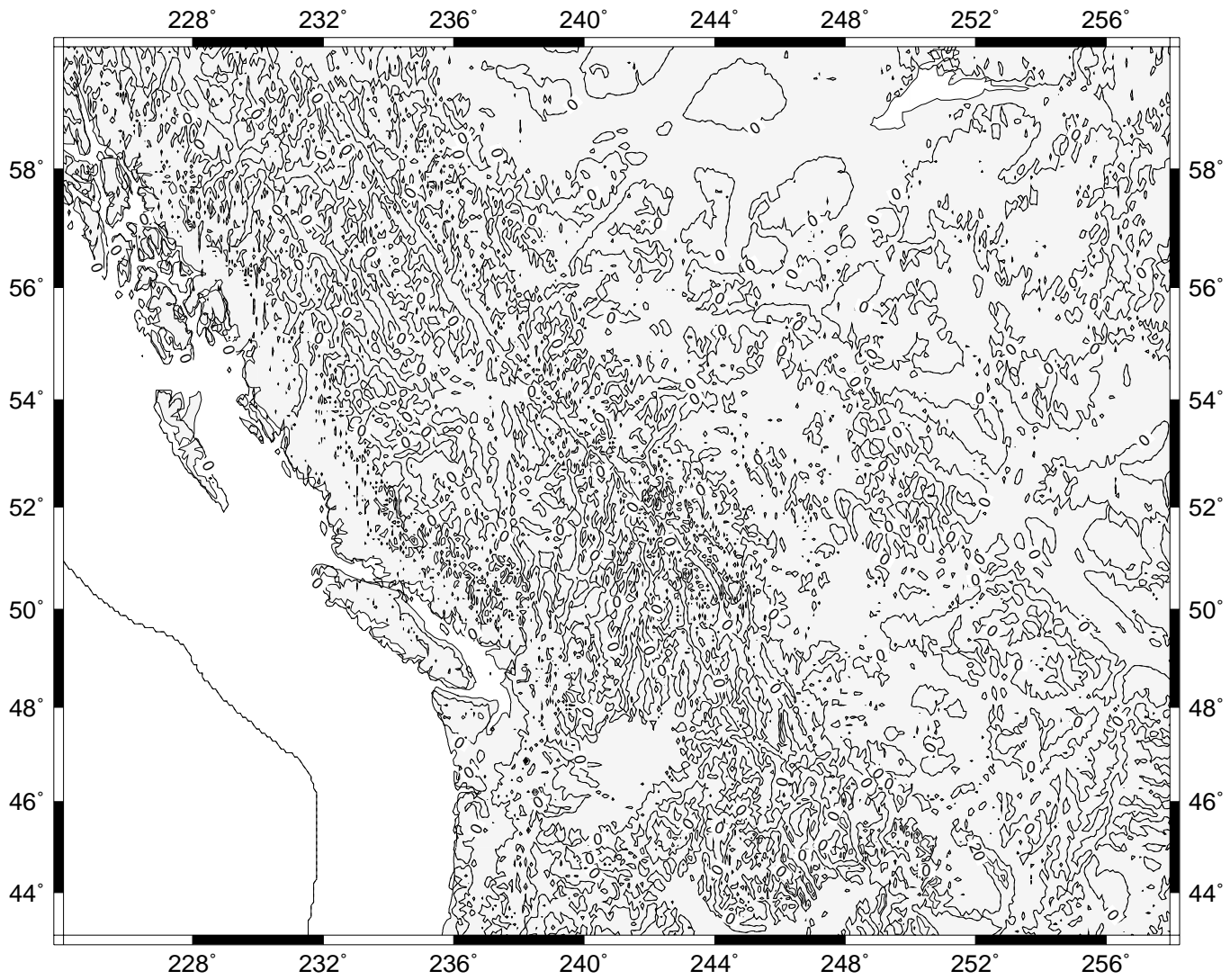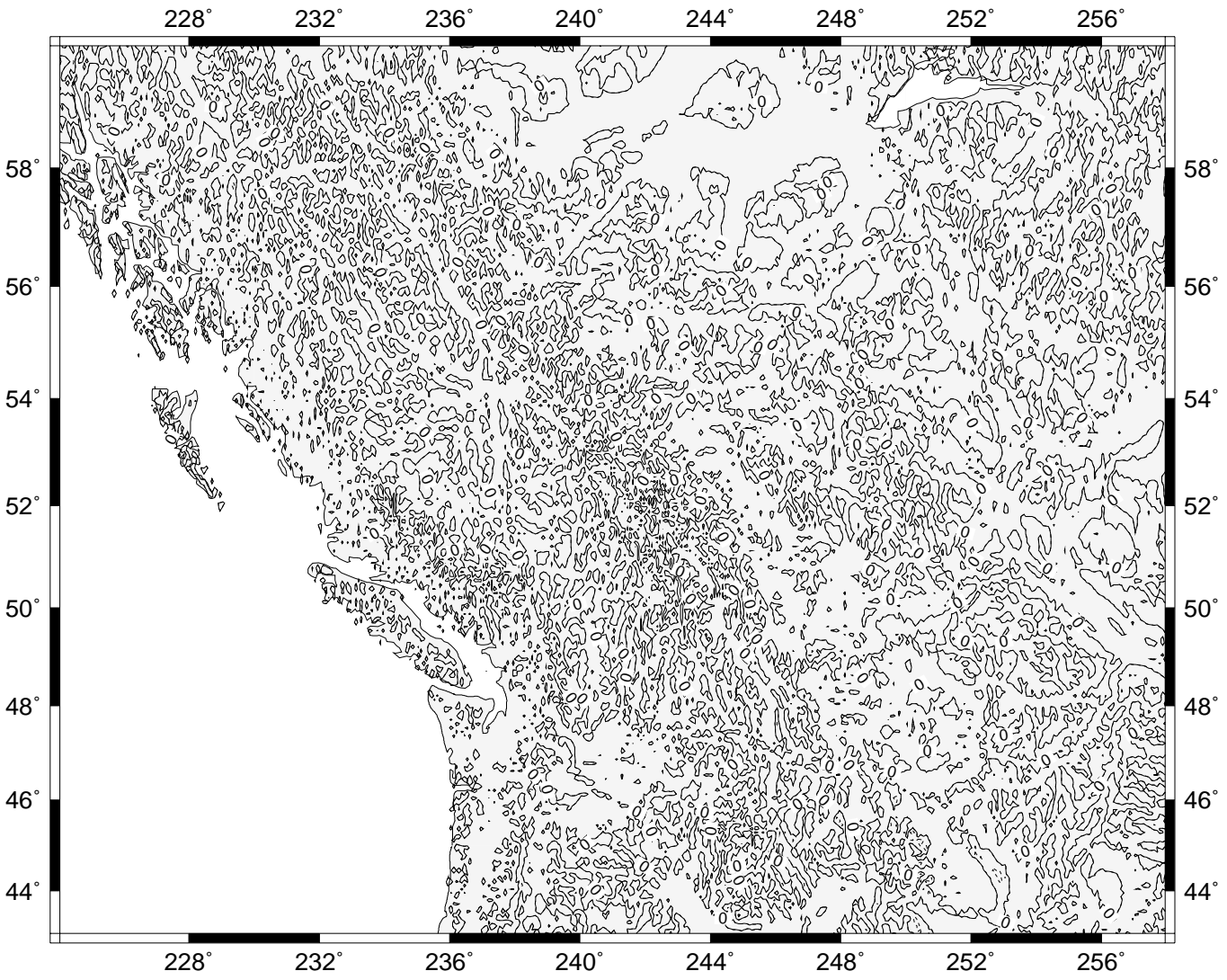
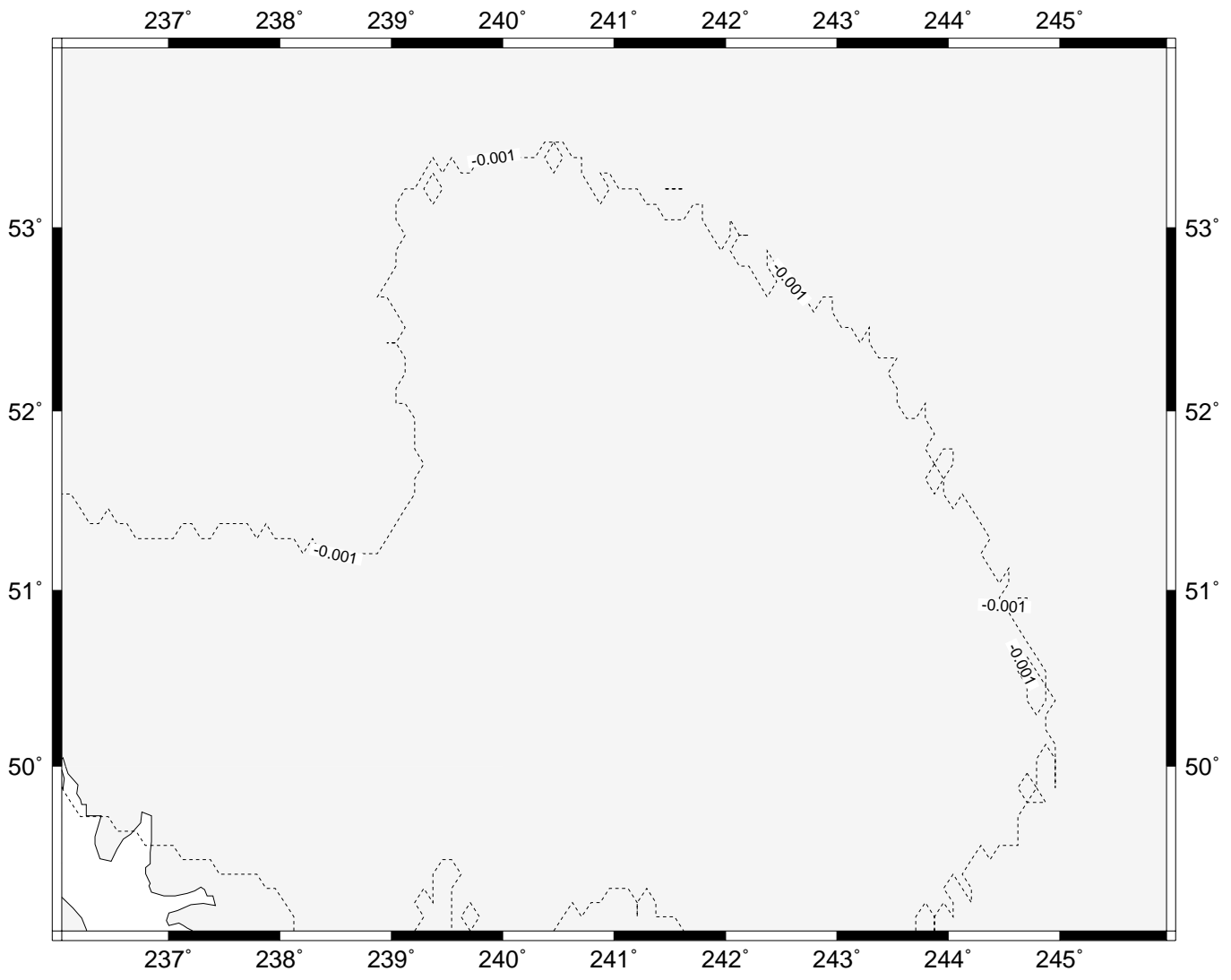Figure 7.9: Direct topographical effect on gravity - near zone (mGal)

81
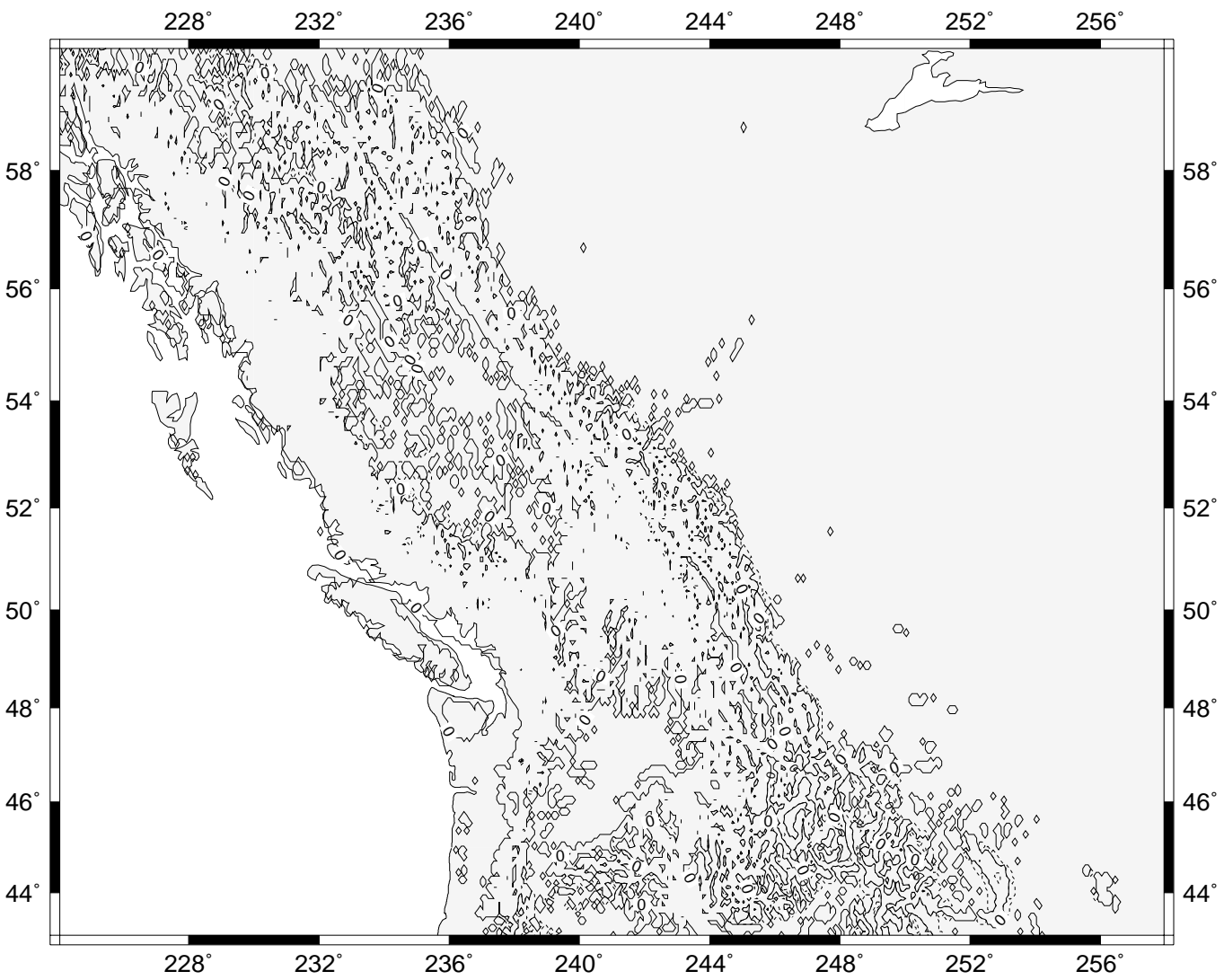
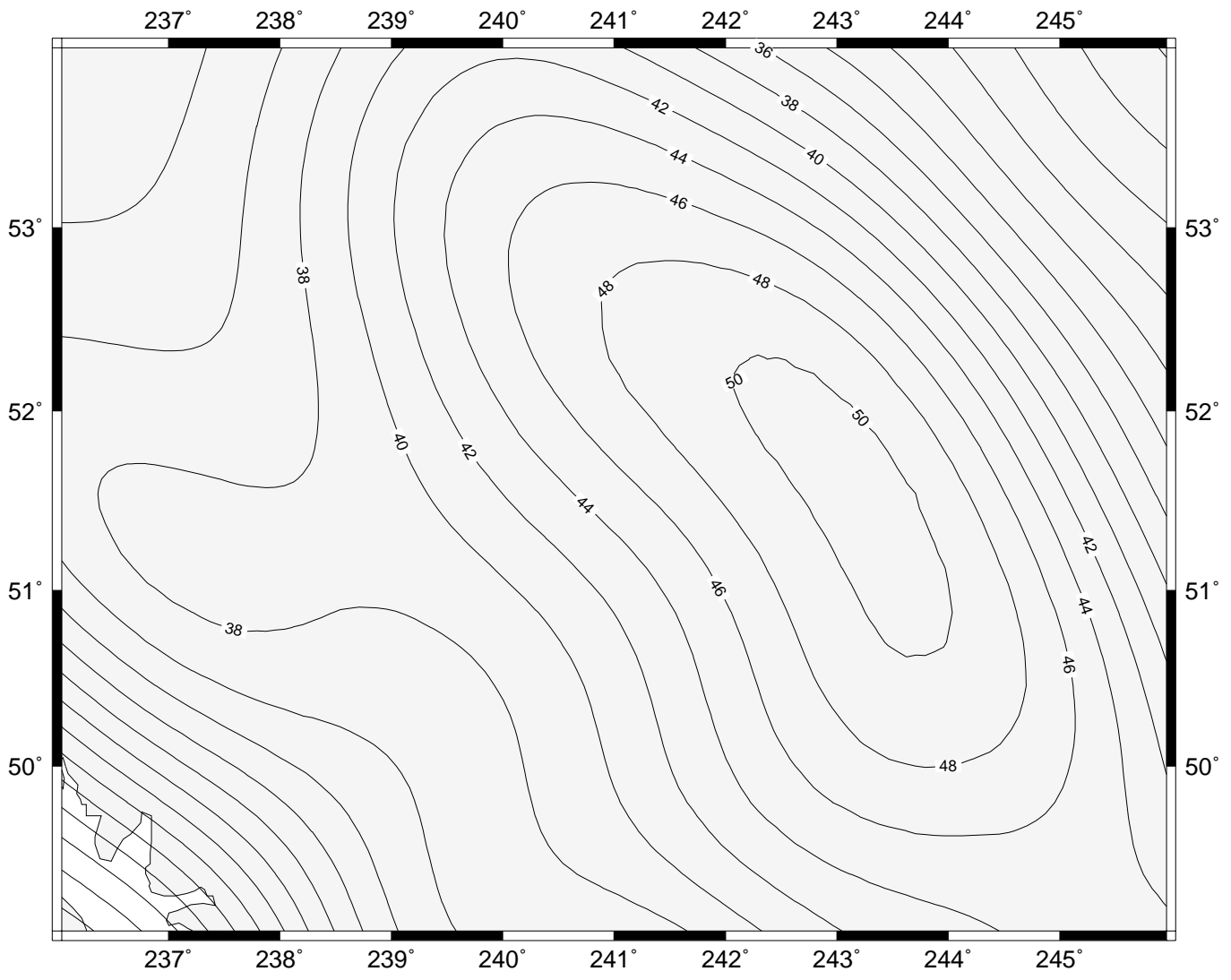Figure 7.10: Secondary indirect topographical effect on gravity - near zone (mGal)

82
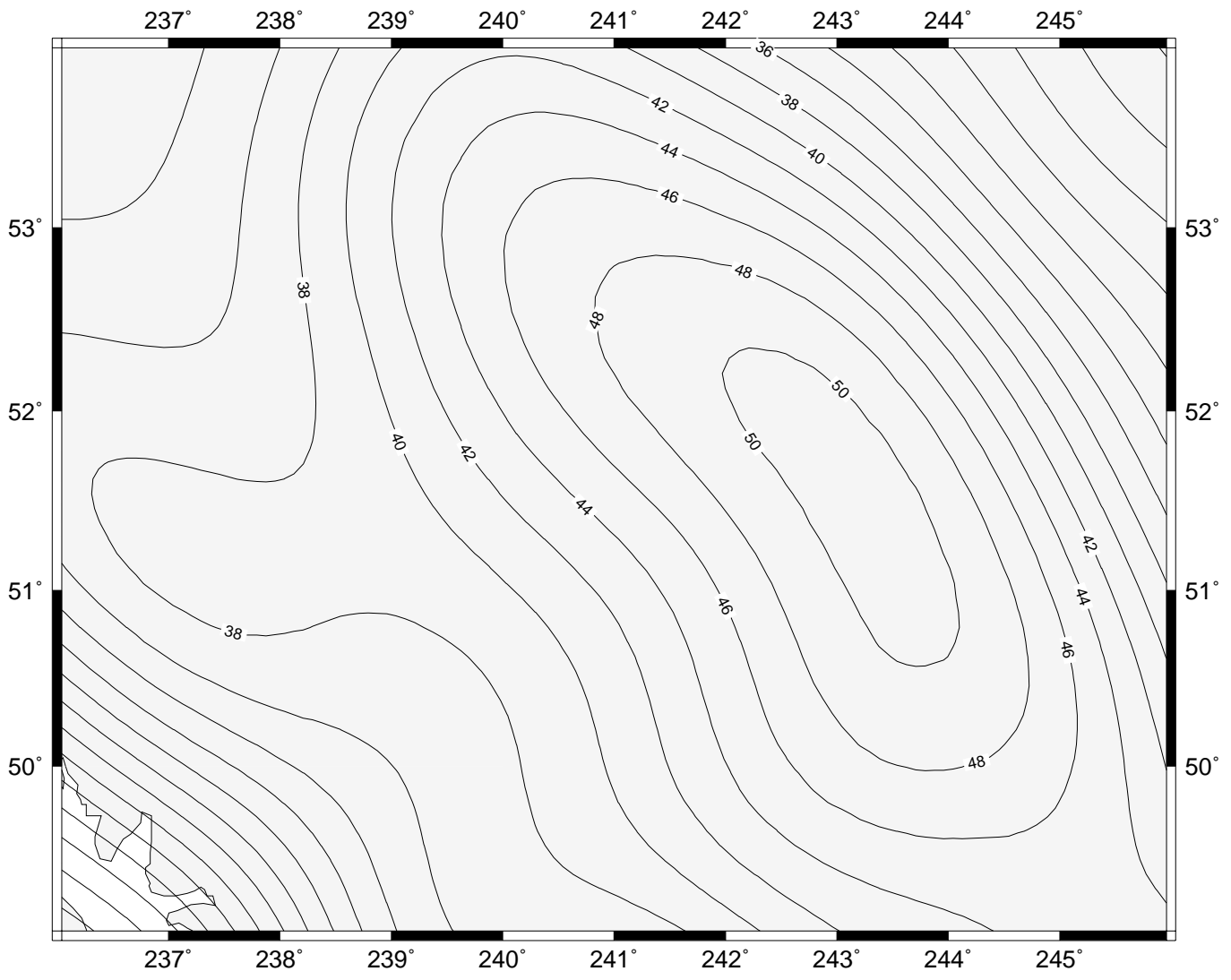
Figure 7.11: Terrain effect on gravity - distant zone (mGal)

83
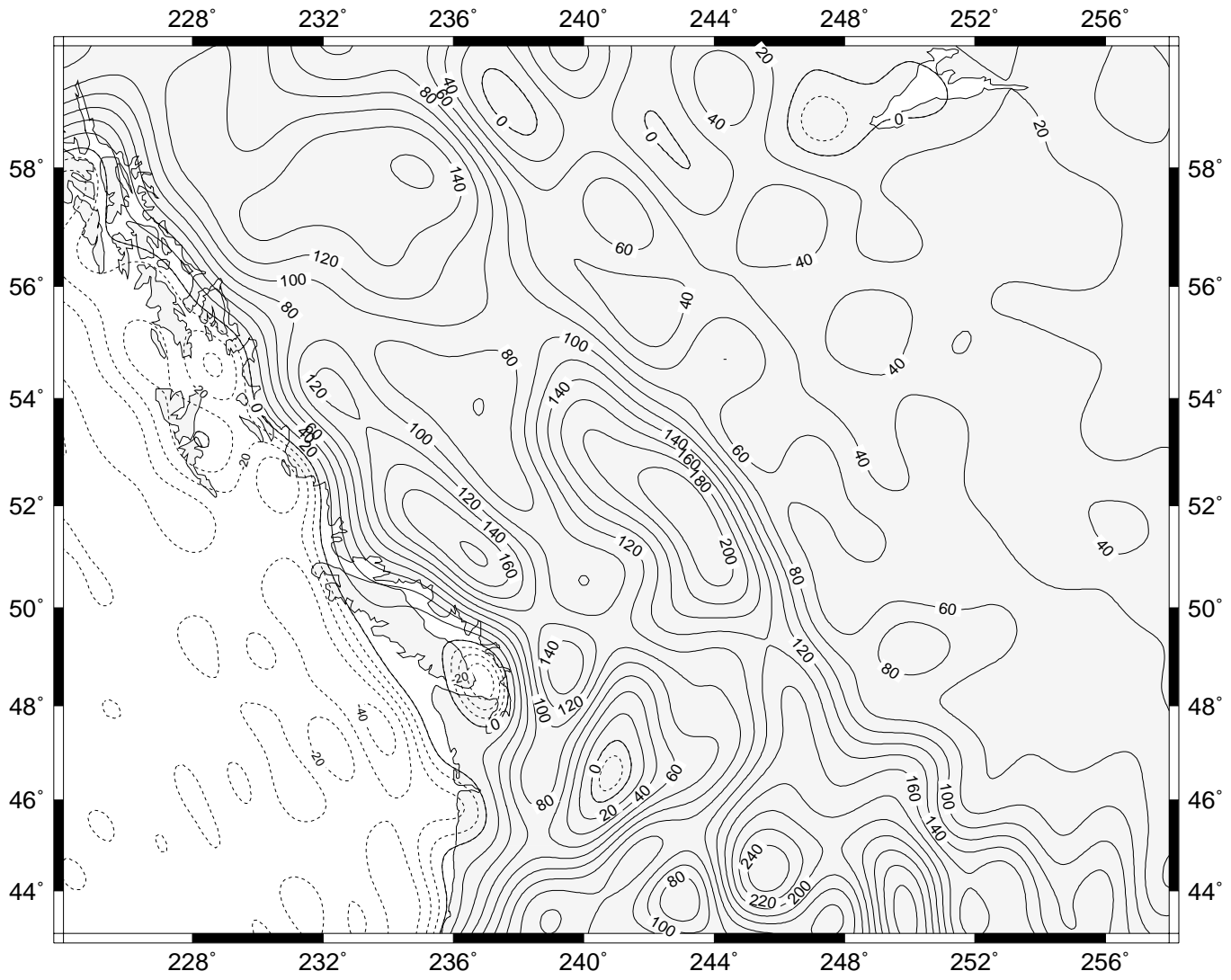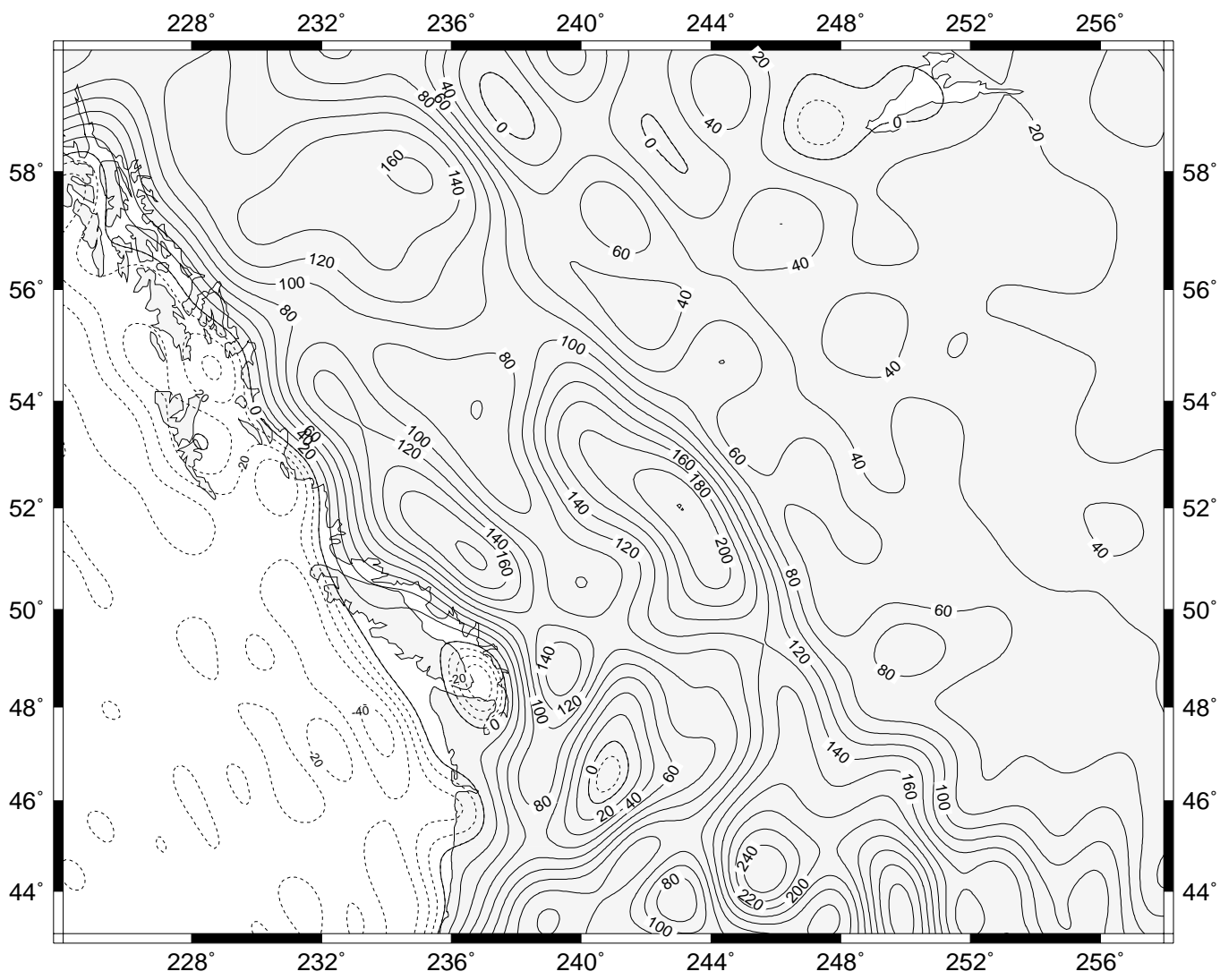
Figure 7.12: Condensed terrain effect on gravity - distant zone (mGal)
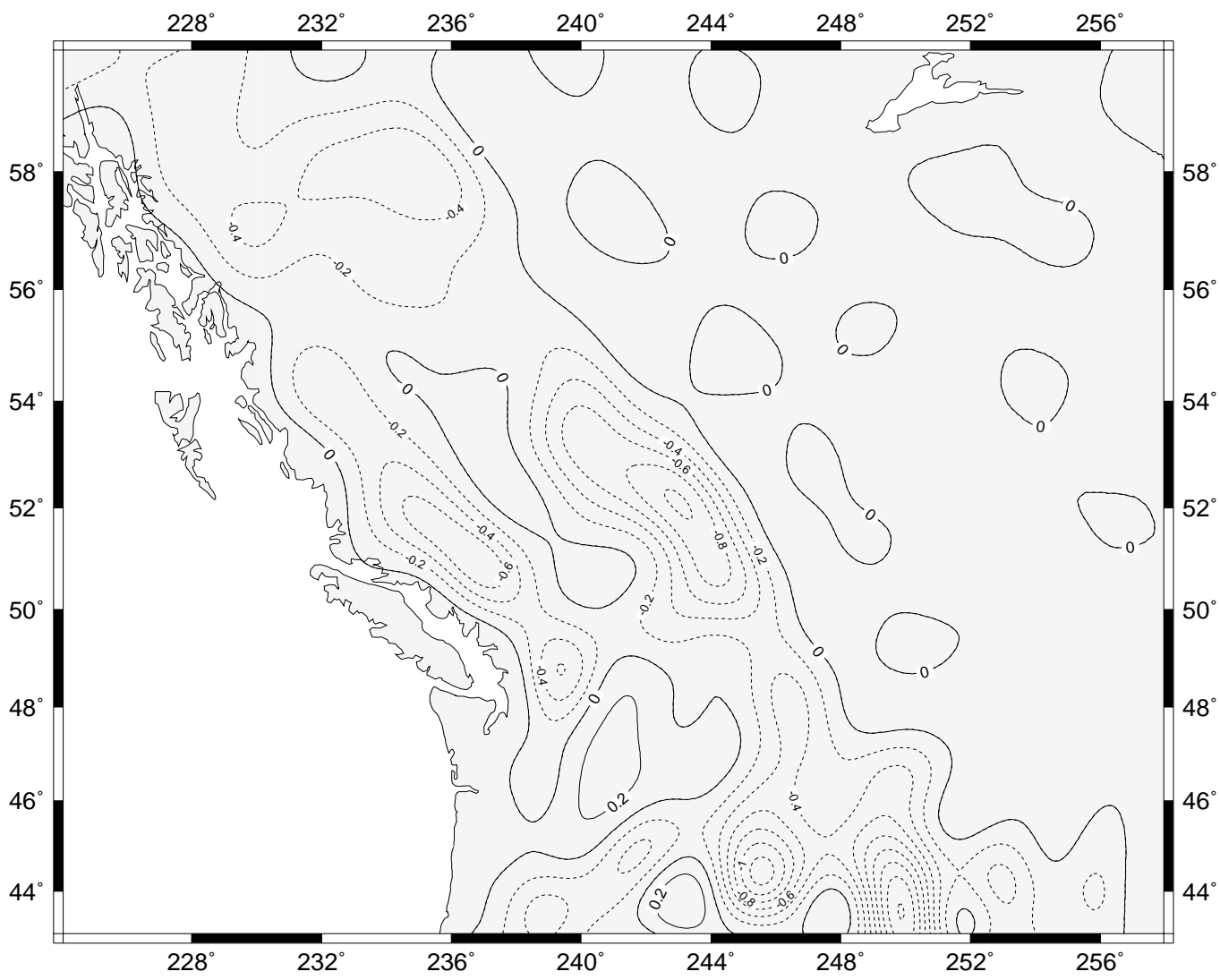
Figure 7.13: Direct topographical effect on gravity - distant zone (mGal)

85
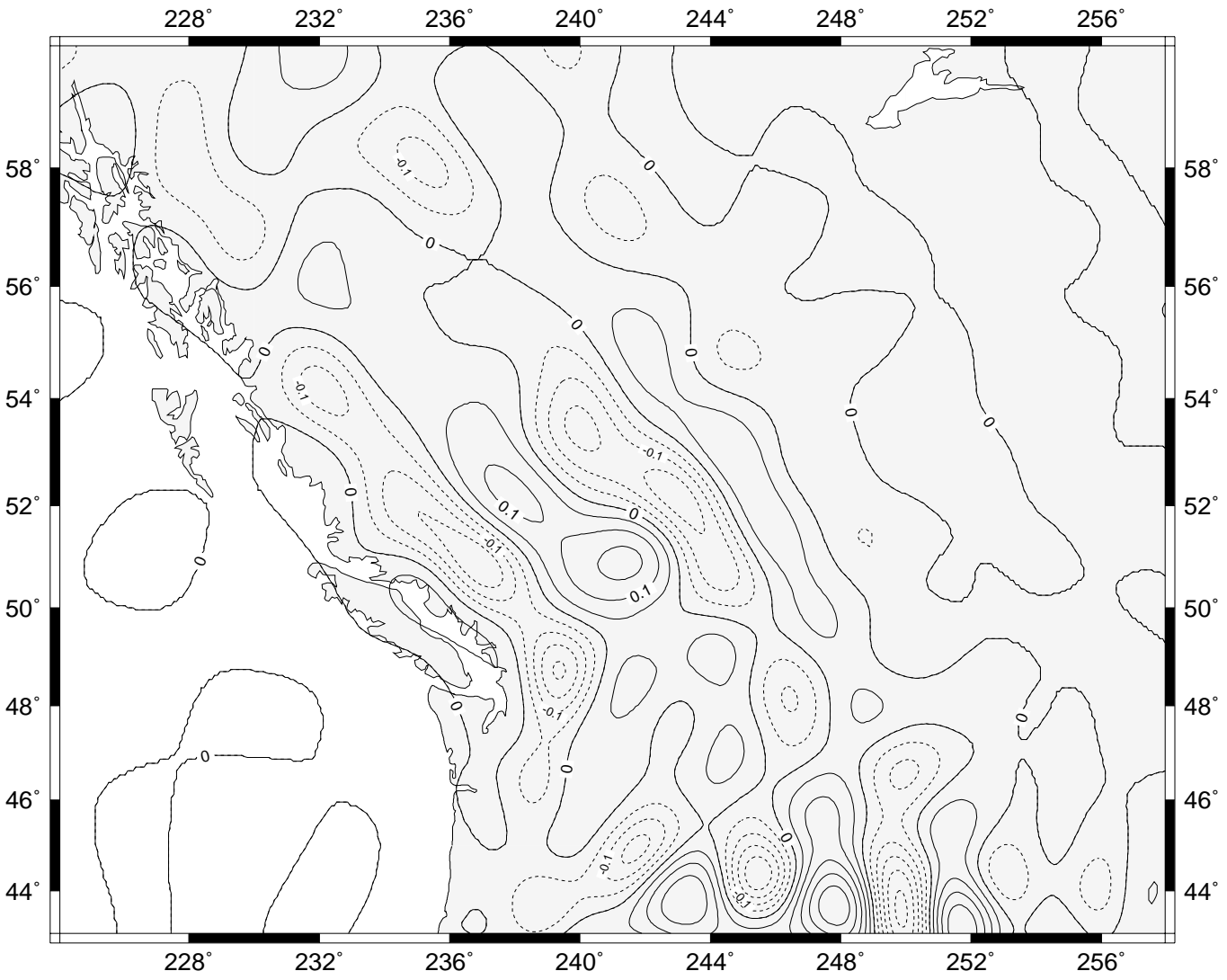
Figure 7.14: Secondary indirect topographical effect on gravity - distant zone (mGal)
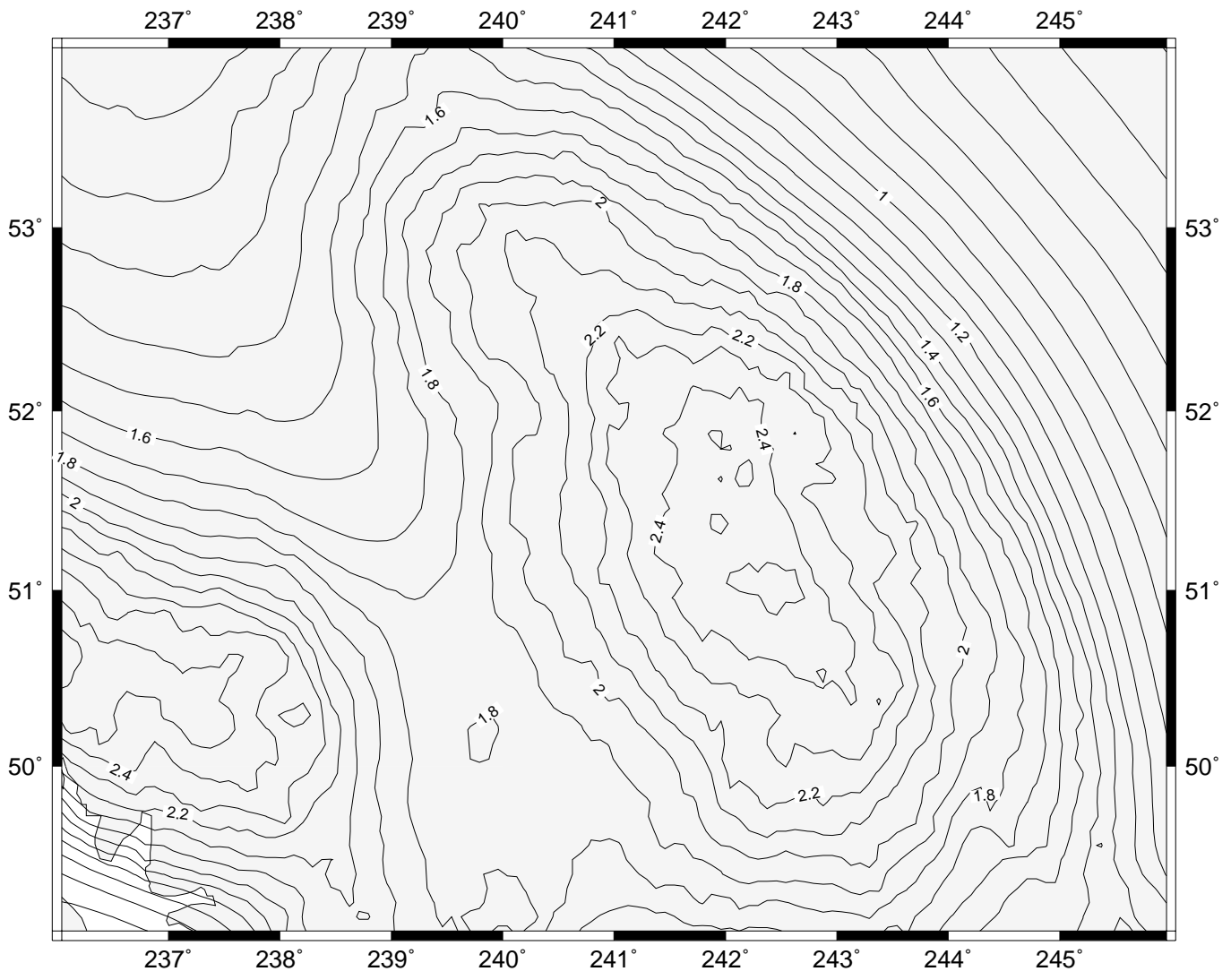
Figure 7.15: Terrain effect on geoid - near zone (m)

Figure 7.16: Condensed terrain effect on geoid – near zone (m)

88
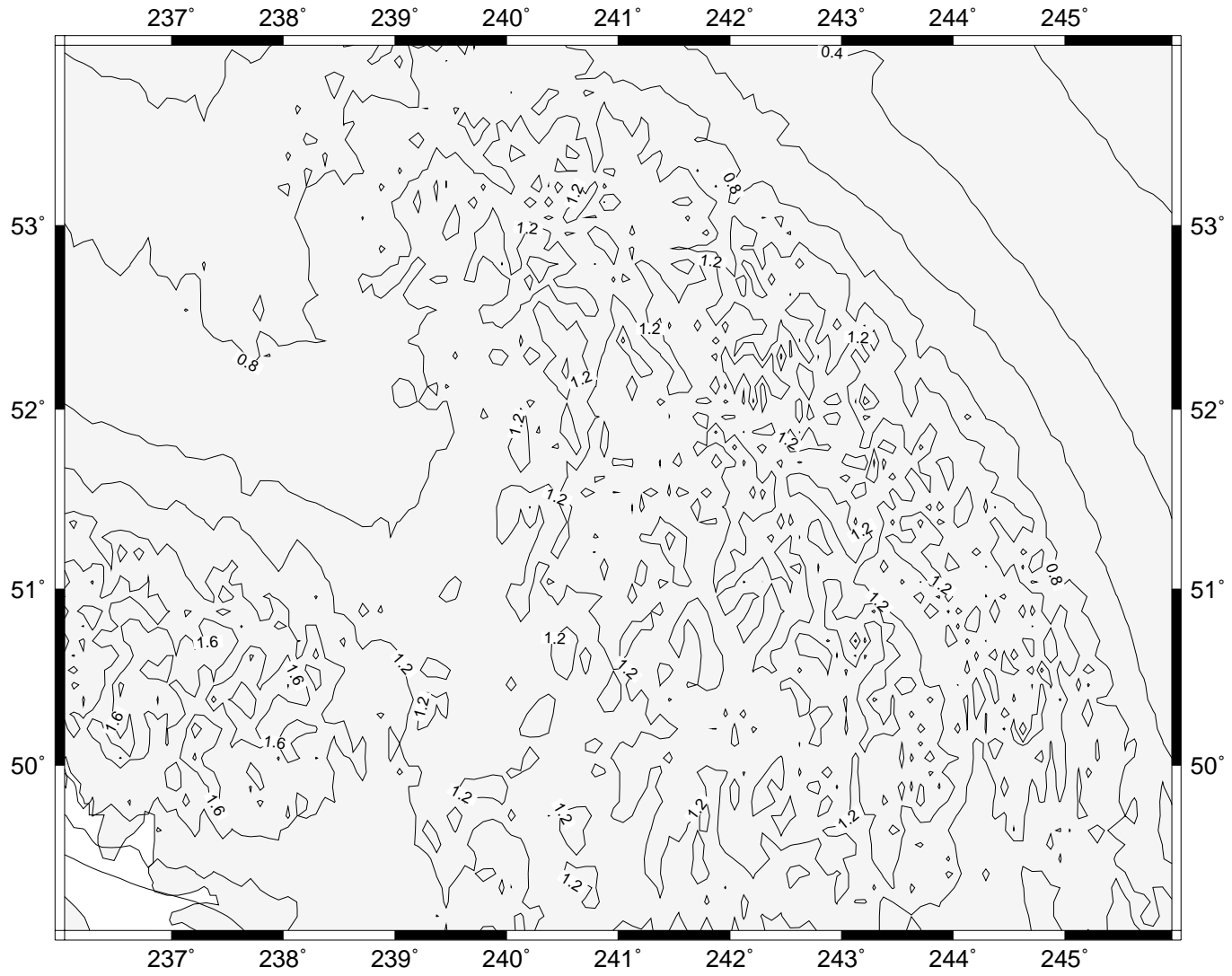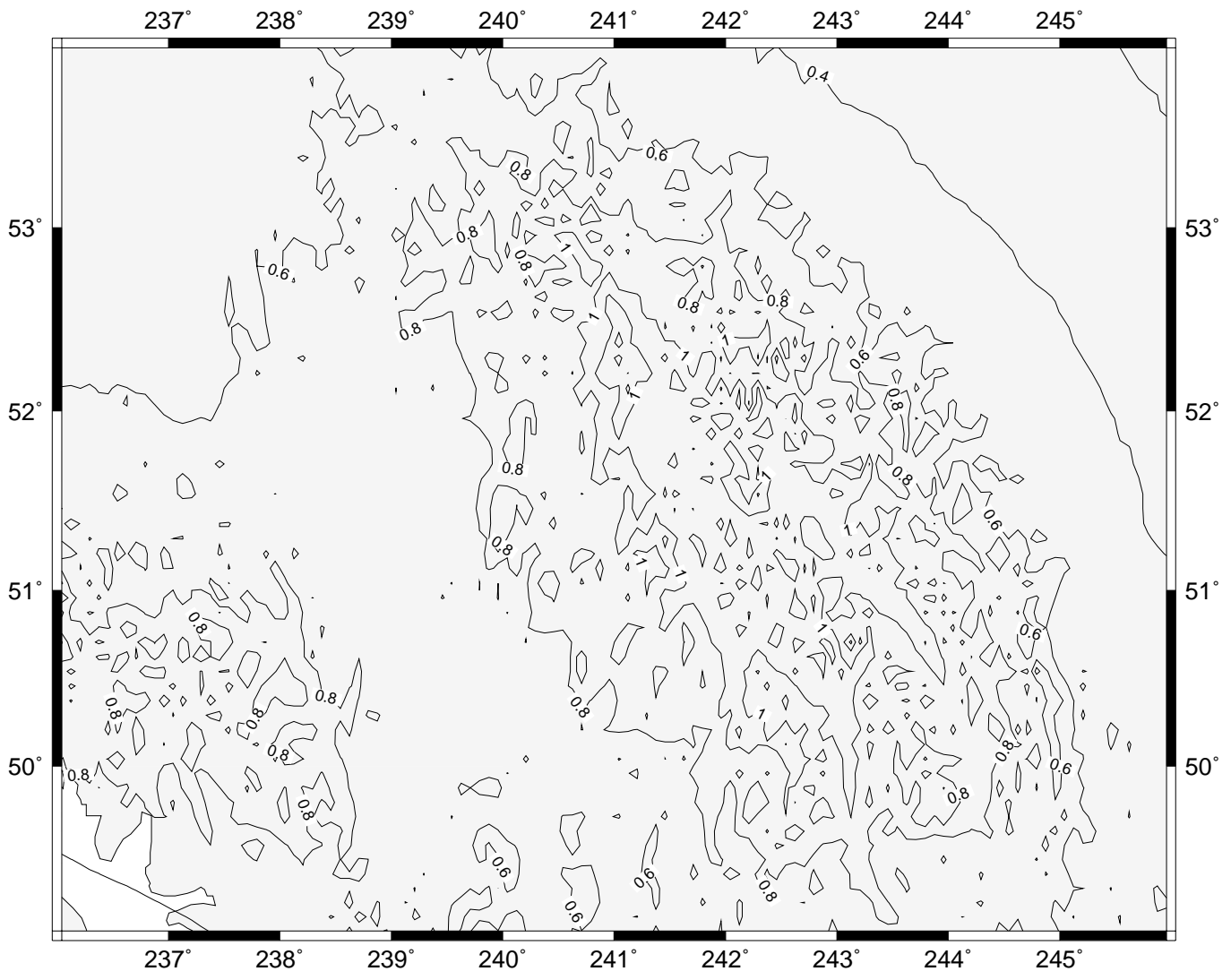
Figure 7.17: Direct topographical effect on geoid - near zone (m)

89

Figure 7.18: Secondary indirect topographical effect on geoid - near zone (m)

Figure 7.19: Terrain effect on geoid - distant zone (m)

91

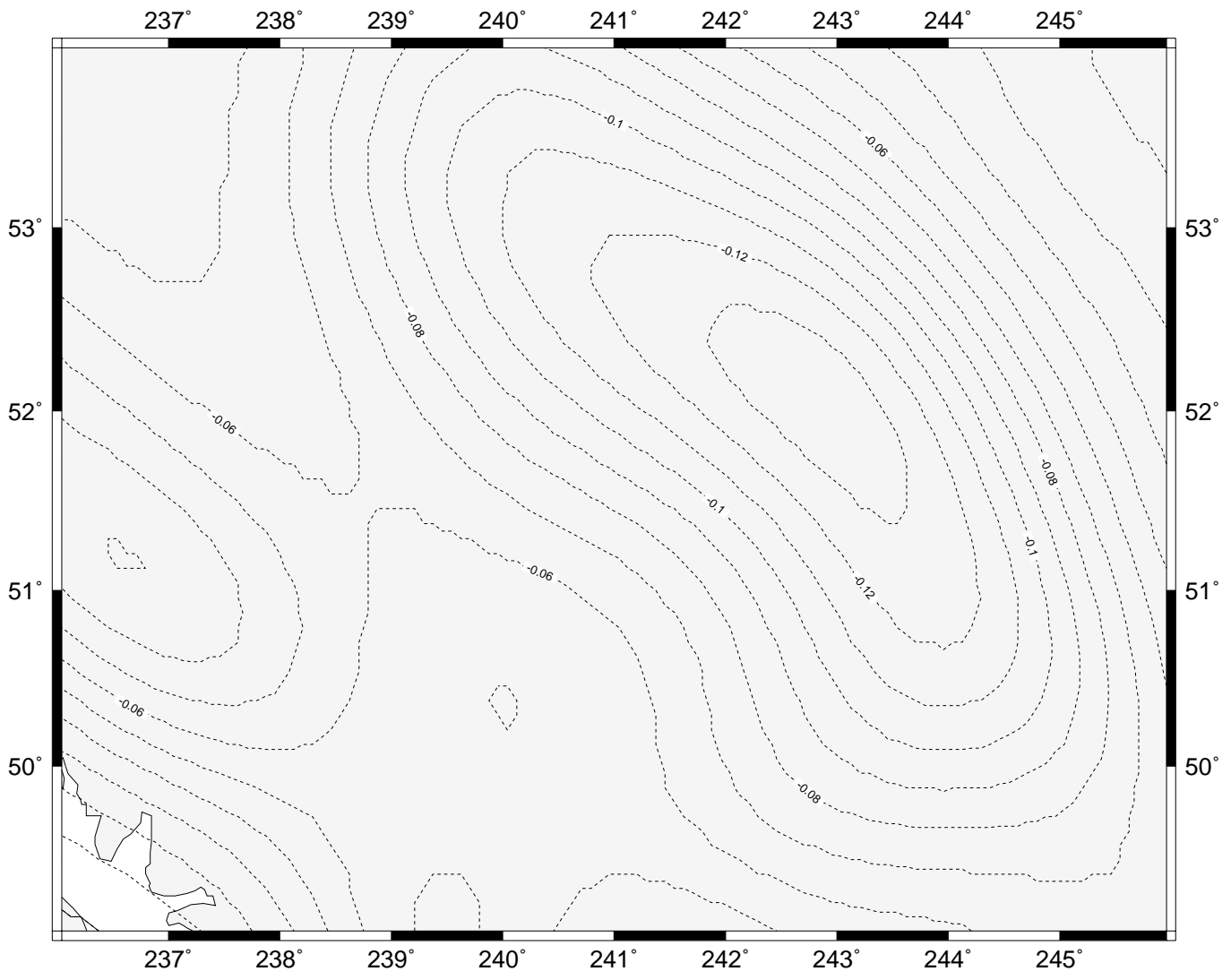Figure 7.20: Condensed terrain effect on geoid – distant zone (m)

92

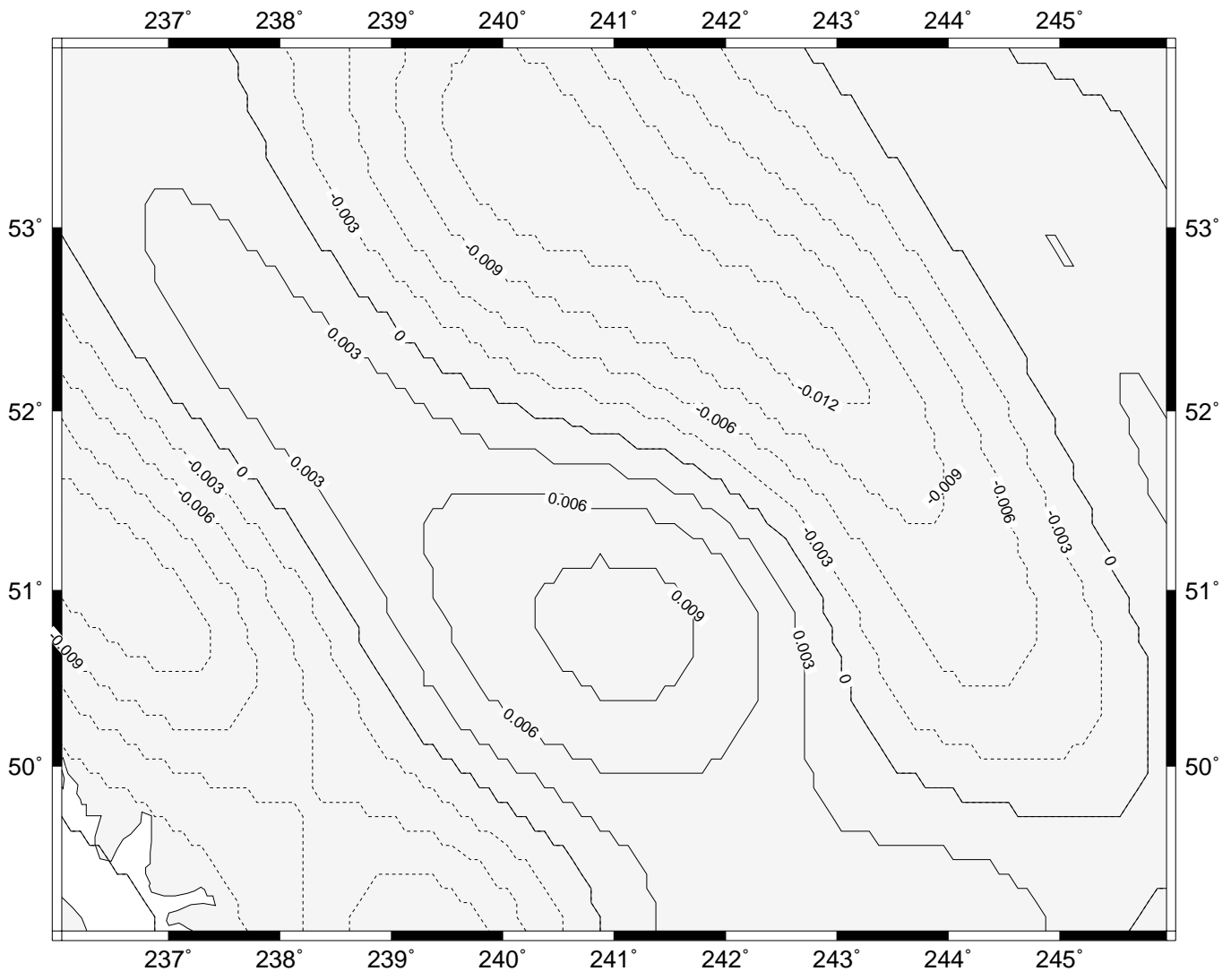Figure 7.21: Direct topographical effect on geoid - distant zone (m)

93

Figure 7.22: Secondary indirect topographical effect on geoid - near zone (m)
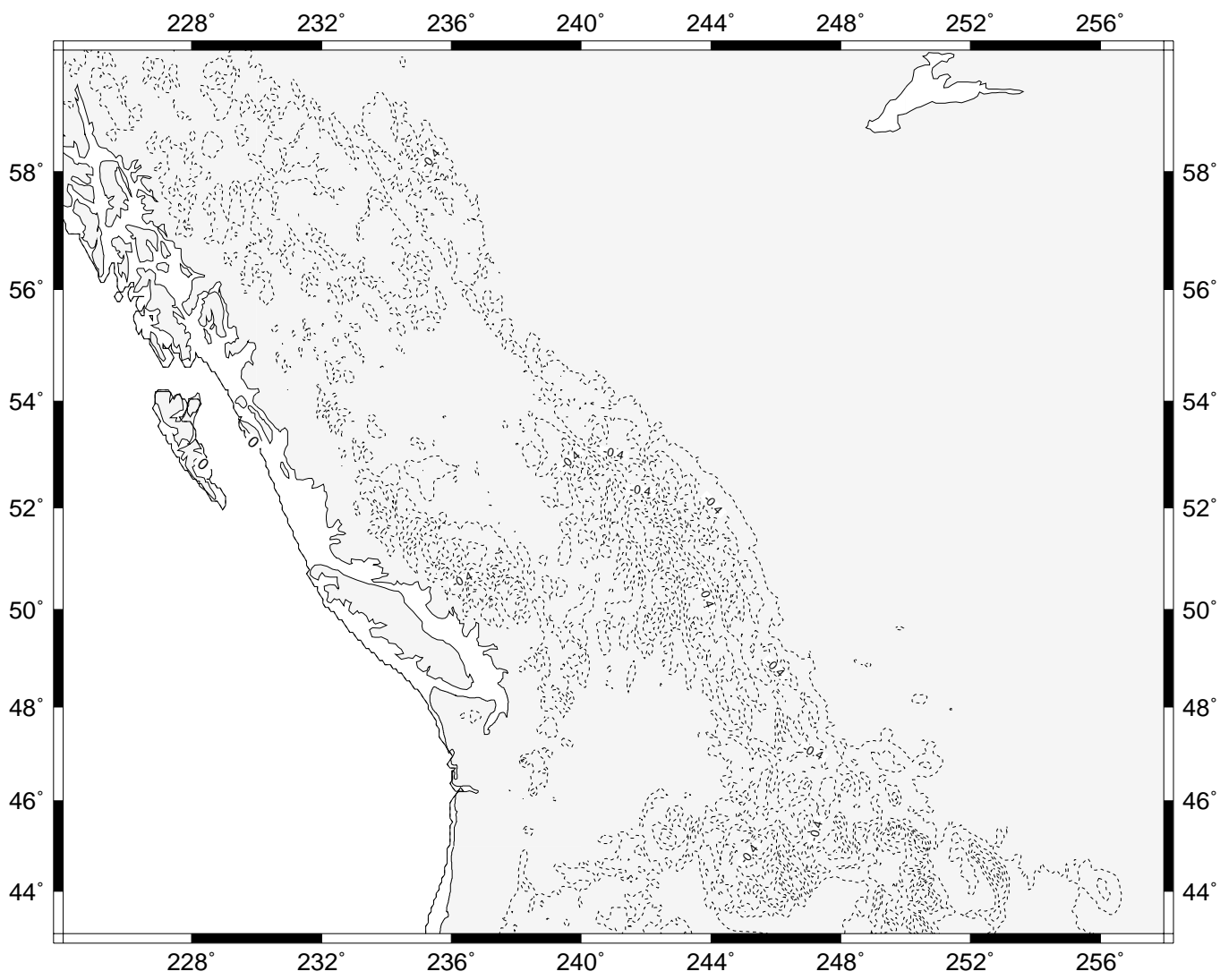
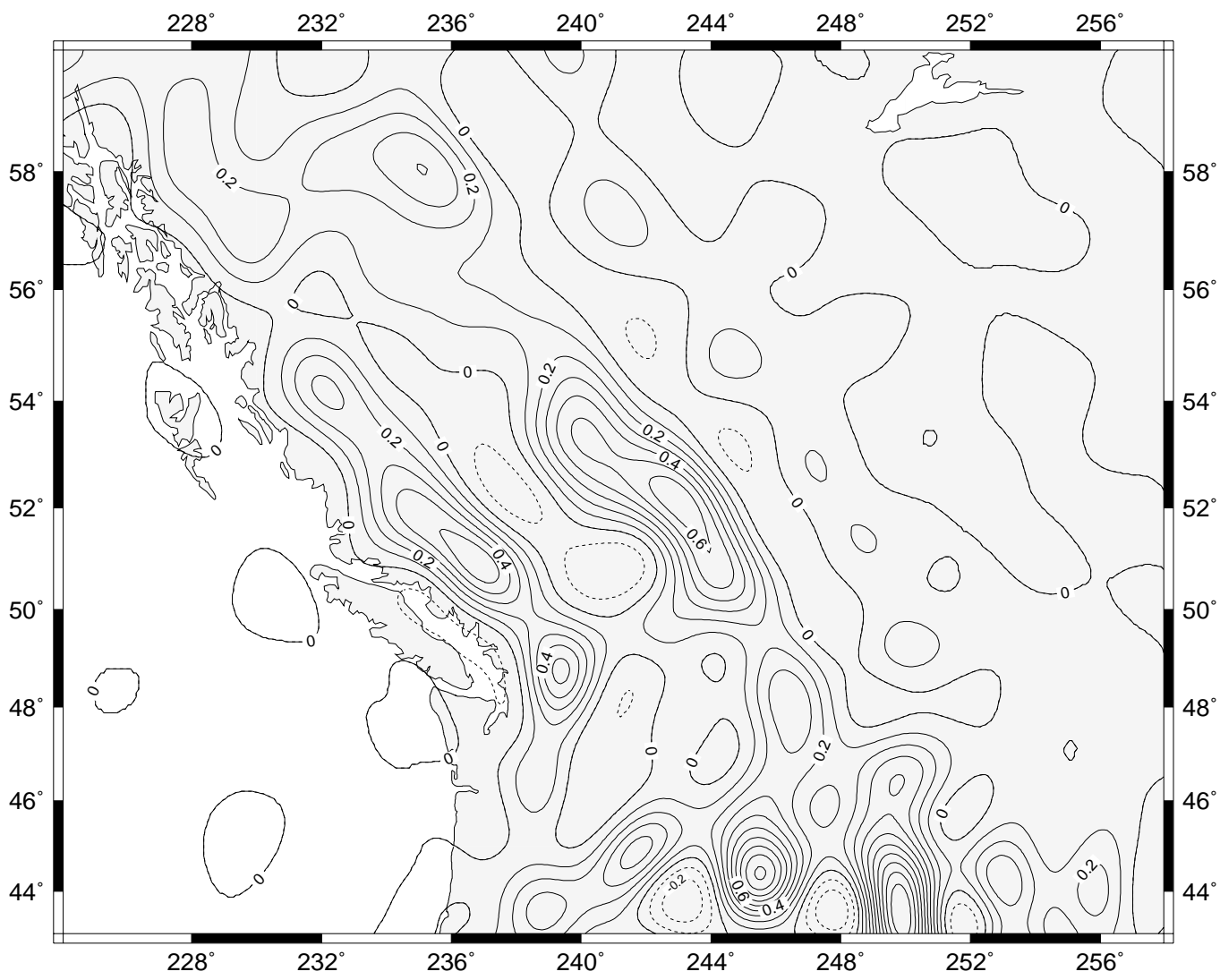Figure 7.23: Primary indirect topographical effect on geoid - near zone (m)

95

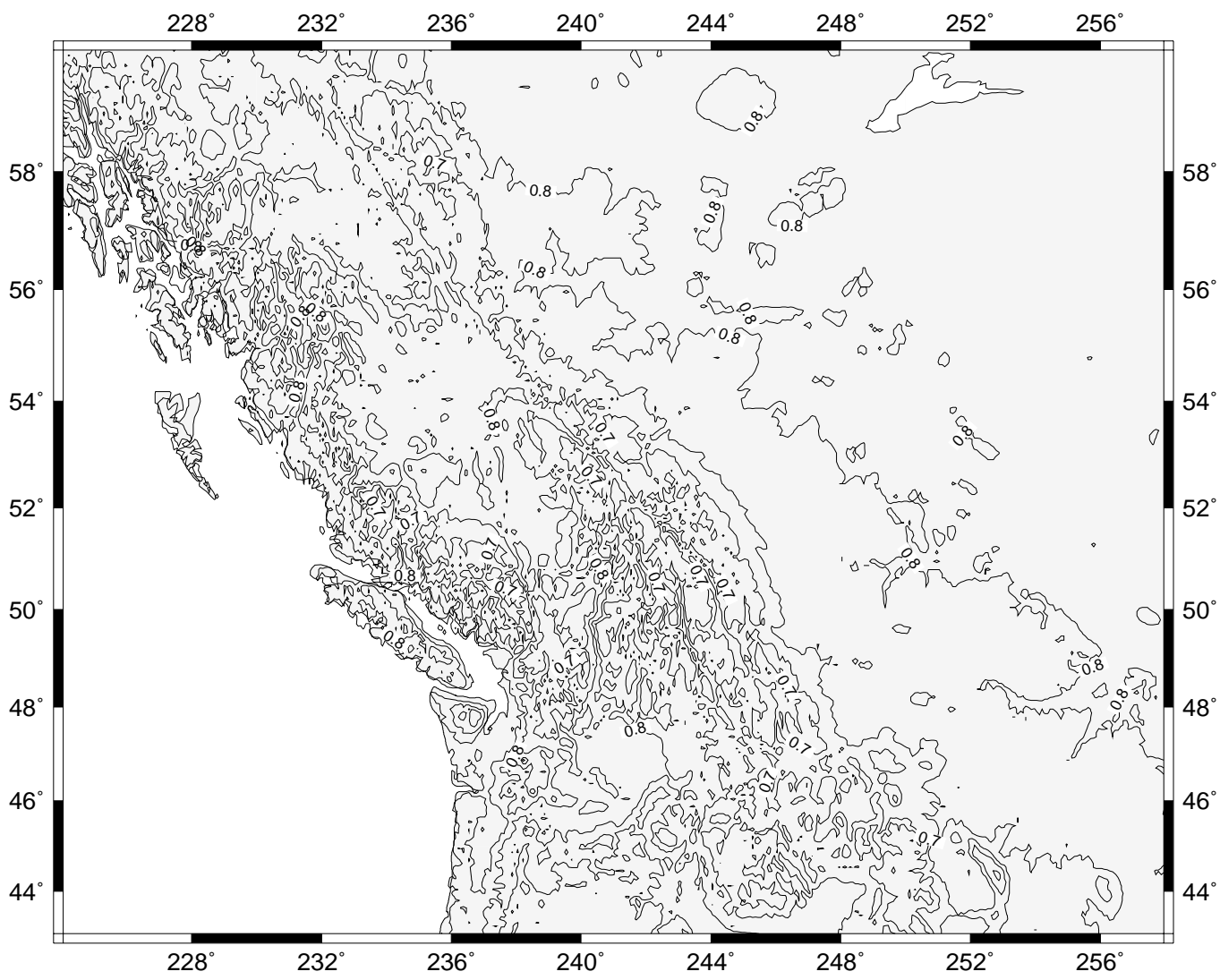Figure 7.24: Primary indirect topographical effect on geoid - distant zone (m)

96

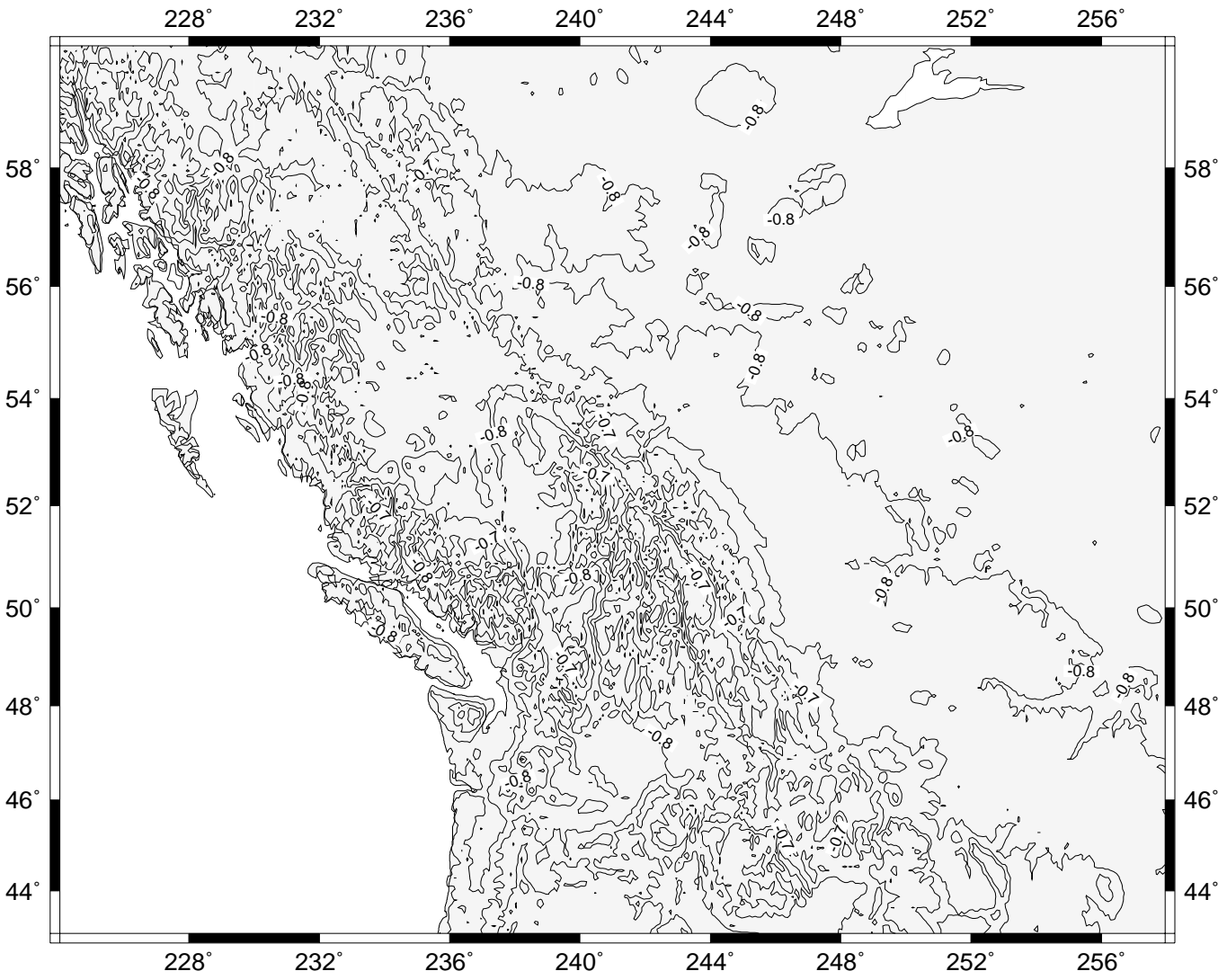Figure 7.25: Direct atmospheric effect on gravity (mGal)

Figure 7.26: Spherical part of direct atmospheric effect on gravity (mGal)

98
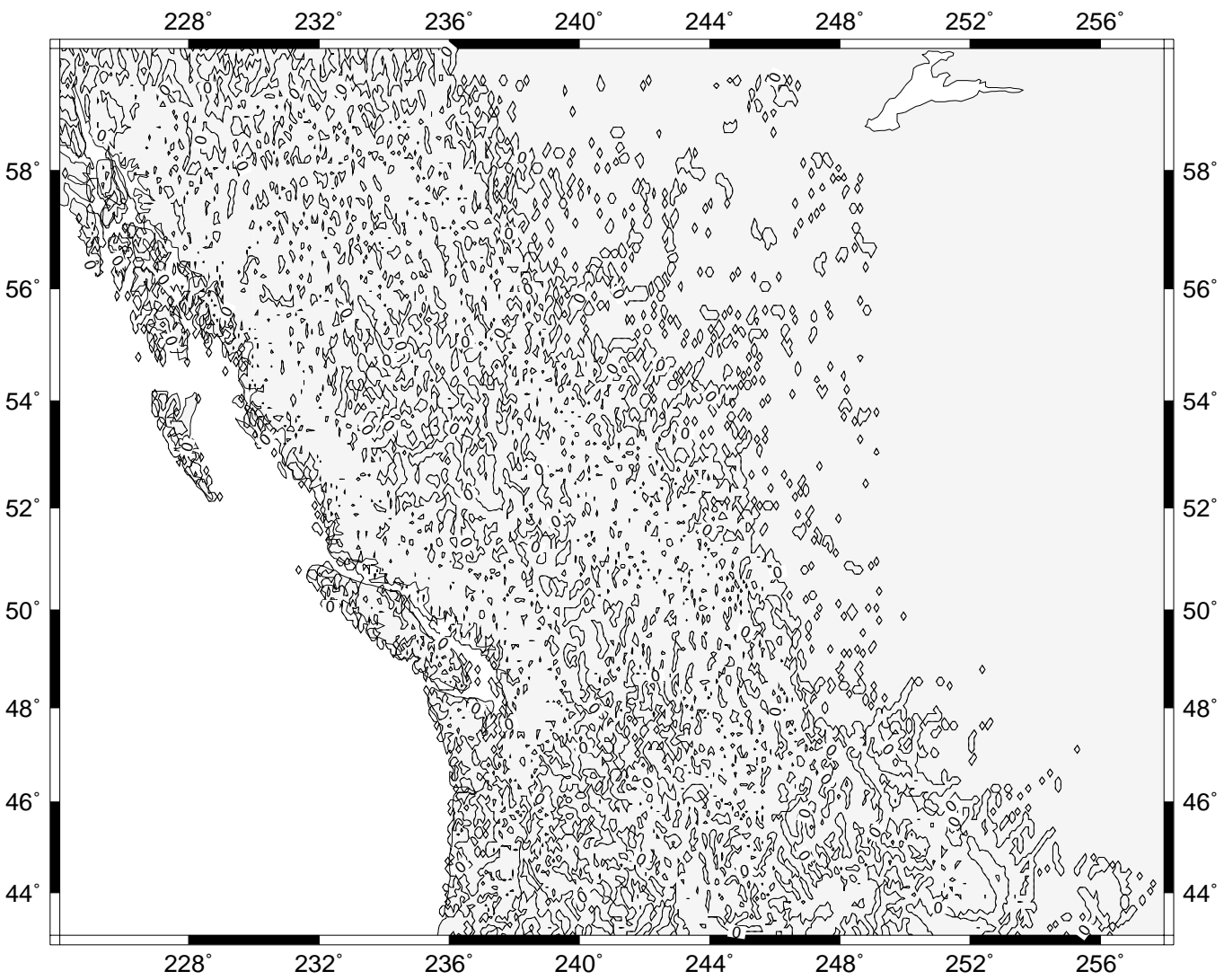
Figure 7.27: Terrain correction to direct atmospheric effect on gravity (mGal)

99

Figure 7.28: Direct atmospheric effect on geoid (m)
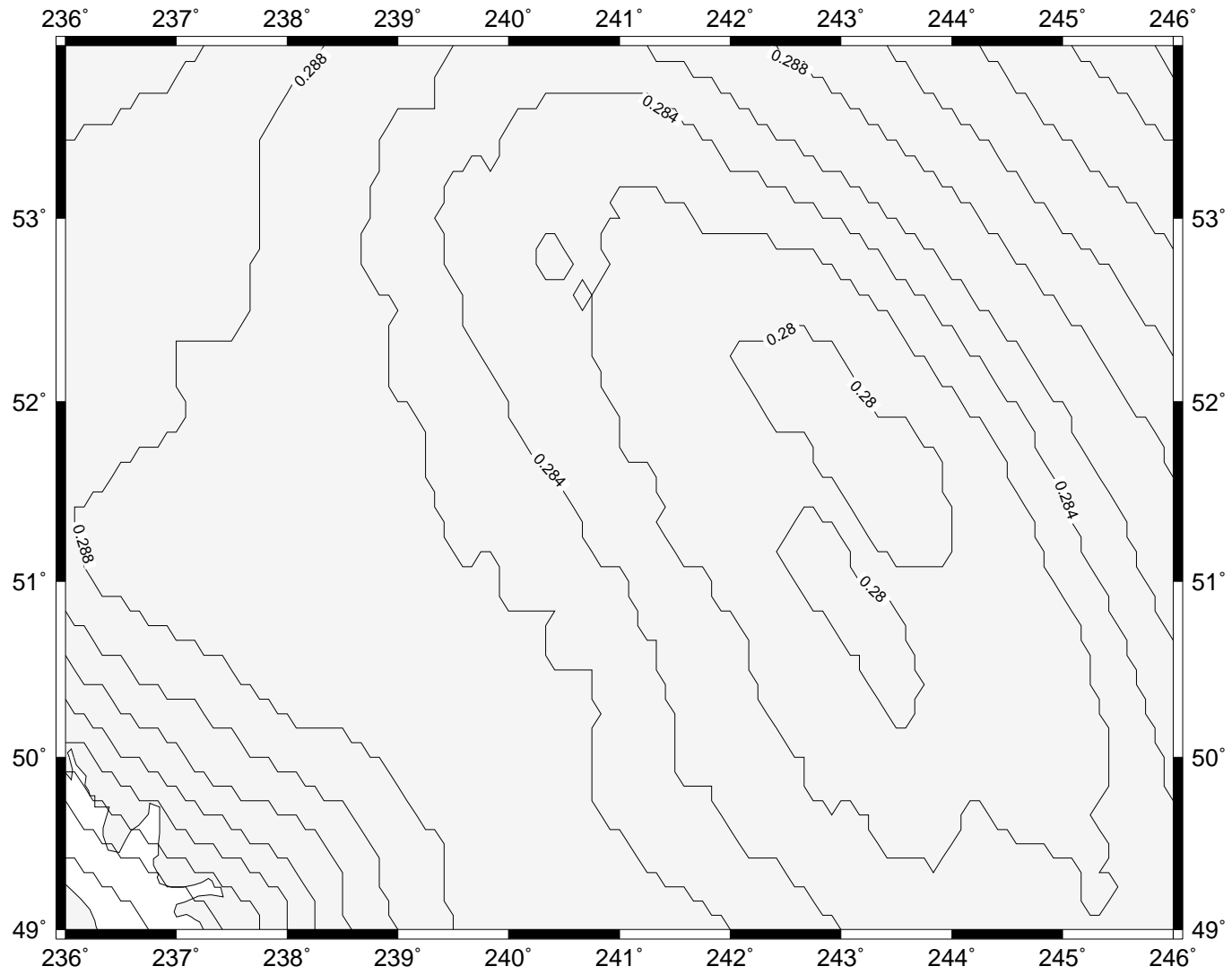
DEGREE VARIANCES: 361–1800

Synthetic Field (b=6.34d6) vs GPM98b

Figure 7.29: Degree variance of the synthetic data A vs GPM98B

DEGREE VARIANCES: 361–1800

Synthetic Field (b=6.35d6) vs GPM98b

Figure 7.30: Degree variance of the synthetic data B vs GPM98B

Figure 7.31: Degree 2160 spheroid A (m)

Figure 7.32: Statistics for the degree 2160 spheroid A (m)

104

Figure 7.33: Degree 2160 spheroid B (m)
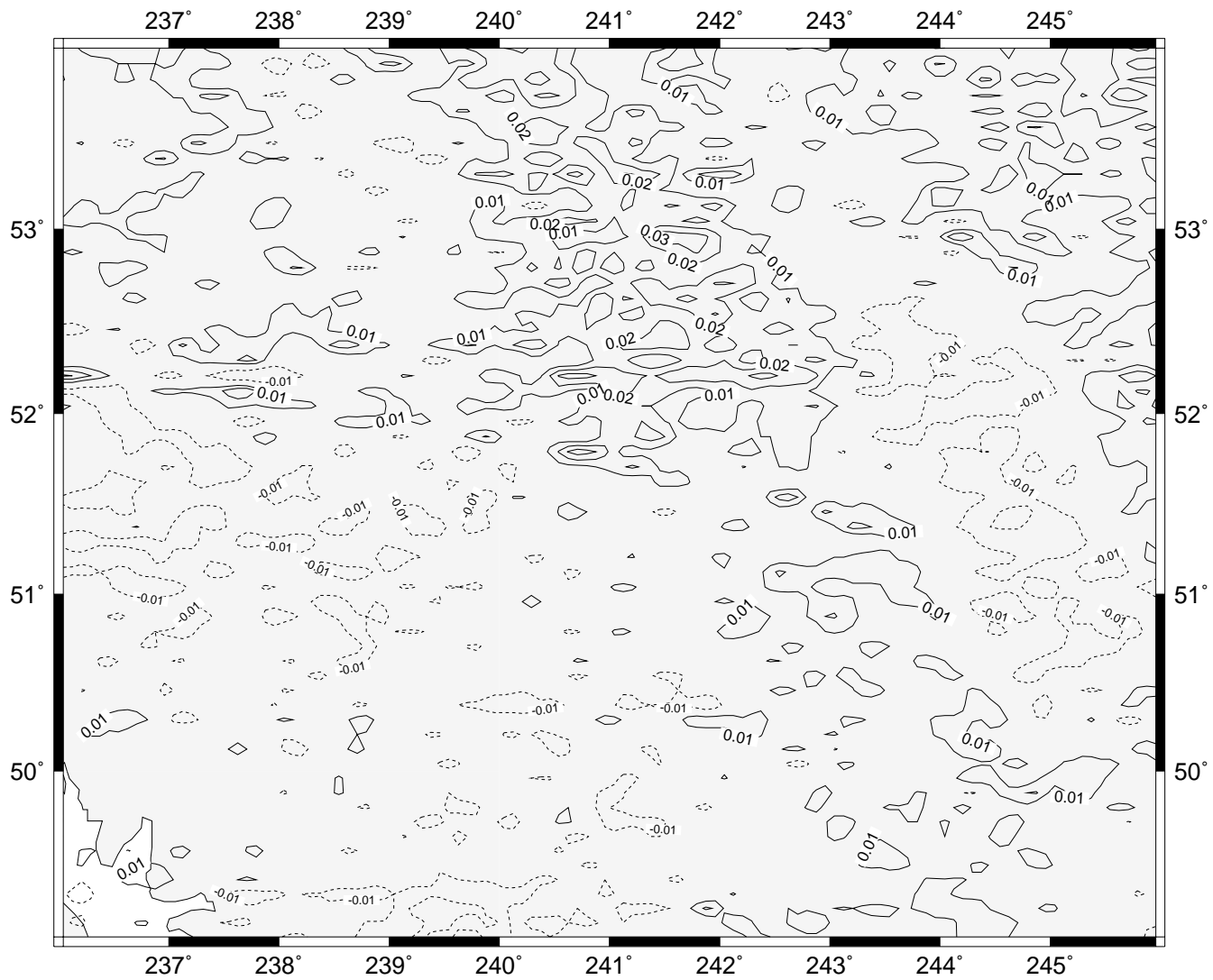
Figure 7.34: Statistics for the degree 2160 spheroid B (m)

Chapter 8

Conclusions and Recommendations

Conclusions of the research presented herewith are summarized in the first part of this chapter. In *Chapter (3)*, the mathema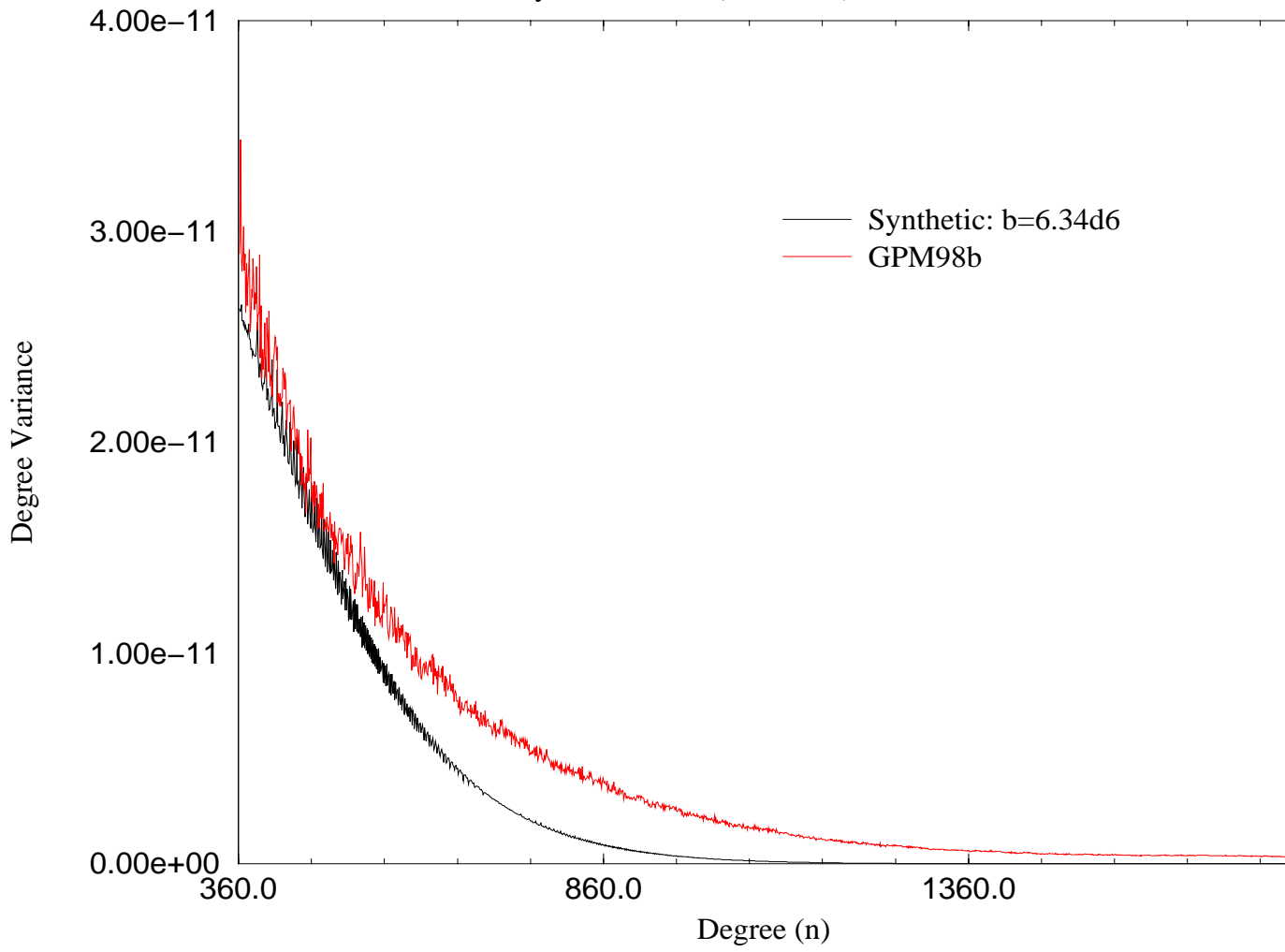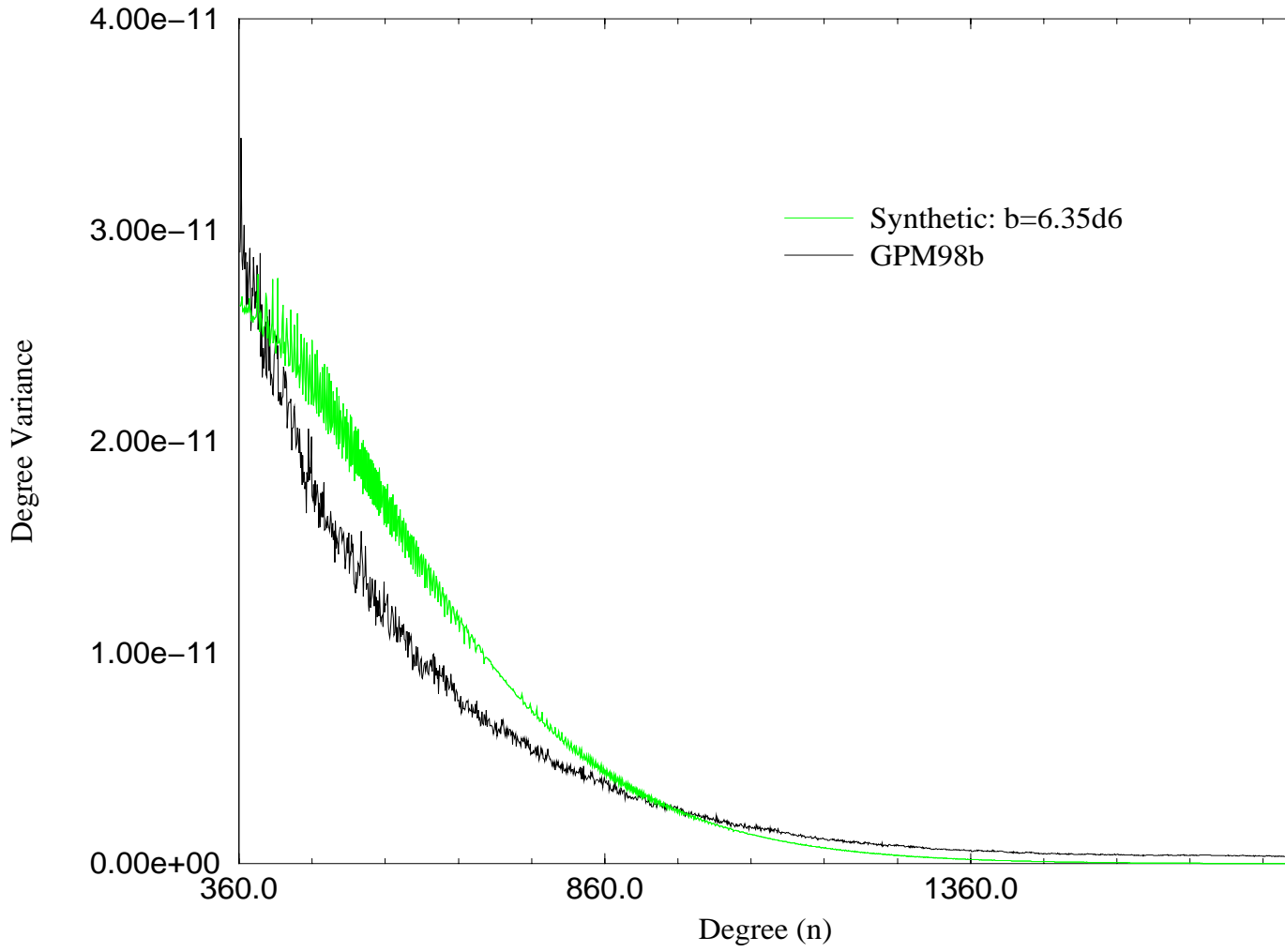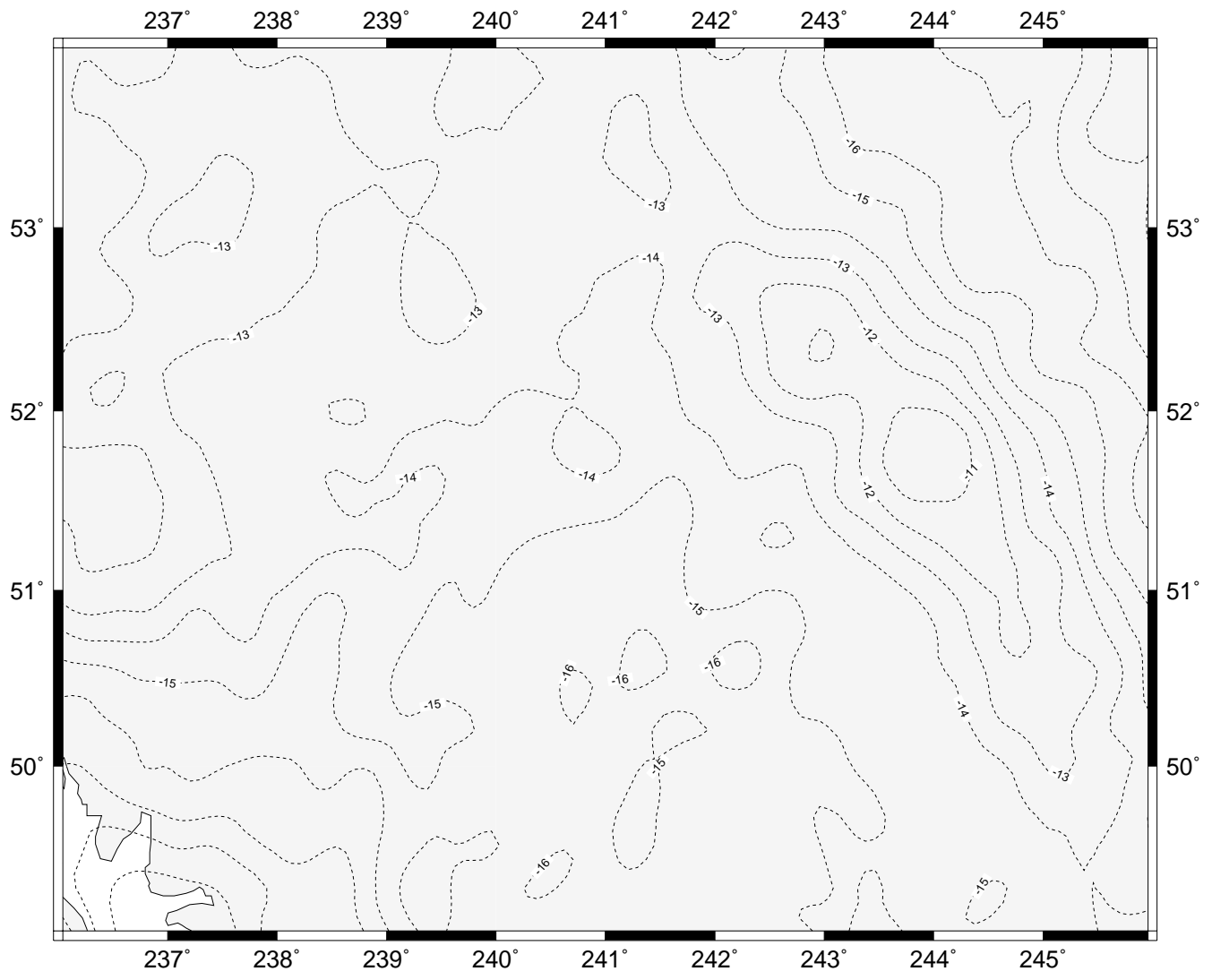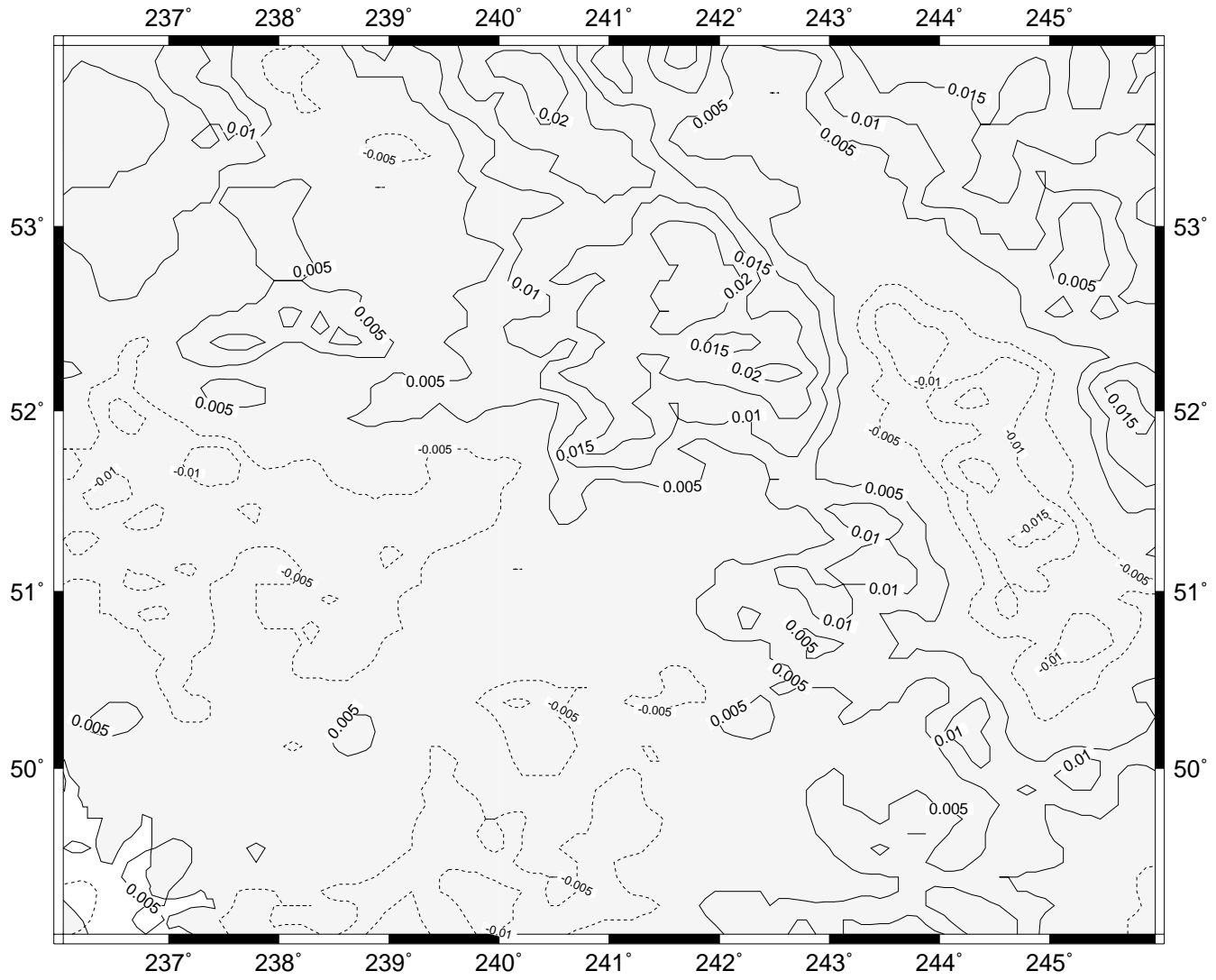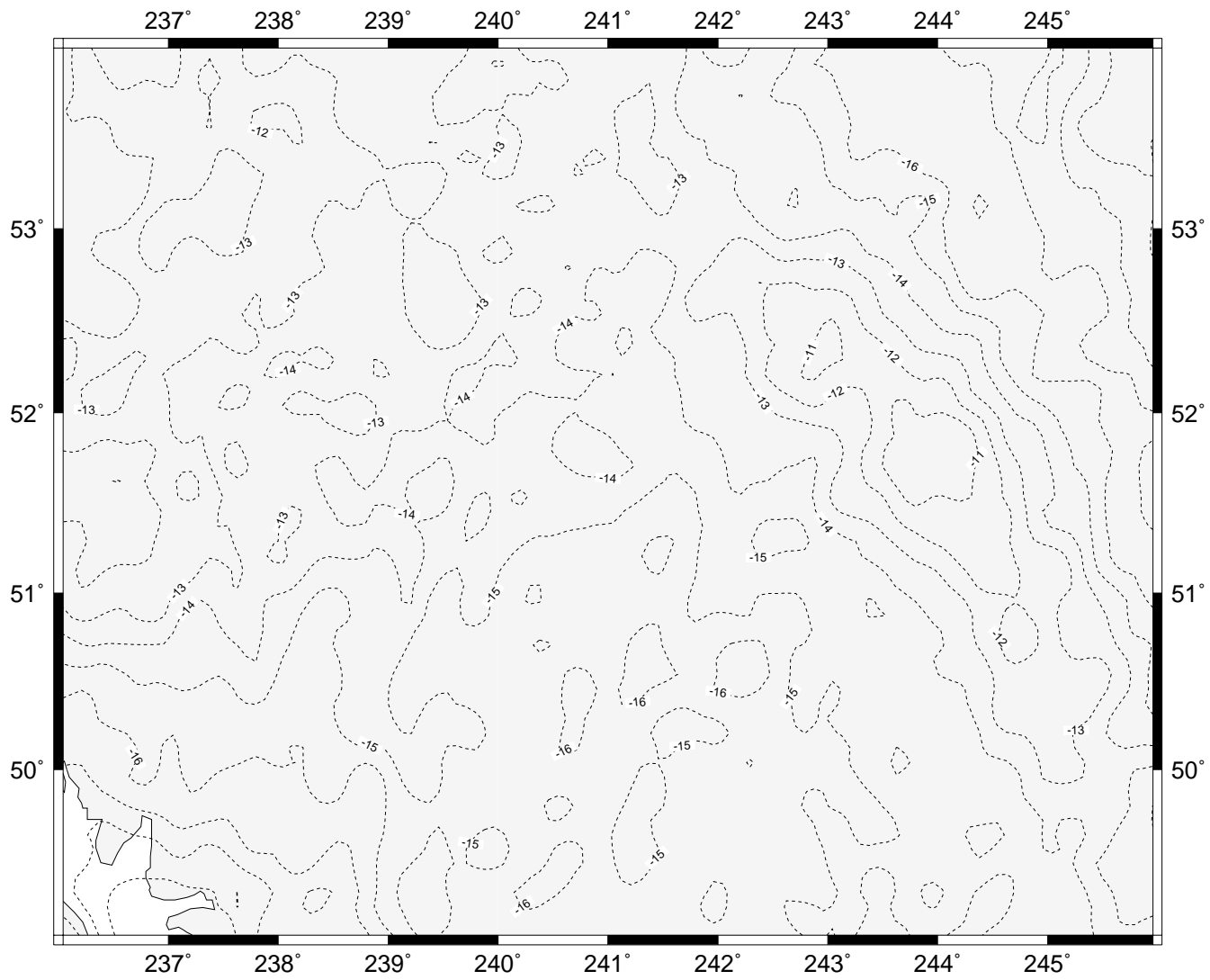tical model for the determination of the gravimetric geoid represented by the geodetic boundary-value problem was derived. The shape and size of the unknown boundary surface (the geoid) were approximated by the geocentric reference sphere. The earth's gravity field was approximated by the normal field generated by the geocentric reference ellipsoid. Based on this formulation, appropriate input data for the model were defined including their derivation from the observed values of gravity. In the last section of this chapter, the entire problem was re-formulated for the reference field generated by a low-frequency reference spheroid which can be derived from a global geopotential model.

Following the theoretical formulations, formulae for the proper gravity reduction were derived in *Chapter (4)*. Using the mass-conservation approach for the condensation of external topographical and atmospheric masses, spherical formulae for the practical evaluation of all topographical and atmospheric effects on gravity and the geoid were derived. The spherical modelling of the topographical masses represents a significant improvement with respect to widely used planar formulae. In this spherical model, the effects of distant topographical masses both on gravity and the geoid can be formulated using the spectral method and spherical harmonic representation

107

of the global topography. Omitting these effects in the geoid computations causes a significant long-wavelength errors to the geoid. The second Helmert condensation was also applied to the atmospheric masses, and all atmospheric effects both in gravity and geoidal space were derived. This step finalized the effort for the derivation of the gravity data which could be used in the boundary-value problems without violating the basic mathematical principles.

Due to large numerical values of the direct and primary indirect topographical effects, the necessity to use the densest and most accurate elevation data seems to be inevitable for the evaluation of the near zones. Effects of distant topographical masses have to be taken into the account using either spatial or spectral techniques. The proper condensation of atmospheric masses brought about numerical values for the direct atmospheric effect similar to those which can be derived from official tables of the internationally adopted corrections. Other atmospheric effects, but the primary indirect atmospheric effect on the geoid, are too small to be applied in the determination of the one-centimetre geoid.

Theoretical derivations leading to the computation of the residual gravity data on the geoid were presented in *Chapter (5)*. The reference part of both the topographical and atmospheric residual potentials was first derived using the spectral method and a global topographical model. The reference topographical and atmospheric effects on gravity were obtained and subsequently deployed for the derivation of the Helmert residual gravity anomaly. Although no numerical values were provided here, derived formulae could easily be implemented.

A practical approach to the numerical evaluation of the residual gravimetric geoid was presented in *Chapter (6)*. First, the appropriate form of the integration kernel was derived from the spherical Stokes function by removing its low-frequency part. To keep the contribution of the distant gravity data as small as possible, the Molodenskij modification of the spheroidal Stokes kernel was employed and appropriate modification coefficients were derived. The weak singularity of the Stokes kernel was removed

analytically. Although the contribution of the distant gravity data was kept small when deploying the modified kernel, its values were still evaluated using the Molodenskij spectral approach and a global gravity model. The accuracy of a numerical approach was then tested using the higher-degree synthetic gravity data. Assuming the same density of gravity data as that in Canada, a centimetre-level accuracy of results can be expected if errorless data are employed.

Recommendations for further research conclude this final chapter. The ellipsoidal correction to the spherical Stokes kernel must be implemented in the near future including its modification and solution of its singularity. Appropriate modifications of existing computer routines for the ellipsoidal correction to the spherical kernel should provide results according to the latest theoretical developments. Estimated values of this effect on the geoidal height are in the centimetre level and thus very important in view of the one-centimetre geoid.

The density and accuracy requirements for the elevation data should be further investigated. Implementation of the anomalous topographical density into formulae is necessary though only a limited knowledge is available today. The density effects might reach the decimetre level for areas with very rough topography. The accuracy of topographical corrections represents one of the major limitations in the present determination of the accurate gravimetric geoid.

Evaluation of the gravitational effect of the distant atmospheric masses might be the next step in the proper atmospheric reduction. Due to the smallness of values of atmospheric corrections, effects of temporal variations of basic atmospheric parameters on the atmospheric corrections to gravity and geoid are not necessary. Because of the reasonable match of values obtained using spherical and ellipsoidal approximations, and density models with variable complexity, there is a low priority for any additional research of gravitational effects of atmospheric masses on the gravimetric geoid.

Gravity information on a denser grid than $5'$ is necessary for the solution of one-centimetre geoid over complex parts of the gravity field. Since this requires more costly observations, there is only a low probability for the determination of the one-centimetre regional gravimetric geoid in the near future. This applies especially to areas with major mountains such as the territory of western Canada. However, this statement should not prevent us from the formulation of suitable theories as was attempted in this dissertation.

References

Anderson, E. G., C. Rizos, and R. S. Mather (1975). Atmospheric effects in physical geodesy. University of New South Wales, Kensigton.

Balmino, G. (1983). A few remarks on the Earth's atmosphere effects on the geoid, the free-air gravity anomalies, the altimetric geoid, and combination procedures in the global geopotential model computation. *Bulettin d'Information*, No. 53, Bureau Gravimetrique International, Brussels.

Bomford, G. (1971). *Geodesy*. 3rd edition, Clarendon Press.

Bruns, H. (1878). *Die Figur der Erde*. Publikation des Königlichen Preussischen Geodätischen Institutes, Berlin.

Cruz, J. Y. (1985). Disturbance vector in space from surface gravity anomalies using complementary models. Report No. 366, Ohio State University, Columbus.

Ecker, E. and E. Mittermayer (1969). Gravity corrections for the influence of the atmosphere. *Bollettino di Geofisica Teoretica ed Applicata*, No. XI., pp. 70-80.

Gauss, C. F. (1828). Bestimmung des Breitenunterschiedes zwischen den Sternwarten von Göttingen und Altona durch Beobachtungen am Ramsdenschen Zenithsector. Vandenhoeck u. Ruprecht, Göttingen.

Gradshteyn, I. S. and I. M. Ryzhik (1980). *Tables of integrals, series, and products.* Academic Press, New York.

Harrie, L. (1993). Some specific problems in the geoid determination. M.Sc. Thesis, Royal Institute of Technology, Stockholm.

Heck, B. (1993). A revision of Helmert's second method of condensation in the geoid and quasigeoid determination. Presented at 7th I.A.G. Symposium "Geodesy and Physics of the Earth", No. 112, Potsdam, October 1992.

Heiskanen, W. A. and H. Moritz (1967). *Physical geodesy.* Freeman and Co., San Francisco.

Helmert, F. R. (1884). *Die mathematische und physikalische Theorien der höheren Geodäsie.* B. G. Taubner, Leipzig.

Hobson, E. W. (1931). *The theory of spherical and ellipsoidal harmonics.* Chelsea, New York.

Hörmander, L. (1976). The boundary problems of physical geodesy. *Archive for Rational Mechanics and Analysis*, 62, pp.1-52.

Huang, J. and P. Vaníček (1999). A faster algorithm for numerical Stokes's integration. Presented at the annual meeting of the Canadian Geophysical Union, Banff, May 9-13.

Huang, J., P. Vaníček, W. Brink, and S. Pagiatakis (1999). Effect of topographical mass density variation on gravity and the geoid. Spring meeting of the American Geophysical Union, Boston, May 31 - June 3.

Huygens, C. (1673). *Horologium Oscillatorium.* Hagae.

Jekeli, C. (1981). The downward continuation to the Earth's surface of truncated spherical and ellipsoidal harmonic series of the gravity and height anomalies. Report No. 323, Ohio State University, Columbus.

Kellogg, O.D. (1929). *Foundations of potential theory.* Springer, Berlin.

Korn, G. A. and T. M. Korn (1968). *Mathematical handbook for scientists and engineers.* McGraw-Hill Book Company, New York.

Lambert, W. D. (1930). Reduction of the observed values of gravity to sea level. *Bulletin Géodésique*, No. 26, pp. 107-181.

Lemoine, F. G., D. E. Smith, L. Kunz, R. Smith, E. C. Pavlis, N. K. Pavlis, S. M. Klosko, D. S. Chinn, M. H. Torrence, R. G. Williamson, C. M. Cox, K. E. Rachlin, Y. M. Wang, S. C. Kenyon, R. Salman, R. Trimmer, R. H. Rapp, and S. Neren (1996). The development of the joint geopotential model. International Association of Geodesy, Springer, Berlin, vol. 117, pp. 461-469.

MacMillan, W. D. (1930). *The theory of the potential.* Dover, New York.

Mader, R. S. (1973). A solution of the geodetic boundary-value problem to order e^3. X-592-73-11, Goddard Space Flight Center, National Aeronautics and Space Administration, Greenbelt.

Martinec, Z. (1993). Effect of lateral density variations of topographical masses in view of improving geoid model accuracy over Canada. Contract report for the Geodetic Survey Division, Natural Resources Canada, Ottawa.

Martinec, Z. and P. Vaníček (1994a). Indirect effect of topography in the Stokes-Helmert technique for a spherical approximation of the geoid. *Manuscripta Geodaetica*, No. 19, pp. 213-219.

Martinec, Z. and P. Vaníček (1994b). Direct topographical effect of Helmert's condensation for a spherical approximation of the geoid. *Manuscripta Geodaetica*, No. 19, pp. 257-268.

Martinec, Z. (1995). Boundary-value problems for gravimetric determination of a precise geoid. Dr.Sc. Thesis, Department of Geophysics, Charles University, Prague.

Martinec, Z. and P. Vaníček (1996). Formulation of the boundary-value problem for the geoid determination with a higher-degree reference field. *Geophysical Journal International*, No. 126, pp. 219-228.

Martinec, Z., P. Vaníček, A. Mainville, and M. Véronneau (1996). Evaluation of topographical effects in precise geoid computation from densely sampled heights. *Journal of Geodesy*, No. 70, pp. 746-754.

Martinec, Z. (1998). Boundary-value problems for gravimetric determination of a precise geoid. *Lecture notes in earth sciences*, 73, Springer.

Merry, C. L. and P. Vaníček (1974). The geoid and datum translation components. *The Canadian Surveyor*, 28, pp. 56-62.

Molodenskij, M. S., V. F. Eremeev, and M. I. Yurkina (1960). *Methods for study of the external gravitational field and figure of the Earth.* Translated from Russian by the Israel program for scientific translations, Office of Technical Services, Department of Commerce, Washington, D.C., 1962.

Moritz, H. (1974). Precise gravimetric geodesy. Report No. 233, Ohio State University, Columbus.

Moritz, H. (1984). Geodetic Reference System 1980. *Bulletin Géodésique*, No. 58, pp. 388-398.

Moritz, H. (1990). *The figure of the earth: theoretical geodesy and the earth interior.* Wichmann, Karlsruhe.

Najafi, M. A. (1996). Contributions towards the computation of a precise regional geoid. Ph.D. Thesis, University of New Brunswick, Fredericton.

Newton, I. (1687). *Philosophiae Naturalis Principia Mathematica.* London.

Paul, M. (1973). A method of evaluation the truncation error coefficients for geoidal heights. *Bulletin Géodésique*, 110, 413-425.

Pizzetti, P. (1911). Sopra il Calcolo Teorico delle Deviazioni del Geoide dall' Ellisoide. Atti Reale Accademia delle Scienze, 46, Torino.

Rektorys, K. (1995). *Survey of applicable mathematics*. Prometheus, Prague.

Rummel, R. and R. Rapp (1976). The influence of the atmosphere on the geoid and potential coefficient determinations from gravity data. *Journal of Geophysical Research*, No. 32, pp. 5639-5642.

Schwarz, K. P., M. G. Sideris, and R. Forsberg (1990). The use of FFT techniques in physical geodesy. *Geophysical Journal International*, No. 100, pp. 485-514.

Somigliana, C. (1929). Teoria Generale del Campo Gravitazionale dell'Ellisoide di Rotazione. *Memoire della Societa Astronomica Italiana*, IV, Milano.

Spiegel, M. R. (1974). *Theory and problems of advanced calculus*. McGraw-Hill Book Company. New York.

Stokes, G. G. (1849). On the variation of gravity on the surface of the Earth. *Transactions of the Cambridge Philosophical Society*, No. 8, pp. 672-695.

Torge, W. (1989). *Gravimetry*. Walter de Gruyter, Berlin & New York.

Tscherning, C. G. (1985). Geoid modelling using the collocation in Scandinavia and Greenland. *Manuscripta Geodaetica*, No. 9.

United States Standard Atmosphere (1976). Joint model of the National Oceanic and Atmospheric Administration, National Aeronautics and Space Administration, and United States Air Force, Washington, D.C.

Vaníček, P. and A. Kleusberg (1986). Towards a new combined geoid for Canada. *Bollettino di Geodesia e Scienze Affini*, No. XLV, p. 2.

Vaníček, P. and E. J. Krakiwsky (1986). *Geodesy: The Concepts.* 2nd corrected edition, North Holland, Amsterdam.

Vaníček, P. and A. Kleusberg (1987). The Canadian geoid – Stokesian approach. *Manuscripta Geodaetica*, No. 12, pp. 86-98.

Vaníček, P., A. Kleusberg, R. G. Chang, H. Fashir, N. Christou, M. Hofman, T. Kling, and T. Arsenault (1987). The Canadian geoid. Technical Report No. 129, University of New Brunswick, Fredericton.

Vaníček, P. and L. E. Sjøberg (1991). Reformulation of Stokes's theory for higher than second-degree reference field and a modification of integration kernels. *Journal of Geophysical Research*, No. 96, pp. 6529-6539.

Vaníček, P., Z. Changyou, and L. E. Sjøberg (1991). A comparison of Stokes's and Hotine's approaches to geoid computation. *Manuscripta Geodaetica*, No. 17, pp. 29-35.

Vaníček, P. and Z. Martinec (1994). The Stokes-Helmert scheme for the evaluation of a precise geoid. *Manuscripta Geodaetica*, No. 19, pp. 119-128.

Vaníček, P., M. Najafi, Z. Martinec, L. Harrie, and L. E. Sjøberg (1995). Higher-degree reference field in the generalized Stokes-Helmert's scheme for geoid computation. *Journal of Geodesy*, No. 70, pp. 176-182.

Vaníček, P., W. Sun, P. Ong, Z. Martinec, M. Najafi, P. Vajda, and B. Ter Horst (1996). Downward continuation of Helmert's gravity. *Journal of Geodesy*, No. 71, pp. 21-34.

Vaníček, P., M. Najafi, P. Novák, and J. Huang (1997). Evaluation of boundary values in generalized Stokes-Helmert problem. Contract report for the Geodetic Survey Division, Natural Resources Canada, Ottawa.

Vaníček, P., J. Huang, P. Novák, S. Pagiatakis, M. Véronneau, Z. Martinec, and W. Featherstone (1999). Determination of boundary values for the Stokes-Helmert problem. *Journal of Geodesy*, No. 73, pp. 180-192.

Wenzel, G. (1998). Ultra-high degree geopotential models GPM98A, B, and C to degree 1800. Proceedings of the joint meeting of the International Gravity Commission and International Geoid Commission, September 7-12, Trieste.

Wichiencharoen, C. (1982). The indirect effects on the computation of geoid undulations. Report No. 336, Ohio State University, Columbus.

Wieser, M. (1987). The global digital terrain model TUG87. Internal report on set-up, origin, and characteristics. Institute of Mathematical Geodesy, Technical University, Graz.

Appendix A

Theoretical Derivations

A.1 Integration kernels $\mathcal{M}_1$ and $\mathcal{M}_2$

Due to the complexity of expressions deployed in the following derivations, a simplified notation is introduced in the following equation for the parameter

$$\eta = \frac{R + H(\Omega')}{R + H(\Omega)} = \frac{R + H'}{R + H} = \frac{r'}{r} \ . \tag{A.1}$$

Following this notation, another unitless quantity is defined as follows

$$\zeta = \frac{r' - r}{r} = \frac{H' - H}{R + H} = \eta - 1 \ . \tag{A.2}$$

Newton's kernel can be developed into a series which is convergent for every $|\zeta| < 1$

$$\mathcal{N}(r, \psi, r') = (r^2 + r'^2 - 2\,r\,r'\cos\psi)^{-\frac{1}{2}} = \frac{1}{r}\,(1 + \eta^2 - 2\,\eta\,\cos\psi)^{-\frac{1}{2}} =$$

$$= \frac{1}{r}\,(2 - 2\,\cos\psi)^{-\frac{1}{2}} \left(1 - \frac{\zeta}{2} + \frac{\zeta^2}{8}\,\frac{1 - 3\cos\psi}{1 - \cos\psi} \right) + \mathcal{O}(\zeta^3) \ . \tag{A.3}$$

Its inverse can similarly be expressed using another convergent series as

$$\mathcal{N}^{-1}(r, \psi, r') = (r^2 + r'^2 - 2\,r\,r'\cos\psi)^{\frac{1}{2}} = r\,(1 + \eta^2 - 2\,\eta\,\cos\psi)^{\frac{1}{2}} =$$

$$= r\,(2 - 2\,\cos\psi)^{\frac{1}{2}} \left(1 + \frac{\zeta}{2} + \frac{\zeta^2}{8}\,\frac{1 + \cos\psi}{1 - \cos\psi} \right) + \mathcal{O}(\zeta^3) \ . \tag{A.4}$$

Equation (4.21) can be formulated for the specified integration limits as

$$\mathcal{M}(r,\psi,r^{'}) \;=\; \frac{r^2}{2}\,(\eta \;+\; 3\;\cos\psi)\,(1\;+\;\eta^2 -\; 2\,\eta\;\cos\psi)^{\frac{1}{2}}\;+$$

$$+\,\frac{r^2}{2}\,(3\;\cos^2\psi\;-\;1)\;\ln\left|\frac{\eta\;-\;\cos\psi\;+\;(1\;+\;\eta^2 -\;2\,\eta\;\cos\psi)^{\frac{1}{2}}}{1\;-\;\cos\psi\;+\;(2\;-\;2\;\cos\psi)^{\frac{1}{2}}}\right|\;-$$

$$-\,\frac{r^2}{2}\,(1\;+\;3\;\cos\psi)\,(2\;-\;2\;\cos\psi)^{\frac{1}{2}}\;. \tag{A.5}$$

Next, Eqns. (A.3) and (A.4) are substituted into the following expression

$$(\eta\;+\;3\;\cos\psi)\,(1\;+\;\eta^2 -\;2\,\eta\;\cos\psi)^{\frac{1}{2}}\;\doteq$$

$$\doteq\;(1\;+\;\zeta\;+\;3\;\cos\psi)\,(2\;-\;2\;\cos\psi)^{\frac{1}{2}}\left(1\;+\;\frac{\zeta}{2}\;+\;\frac{\zeta^2}{8}\,\frac{1+\cos\psi}{1-\cos\psi}\right)\,, \tag{A.6}$$

and similarly into the logarithmic function

$$\ln\left|\frac{\eta\;-\;\cos\psi\;+\;(1\;+\;\eta^2 -\;2\,\eta\;\cos\psi)^{\frac{1}{2}}}{1\;-\;\cos\psi\;+\;(2\;-\;2\;\cos\psi)^{\frac{1}{2}}}\right|\;\doteq$$

$$\doteq\;\ln\left|1\;+\;\frac{\zeta\;+\;(2\;-\;2\;\cos\psi)^{\frac{1}{2}}\left(\frac{\zeta}{2}\;+\;\frac{\zeta^2}{8}\,\frac{1+\cos\psi}{1-\cos\psi}\right)}{1\;-\;\cos\psi\;+\;(2\;-\;2\;\cos\psi)^{\frac{1}{2}}}\right|\;. \tag{A.7}$$

This logarithm can be expanded into the Taylor series which is convergent for every $|\zeta|\;<\;1$ and $\psi\;>\;0$

$$\ln\left|1\;+\;\frac{\zeta\;+\;(2\;-\;2\;\cos\psi)^{\frac{1}{2}}\left(\frac{\zeta}{2}\;+\;\frac{\zeta^2}{8}\,\frac{1+\cos\psi}{1-\cos\psi}\right)}{1\;-\;\cos\psi\;+\;(2\;-\;2\;\cos\psi)^{\frac{1}{2}}}\right|\;=$$

$$=\;\zeta\,\frac{1\;+\;(2\;-\;2\;\cos\psi)^{\frac{1}{2}}\left(\frac{1}{2}\;+\;\frac{\zeta}{8}\,\frac{1+\cos\psi}{1-\cos\psi}\right)}{1\;-\;\cos\psi\;+\;(2\;-\;2\;\cos\psi)^{\frac{1}{2}}}\;-$$

$$-\,\frac{\zeta^2}{2}\left[\frac{1\;+\;(2\;-\;2\;\cos\psi)^{\frac{1}{2}}\left(\frac{1}{2}\;+\;\frac{\zeta}{8}\,\frac{1+\cos\psi}{1-\cos\psi}\right)}{1\;-\;\cos\psi\;+\;(2\;-\;2\;\cos\psi)^{\frac{1}{2}}}\right]^2\;+\;\dots \tag{A.8}$$

The second term from this series is taken into the account only rendering truncation errors negligible. Performing algebraic operations in Eqns. (A.6) and (A.8), then Eqn. (A.5) can be written as

$$
\mathcal{M}(r, \psi, r^{'}) \; \doteq \; \frac{r^2}{2} \; \zeta \; \frac{2 + (2 - 2 \; \cos \psi)^{\frac{1}{2}}}{1 - \cos \psi + (2 - 2 \; \cos \psi)^{\frac{1}{2}}} \; +
$$

$$
+ \; \frac{3 \; r^2}{4} \; \zeta^2 \; \frac{3 - 4 \cos \psi + \cos^2 \psi + 2 \; (1 - \cos \psi) \; (2 - 2 \cos \psi)^{\frac{1}{2}}}{(2 - 2 \cos \psi)^{\frac{1}{2}} \; \left[\; 1 - \cos \psi + (2 - 2 \cos \psi)^{\frac{1}{2}} \; \right]^2} \; . \tag{A.9}
$$

The sought integration kernels can be obtained from this expression substituting for ζ and ζ^2. They are subsequently used for the evaluation of the distant-zone effect.

A.2   Integration kernels $\mathcal{H}_1$, $\mathcal{H}_2$, and $\mathcal{H}_3$

In the case of the primary indirect topographical effect on gravity, the computation point is on the reference sphere. Introducing following two unitless quantities

$$
\eta \; = \; \frac{r}{R} \; = \; \frac{R \; + \; H}{R} \; = \; 1 \; + \; \zeta \; , \tag{A.10}
$$

and

$$
\eta^{'} \; = \; \frac{r^{'}}{R} \; = \; \frac{R \; + \; H^{'}}{R} \; = \; 1 \; + \; \zeta^{'} \; , \tag{A.11}
$$

the integration kernel $\mathcal{M}$ given by Eqn. (4.21) is now sought in the form

$$
\mathcal{M}(R, \psi, r, r^{'}) \; = \; \frac{R^2}{2} \; (\eta^{'} \; + \; 3 \; \cos \psi) \; (1 \; + \; \eta^{' \, 2} - \; 2 \; \eta^{'} \cos \psi)^{\frac{1}{2}} \; +
$$

$$
+ \; \frac{R^2}{2} \; (3 \; \cos^2 \psi \; - \; 1) \; \ln \left| \frac{\eta^{'} \; - \; \cos \psi \; + \; (1 \; + \; \eta^{' \, 2} - \; 2 \; \eta^{'} \cos \psi)^{\frac{1}{2}}}{\eta \; - \; \cos \psi \; + \; (1 \; + \; \eta^2 - \; 2 \; \eta \; \cos \psi)^{\frac{1}{2}}} \right| \; -
$$

$$
- \; \frac{R^2}{2} \; (\eta \; + \; 3 \; \cos \psi) \; (1 \; + \; \eta^2 - 2 \; \eta \; \cos \psi)^{\frac{1}{2}} \; . \tag{A.12}
$$

Substitutions introduced in Eqns. (A.3) and (A.4) are employed to derive following three expressions

$$(\eta' + 3 \cos \psi)(1 + \eta'^2 - 2 \eta' \cos \psi)^{\frac{1}{2}} \doteq$$

$$\doteq (1 + \zeta' + 3 \cos \psi)(2 - 2 \cos \psi)^{\frac{1}{2}} \left(1 + \frac{\zeta'}{2} + \frac{\zeta'^2}{8} \frac{1 + \cos \psi}{1 - \cos \psi} \right) , \quad (A.13)$$

$$(\eta + 3 \cos \psi)(1 + \eta^2 - 2 \eta \cos \psi)^{\frac{1}{2}} \doteq$$

$$\doteq (1 + \zeta + 3 \cos \psi)(2 - 2 \cos \psi)^{\frac{1}{2}} \left(1 + \frac{\zeta}{2} + \frac{\zeta^2}{8} \frac{1 + \cos \psi}{1 - \cos \psi} \right) , \quad (A.14)$$

$$\ln \left| \frac{\eta' - \cos \psi + (1 + \eta'^2 - 2 \eta' \cos \psi)^{\frac{1}{2}}}{\eta - \cos \psi + (1 + \eta^2 - 2 \eta \cos \psi)^{\frac{1}{2}}} \right| \doteq$$

$$\doteq \ln \left| 1 + \frac{\zeta' - \zeta + (2 - 2 \cos \psi)^{\frac{1}{2}} \left(\frac{\zeta' - \zeta}{2} + \frac{\zeta'^2 - \zeta^2}{8} \frac{1 + \cos \psi}{1 - \cos \psi} \right)}{\zeta - \cos \psi + (1 - \zeta^2 - 2 \zeta \cos \psi)^{\frac{1}{2}}} \right| . \quad (A.15)$$

After few algebraic operations, the above expressions can significantly be simplified, and the kernel $\mathcal{M}$ is derived in the form

$$\mathcal{M}(R, \psi, r, r') = \frac{3R^2}{4} (\zeta' - \zeta)(2 - 2 \cos \psi)^{\frac{1}{2}}(1 + \cos \psi) +$$

$$+ \frac{R^2}{8} (\zeta'^2 - \zeta^2) \frac{(3 \cos^2 \psi - 1)(1 + \cos \psi)}{(2 - 2 \cos \psi)^{\frac{1}{2}} \left[\eta - \cos \psi + (1 + \eta^2 - 2\eta \cos \psi)^{\frac{1}{2}} \right]} -$$

$$- \frac{R^2}{8} (\zeta' - \zeta)^2 (3 \cos^2 \psi - 1) \frac{3 - \cos \psi + 2 (2 - 2 \cos \psi)^{\frac{1}{2}}}{\left[\eta - \cos \psi + (1 + \eta^2 - 2\eta \cos \psi)^{\frac{1}{2}} \right]^2} +$$

$$+ \frac{R^2}{4} (\zeta' - \zeta)(3 \cos^2 \psi - 1) \frac{2 + (2 - 2 \cos \psi)^{\frac{1}{2}}}{\eta - \cos \psi + (1 + \eta^2 - 2\eta \cos \psi)^{\frac{1}{2}}} +$$

$$+ \frac{R^2}{8} (\zeta'^2 - \zeta^2) \frac{5 + 3 \cos^2 \psi}{(2 - 2 \cos \psi)^{\frac{1}{2}}} . \quad (A.16)$$

121

A.3 Integration kernels $\mathcal{K}_1$ and $\mathcal{K}_2$

The integration kernels for the direct topographical effect on gravity can be derived deploying the same approach described in Apx. (A.1). Using the same substitutions, the integration kernel $\mathcal{K}$, see Eqn. (4.59), can be first written as

$$\mathcal{K}(r, \psi, r') = r \, \frac{(3 + \eta^2) \, \cos \psi + \eta \, (1 - 6 \, \cos^2 \psi)}{(1 + \eta^2 - 2 \, \eta \, \cos \psi)^{\frac{1}{2}}} \, +$$

$$+ \, r \, (3 \cos^2 \psi - 1) \, \ln \left| \frac{\eta - \cos \psi + (1 + \eta^2 - 2 \, \eta \, \cos \psi)^{\frac{1}{2}}}{1 - \cos \psi + (2 - 2 \, \cos \psi)^{\frac{1}{2}}} \right| \, -$$

$$- \, r \, \frac{1 + 4 \, \cos \psi - 6 \, \cos^2 \psi}{(2 - 2 \, \cos \psi)^{\frac{1}{2}}} \, , \tag{A.17}$$

and subsequently developed into the form

$$\mathcal{K}(r, \psi, r') = -\frac{r}{2} \, \zeta \, (2 - 2 \cos \psi)^{-\frac{1}{2}} \, -$$

$$- \, \frac{r}{8} \, \zeta^2 \, \frac{3 - 10 \cos \psi + 3 \cos^2 \psi - 2 \, (3 \cos \psi - 1) \, (2 - 2 \cos \psi)^{\frac{1}{2}}}{(2 - 2 \cos \psi)^{\frac{1}{2}} \left[1 - \cos \psi + (2 - 2 \cos \psi)^{\frac{1}{2}} \right]^2} \, . \tag{A.18}$$

A.4 Integration kernels $\mathcal{N}_1$, $\mathcal{N}_2$, and $\mathcal{N}_3$

The auxiliary integration kernels which are required for the evaluation of the residual atmospheric potential are derived here. Three geocentric radii $r(\Omega)$, $r_1(\Omega')$, and $r_2(\Omega')$ define positions of the computation point, the lower integration limit, and the upper integration limit. Spatial distances for these three positions are defined as

$$i = 1, \, 2 \, : \, \mathcal{N}^{-1}(r, \psi, r_i) = (r^2 + r_i^2 - 2 \, r \, r_i \cos \psi)^{\frac{1}{2}} = l_i \, , \tag{A.19}$$

and a logarithm of the following expression is as follows

$$x = \ln \frac{r_2 - r \, \cos \psi + l_2}{r_1 - r \, \cos \psi + l_1} \, . \tag{A.20}$$

Using these substitutions, the integrals (4.101), (4.102), and (4.103) are derived as

$$\mathcal{N}_1(r, \psi, r_1, r_2) = \int_{\xi=r_1}^{r_2} \mathcal{N}(r, \psi, \xi) \, \xi^2 \, d\xi \; =$$

$$= \; \frac{1}{2} \left[\, r_2 \, l_2 \, - \, r_1 \, l_1 + \, 3 \, r \cos \psi \, (l_2 - \, l_1) \, + \, r^2 \, x \, (3 \cos^2 \psi \, - \, 1) \right] \, , \qquad \text{(A.21)}$$

$$\mathcal{N}_2(r, \psi, r_1, r_2) \; = \; \int_{\xi=r_1}^{r_2} \mathcal{N}(r, \psi, \xi) \, \xi^3 \, d\xi \; =$$

$$= \; \frac{1}{6} \left[\, 2 \, (r_2^2 \, l_2 \, - \, r_1^2 \, l_1) + \, 5 \, r \cos \psi \, (r_2 \, l_2 - \, r_1 \, l_1) \, + \right.$$

$$\left. + \; r^2 \, (15 \cos^2 \psi \, - \, 4) \, (l_2 - \, l_1) \, + \, 3 \, r^3 \, x \, \cos \psi \, (5 \cos^2 \psi \, - \, 3) \right] \, , \qquad \text{(A.22)}$$

$$\mathcal{N}_3(r, \psi, r_1, r_2) \; = \; \int_{\xi=r_1}^{r_2} \mathcal{N}(r, \psi, \xi) \, \xi^4 \, d\xi \; =$$

$$= \; \frac{1}{24} \left[\, 6 \, (r_2^3 \, l_2 \, - \, r_1^3 \, l_1) \, + \, 14 \, r \cos \psi \, (r_2^2 \, l_2 - \, r_2^2 \, l_2) \, + \right.$$

$$+ \, r^2 \, (35 \cos^2 \psi \, - \, 9) \, (r_2 \, l_2 - \, r_1 \, l_1) \, + \, 5 \, r^3 \cos \psi \, (21 \cos^2 \psi \, - \, 11) \, (l_2 - \, l_1) \, +$$

$$\left. + \; 3 \, r^4 \, x \, (35 \cos^4 \psi \, - \, 30 \cos^2 \psi \, + \, 3) \right] \, . \qquad \text{(A.23)}$$

A.5   Integration kernels $\mathcal{J}_1$, $\mathcal{J}_2$, and $\mathcal{J}_3$

Additional substitutions are introduced here

$$i \; = \; 1, \, 2 \; : \; \alpha_i \; = \; \frac{r \; - \; r_i \cos \psi}{l_i} \, , \qquad \text{(A.24)}$$

$$i \; = \; 1, \, 2 \; : \; \beta_i \; = \; \frac{\alpha_i \, - \; \cos \psi}{r_i \, - \; r \; \cos \psi \, + \, l_i} \, . \qquad \text{(A.25)}$$

The integration kernels (4.113), (4.114), and (4.115) are then derived as follows

$$
\mathcal{J}_1(r,\psi,r_1,r_2) \; = \; \left.\frac{\partial}{\partial r}\right|_r \; \int_{\xi=r_1}^{r_2} \mathcal{N}(r,\psi,\xi)\,\xi^2\,d\xi \; =
$$

$$
= \; \frac{1}{2}\,\Big[\; r_2\,\alpha_2 \; - \; r_1\,\alpha_1 \; + \; 3\cos\psi\,(l_2 \; - \; l_1) \; + \; 2\,r\,x\,(3\cos^2\psi \; - \; 1) \; +
$$

$$
+ \; 3\,r\cos\psi\,(\alpha_2 \; - \; \alpha_1) \; + \; r^2\,(3\cos^2\psi \; - \; 1)\,(\beta_2 \; - \; \beta_1)\;\Big]\;, \qquad\qquad \text{(A.26)}
$$

$$
\mathcal{J}_2(r,\psi,r_1,r_2) \; = \; \left.\frac{\partial}{\partial r}\right|_r \; \int_{\xi=r_1}^{r_2} \mathcal{N}(r,\psi,\xi)\,\xi^3\,d\xi \; =
$$

$$
= \; \frac{1}{6}\,\Big[\; 2\,(r_2^2\,\alpha_2 \; - \; r_1^2\,\alpha_1) \; + \; 5\cos\psi\,(r_2\,l_2 \; - \; r_1\,l_1) \; +
$$

$$
+ \; r\,(30\cos^2\psi \; - \; 8)\,(l_2 \; - \; l_1) \; + \; 5\,r\cos\psi\,(r_2\,\alpha_2 \; - \; \alpha_1\,l_1) \; +
$$

$$
+ \; r^2\,(15\cos^2\psi \; - \; 4)\,(\alpha_2 \; - \; \alpha_1) \; + \; 9\,r^2\,x\;\cos\;\psi\,(5\cos^2\psi - 3) \; +
$$

$$
+ \; 3\,r^3\cos\psi\,(5\cos^2\psi - 3)\,(\beta_2 \; - \; \beta_1)\;\Big]\;, \qquad\qquad \text{(A.27)}
$$

$$
\mathcal{J}_3(r,\psi,r_1,r_2) \; = \; \left.\frac{\partial}{\partial r}\right|_r \; \int_{\xi=r_1}^{r_2} \mathcal{N}(r,\psi,\xi)\,\xi^4\,d\xi \; =
$$

$$
= \; \frac{1}{24}\,\Big[\; 6\,(r_2^3\,\alpha_2 \; - \; r_1^3\,\alpha_1) \; + \; 14\cos\psi\,(r_2^2\,l_2 \; - \; r_1^2\,l_1) \; +
$$

$$
+ \; 14\,r\cos\psi\,(r_2^2\,\alpha_2 \; - \; r_1^2\,\alpha_1) \; + \; 2\,r\,(35\cos^2\psi \; - \; 9)\,(r_2\,l_2 \; - \; r_1\,l_1) \; +
$$

$$
+ \; r^2\,(35\cos^2\psi - 9)\,(r_2\,\alpha_2 - r_1\,\alpha_2) \; + \; 15\,r^2\cos\psi\,(21\cos^2\psi - 11)\,(l_2 - l_1) \; +
$$

$$
+ \; 5\,r^3\cos\psi\,(21\cos^2\psi - 11)\,(\alpha_2 - \alpha_1) \; + \; 12\,r^3\,x\,(35\cos^4\psi - 30\cos^2\psi + 3) \; +
$$

$$
+ \; 3\,r^4\,(35\cos^4\psi \; - \; 30\cos^2\psi \; + \; 3)\,(\beta_2 \; - \; \beta_1)\;\Big]\;. \qquad\qquad \text{(A.28)}
$$

Appendix B

Computer Realizations

The computer realization of some important formulae derived in the dissertation is presented in this appendix. Six different subroutines in a form of the FORTRAN source code represent main parts of programs written for numerical evaluation of quantities described in the sequel. All variables were implicitly declared using the double precision. The declaration is not included in the codes.

First two subroutines were deployed for numerical evaluation of integration kernels for the residual topographical potential and the direct topographical effect on gravity. Values of integration kernels for the spherical terrain correction and its condensed counterpart can also be obtained. Integration kernels for the residual atmospheric potential and the direct atmospheric effect on gravity are then computed using the third and fourth subroutines.

The evaluation of the modified spheroidal Stokes kernel can be done using the fifth subroutine. The analytical solution of the modified spheroidal Stokes kernel can be found in the last subroutine. They both form the computational core of the Stokes integrator employed recently for the numerical evaluations of the accurate gravimetric geoid at the University of New Brunswick.

B.1   Residual topographical potential

```
      subroutine topot(csi,rha,row,rup,dkx,dky,dkz)
c === input:   1.  csi - cosine of spherical distance
c              2.  rha - radius of computation point
c              3.  row - lower bound of newton integral
c              4.  rup - upper bound of newton integral
c === output:  1.  dkx - integration kernel of topographical potential
c              2.  dky - integration kernel of condensation potential
c              3.  dkz - integration kernel of residual potential
      tow=row/rha
      tup=rup/rha
      sow=dsqrt(1.d0+tow*tow-2.d0*tow*csi)
      sup=dsqrt(1.d0+tup*tup-2.d0*tup*csi)
      zow=tow-csi+sow
      zup=tup-csi+sup
      dk1=(3.d0*csi*csi-1.d0)*dlog(zup/zow)
      dk2=(tow+3.d0*csi)*sow
      dk3=(tup+3.d0*csi)*sup
      dkx=rha*rha*(dk1+dk3-dk2)/2.d0
      hip=(rup-row)/row
      tip=rha/row
      sig=(rup-row)*(1.d0+1.5d0*hip+hip*hip)
      dis=dsqrt(1.d0+tip*tip-2.d0*tip*csi)
      dky=row*sig/dis
      dkz=dkx-dky
      return
      end
```

B.2　Direct topographical effect

```
      subroutine topef(csi,rha,rem,row,rup,dkx,dky,dkz)
c === input:   1.  csi - cosine of spherical distance
c             2.  rha - radius of computation point
c             3.  rem - mean radius of earth
c             4.  row - lower bound of newton integral
c             5.  rup - upper bound of newton integral
c === output:  1.  dkx - integration kernel of topographical gravitation
c             2.  dky - integration kernel of condensation gravitation
c             3.  dkz - integration kernel of residual gravitation
      tow=row/rha
      tup=rup/rha
      sow=dsqrt(1.d0+tow*tow-2.d0*tow*csi)
      sup=dsqrt(1.d0+tup*tup-2.d0*tup*csi)
      zow=tow-csi+sow
      zup=tup-csi+sup
      dk1=(3.d0*csi*csi-1.d0)*dlog(zup/zow)
      dk2=(tow*tow*csi+3.d0*csi+(1.d0-6.d0*csi*csi)*tow)/sow
      dk3=(tup*tup*csi+3.d0*csi+(1.d0-6.d0*csi*csi)*tup)/sup
      dkx=rha*(dk1+dk3-dk2)
      sig=(rup*rup*rup-row*row*row)/(3.d0*rem*rem)
      tip=rha/rem
      dis=dsqrt(1.d0+tip*tip-2.d0*tip*csi)
      dky=sig*(csi-tip)/(dis*dis*dis)
      dkz=dkx-dky
      return
      end
```

127

B.3   Residual atmospheric potential

```
      subroutine atpot(csi,rem,rha,row,rup,dkx,dky,dkz)
c === input:   1.   csi - cosine of spherical distance
c             2.   rem - mean radius of earth
c             3.   rha - radius of computation point
c             4.   row - lower bound of newton integral
c             5.   rup - upper bound of newton integral
c === output:  1.   dkx - integration kernel of atmospheric potential
c             2.   dky - integration kernel of condensation potential
c             3.   dkz - integration kernel of residual potential
      de0=+1.2226662d+0
      alp=-1.1435850d-4
      bet=+3.4057150d-9
      tow=row/rha
      tup=rup/rha
      sow=dsqrt(1.d0+tow*tow-2.d0*tow*csi)
      sup=dsqrt(1.d0+tup*tup-2.d0*tup*csi)
      zow=tow-csi+sow
      zup=tup-csi+sup
      res=dlog(zup/zow)
      bam=sup-sow
      cam=sup*tup-sow*tow
      dam=sup*tup*tup-sow*tow*tow
      eam=sup*tup*tup*tup-sow*tow*tow*tow
      rt1=3.d0*csi*bam+cam+(3.d0*csi*csi-1.d0)*res
      rt2=(15.d0*csi*csi-4.d0)*bam+5.d0*csi*cam+
     &2.d0*dam+3.d0*csi*(5.d0*csi*csi-3.d0)*res
```

```
      rt3=5.d0*csi*(21.d0*csi*csi-11.d0)*bam+14.d0*csi*dam+
     &3.d0*(35.d0*csi*csi*csi*csi-30.d0*csi*csi+3.d0)*res+
     &(35.d0*csi*csi-9.d0)*cam+6.d0*eam
      dkx=rha*rha*(de0-alp*rem+bet*rem*rem)*rt1/2.d0+
     &rha*rha*rha*(alp-2.d0*bet*rem)*rt2/6.d0+
     &rha*rha*rha*rha*bet*rt3/24.d0
      tip=rha/rem
      dis=dsqrt(1.d0+tip*tip-2.d0*tip*csi)
      rt1=(tup*tup*tup-tow*tow*tow)/3.d0
      rt2=(tup*tup*tup*tup-tow*tow*tow*tow)/4.d0
      rt3=(tup*tup*tup*tup*tup-tow*tow*tow*tow*tow)/5.d0
      dky=rha*rha*(de0-alp*rem+bet*rem*rem)*rt1/dis+
     &rha*rha*rha*(alp-2.d0*bet*rem)*rt2/dis+
     &rha*rha*rha*rha*bet*rt3/dis
      dkz=dkx-dky
      return
      end
```

B.4   Direct atmospheric effect

```
      subroutine atmef(csi,rem,rha,row,rup,dkx,dky,dkz)
c === input:   1.   csi - cosine of spherical distance
c              2.   rem - mean radius of earth
c              3.   rha - radius of computation point
c              4.   row - lower bound of newton integral
c              5.   rup - upper bound of newton integral
c === output:  1.   dkx - integration kernel of atmospheric gravitation
c              2.   dky - integration kernel of condensation gravitation
c              3.   dkz - integration kernel of residual gravitation
      de0=+1.2226662d+0
      alp=-1.1435850d-4
      bet=+3.4057150d-9
      tow=row/rha
      tup=rup/rha
      sow=dsqrt(1.d0+tow*tow-2.d0*csi*tow)
      sup=dsqrt(1.d0+tup*tup-2.d0*csi*tup)
      zow=tow-csi+sow
      zup=tup-csi+sup
      res=dlog(zup/zow)
      bam=sup-sow
      cam=sup*tup-sow*tow
      dam=sup*tup*tup-sow*tow*tow
      qow=(1.d0-tow*csi)/sow
      qup=(1.d0-tup*csi)/sup
      gow=(qow-csi)/zow
      gup=(qup-csi)/zup
```

```
deq=qup-qow
deg=gup-gow
fam=tup*qup-tow*qow
gam=tup*tup*qup-tow*tow*qow
ham=tup*tup*tup*qup-tow*tow*tow*qow
rt1=3.d0*(csi*bam+csi*deq)+fam+
&(3.d0*csi*csi-1.d0)*(2.d0*res+deg)
rt2=(30.d0*csi*csi-8.d0)*bam+5.d0*(csi*cam+csi*fam)+
&3.d0*csi*(5.d0*csi*csi-3.d0)*(3.d0*res+deg)+
&2.d0*gam+(15.d0*csi*csi-4.d0)*deq
rt3=5.d0*csi*(21.d0*csi*csi-11.d0)*(3.d0*bam+deq)+
&(35.d0*csi*csi-9.d0)*(2.d0*cam+fam)+6.d0*ham+
&3.d0*(35.d0*csi*csi*csi*csi-30.d0*csi*csi+3.d0)*
&(4.d0*res+deg)+14.d0*csi*(dam+gam)
dkx=rha*(de0-alp*rem+bet*rem*rem)*rt1/2.d0
&+rha*rha*(alp-2.d0*bet*rem)*rt2/6.d0
&+rha*rha*rha*bet*rt3/24.d0
tip=rha/rem
sig=(de0-alp*rem+bet*rem*rem)*(rup*rup*rup-row*row*row)/3.d0+
&(alp-2.d0*bet*rem)*(rup*rup*rup*rup-row*row*row*row)/4.d0+
&bet*(rup*rup*rup*rup*rup-row*row*row*row*row)/5.d0
sig=sig/rem/rem
dis=dsqrt(1.d0+tip*tip-2.d0*tip*csi)
dky=sig*(csi-tip)/(dis*dis*dis)
dkz=dkx-dky
return
end
```

B.5   Modified spheroidal Stokes's kernel

```
      subroutine integ(csi,nlr,tkc,ftc)
c === input:   1.  csi - cosine of spherical distance
c             2.  nlr - degree of modified spheroidal stokes fct
c             3.  tkc - coefficients of modified spheroidal stokes fct
c === output:  1.  ftc - value of modified spheroidal stokes fct
      dimension tkc(*)
      rsi=(1.d0-csi)/2.d0
      tsi=dsqrt(rsi)
      ftc=1.d0-5.d0*csi+1.d0/tsi-6.d0*tsi-3.d0*csi*dlog(tsi+rsi)
      sun=0.d0
      sum=tkc(1)/2.d0
      sum=sum+3.d0*tkc(2)*csi/2.d0
      prm=1.d0
      prv=csi
      do n=2,nlr
      prs=prm
      prm=prv
      prv=(2.d0*n-1.d0)*csi*prm-(n-1.d0)*prs
      prv=prv/n
      sun=sun+(2.d0*n+1.d0)*prv/(n-1.d0)
      sum=sum+(2.d0*n+1.d0)*prv*tkc(n+1)/2.d0
      end do
      ftc=ftc-sun-sum
      return
      end
```

B.6 Integral of modified spheroidal Stokes's kernel

```
      subroutine stokes(csr,nlr,tkc,epc)
c === input:   1.  csr - cosine of spherical distance
c              2.  nlr - degree of spheroidal stokes fct
c              3.  tkc - modification coefficients
c === output:  1.  epc - integral of modified spheroidal stokes fct
      dimension tkc(*)
      tsi=dsqrt((1.d0-csr)/2.d0)
      epc=4.d0*tsi-5.d0*tsi*tsi-
     &6.d0*tsi*tsi*tsi+7.d0*tsi*tsi*tsi*tsi-
     &6.d0*tsi*tsi*(1.d0-tsi*tsi)*dlog(tsi+tsi*tsi)
      sun=0.d0
      sum=tkc(1)*(csr-1.d0)/2.d0+3.d0*tkc(2)*(csr*csr-1.d0)/4.d0
      prm=csr
      prv=(3.d0*csr*csr-1.d0)/2.d0
      do n=2,nlr
      prs=prm
      prm=prv
      prv=(2.d0*n+1.d0)*csr*prm-n*prs
      prv=prv/(n+1)
      sun=sun+(prv-prs)/(n-1.d0)
      sum=sum+tkc(n+1)*(prv-prs)/2.d0
      end do
      epc=epc+sun+sum
      return
      end
```

Vita

Candidate's full name : Pavel Novák

Date / place of birth : September 21, 1965 / Pilsen, Czech Republic

Permanent address : Lud'ka Pika 1

320 05 Pilsen

Czech Republic

Phone: + 420 19 278779

E-mail: novak@asu.cas.cz

Schools attended : Elementary school, Pilsen, 1972 − 1980

Grammar school in Pilsen, 1980 − 1984

Universities attended : Czech Technical University, Prague, 1984 − 1989

University of New Brunswick, Fredericton, 1996 − 1999

University degree : Master of Engineering, Czech Technical University, 1989

Publications :

Novák, P. (1993). Astronomical observations in the Czechoslovak GPS reference network. *Scientific Newspapers of the Technical University Dresden*, No. 42, Dresden.

Karský, G., J. Kostelecký, *P. Novák*, and J. Šimek (1993). Realization of the GPS reference network on the territory of the Czech and Slovak Republics. *Reports of the Research Institute of Geodesy, Topography, and Cartography*, Prague.

Novák, P., J. Kostelecký, and L. Skořepa (1994). Preliminary analysis of continuous GPS observations. *Reports on Geodesy*, Warsaw Institute of Technology, No. 5(13), pp. 185-209, Warsaw.

Novák, P. and G. Karský (1994). The Czech and Slovak reference network of the zero order (solution 1993). *Reports of the Research Institute of Geodesy, Topography, and Cartography*, Prague.

Karský, G. and *P. Novák* (1994). Preliminary analysis of the Czech GPS reference network. *Geodetic and Cartographic Horizon*, No. 1, pp. 218-222, Prague.

Novák, P. and V. Skoupý (1994). Astronomical observations in the GPS project CS-NULRAD'92. *Geodetic and Cartographic Horizon*, No. 3, pp. 45-47, Prague.

Novák, P. and G. Karský (1994). Analysis of the Czech GPS reference network. *Geodetic and Cartographic Horizon*, No. 9, pp. 183-189, Prague.

Novák, P., G. Karský, and L. Skořepa (1994). Accuracy of the GPS technology on very short baselines. *Geodetic and Cartographic Horizon*, No. 11, pp. 227-231, Prague.

Novák, P. (1995). International GPS Service for Geodynamics in 1995. *Geodetic and Cartographic Horizon*, No. 10, pp. 183-189, Prague.

Marek, P. and *P. Novák* (1995). Central European Geodynamics Reference Network. Czech solution 1994. *Reports on Geodesy*, Warsaw University of Technology, No. (3)16, pp. 341-350, Warsaw.

Marek, P., *P. Novák*, and J. Šimek (1995). GPS-based investigations of recent crustal movements in the seismoactive area Western Bohemia – Vogtland. *Reports on Geodesy*, Warsaw University of Technology, No. (3)16, pp. 361-368, Warsaw.

Skořepa, Z. and *P. Novák* (1996). GPS survey in the "Staré Město pod Sněžníkem" experimental network. *Geodetic and Cartographic Horizon*, No. 7, pp. 138-142, Prague.

Kostelecký, J., *P. Novák*, L. Skořepa, and J. Šimek (1996). Analysis of continuous GPS observations for geodynamics purposes. *GPS Trends in Precise Terrestrial, Airborne, and Spaceborne Applications*, Springer, pp. 65-69, Berlin.

Cimbálník, M., D. Dušátko, P. Janus, G. Karský, J. Kostelecký, L. Laža, Z. Nevosád, *P. Novák*, J. Provázek, J. Říkal, L. Skořepa, J. Šimek, M. Talich, V. Vatrt, and L. Zajíček (1998). *Geodetic reference systems in the Czech Republic*. Research Institute of Geodesy, Topography, and Cartography & Military Geographical Institute, Prague, 188 pp.

Vaníček, P., J. Huang, *P. Novák*, S. Pagiatakis, M. Véronneau, Z. Martinec, and W. Featherstone (1999). Determination of boundary values for the Stokes-Helmert problem. *Journal of Geodesy*, No. 73, pp. 180-192.

Vaníček, P. and *P. Novák* (1999). On the correct determination of transformation parameters of a horizontal geodetic datum. Submitted to *Geomatica*.

Reports and Presentations :

Novák, P. (1989). Semi-dynamic method of the satellite geodesy and its applications for laser ranging to the LAGEOS. Master of Engineering thesis, Czech Technical University, Department of Geodesy and Cartography, Prague.

Novák, P. (1991). Determination of the astronomical latitude and longitude using the circumzenithal VÚGTK 50/500. Contract report for the German Research Council, Bonn.

Novák, P. (1992). Some aspects of the circumzenithal VÚGTK 50/500. Research report of the Technical University Berlin, Department of Geodesy and Photogrammetry, Berlin.

Novák, P. (1992). On the astronomical levelling. Research report of the Technical University Berlin, Department of Geodesy and Photogrammetry, Berlin.

Skoupý, V. and *P. Novák* (1992). Astronomical observations in the GPS campaign CS-NULRAD'92. Research report of the Research Institute of Geodesy, Topography, and Cartography, Prague.

Brož, J., P. Dubišar, P. Holota, G. Karský, J. Kostelecký, L. Livora, *P. Novák*, J. Šimek, Z. Šimon, and P. Vyskočil (1992). Geodesy and the dynamics of the Earth. Research report of the Research Institute of Geodesy, Topography, and Cartography, Prague.

Novák, P. (1993). Interconnection of Czech and German GPS reference networks. Analysis of the GPS project CZ-BRD'93. Research report of the Research Institute of Geodesy, Topography, and Cartography, Prague.

Novák, P. and G. Karský (1993). Czech and Slovak spatial reference network of the zero order. Analysis of the GPS project CS-NULRAD'92. Research report of the Research Institute of Geodesy, Topography, and Cartography, Prague.

Novák, P. and J. Kostelecký (1994). Densification of the Czech GPS reference network. Sector A. Contract report for the Czech Office of Surveying, Mapping, and Cadastre, Prague.

Kostelecký, J. and *P. Novák* (1994). Densification of the Czech GPS reference network. Sector B. Contract report for the Czech Office of Surveying, Mapping, and Cadastre, Prague.

Kostelecký, J., P. Marek, *P. Novák*, and L. Skořepa (1994). Realization of the ETRF coordinate frame on the territory of the Czech Republic for civilian and military purposes. Proceedings of the seminar "Role of modern geodesy in armed forces", Budapest, November 1994.

Kostelecký, J., *P. Novák*, and J. Šimek (1994). On the long term behaviour of long baselines determined by GPS. Initial stage of the analysis. Presented at the "First CERGOP Conference", Warsaw, February 1994.

Novák, P. (1994). Some aspects of the GPS reference frame on the territory of the Czech and Slovak Republics. Presented at the workshop "Geodetic Networks", Bratislava, May 1994.

Novák, P., J. Kostelecký, and L. Skořepa (1994). Densification of the Czech GPS reference network. Sector C. Contract report for the Czech Office of Surveying, Mapping, and Cadastre, Prague.

Kostelecký, J. and *P. Novák* (1994). Densification of the Czech GPS reference network. Sector D. Contract report for the Czech Office of Surveying, Mapping, and Cadastre, Prague.

Novák, P., J. Kostelecký, and L. Skořepa (1994). Densification of the Czech GPS reference Network. Sectors E and F. Contract report for the Czech Office of Surveying, Mapping, and Cadastre, Prague.

Kostelecký, J., *P. Novák*, and J. Šimek (1994). National report of the Czech Republic on the participation in the international GPS campaign "Interconnection of the First Order Horizontal Networks", presented at the international working meeting on the results of the campaign, Vienna, May 1994.

Novák, P., J. Kostelecký, and L. Skořepa (1994). Densification of the Czech GPS reference network. Sectors G, H, and J. Contract report for the Czech Office of Surveying, Mapping, and Cadastre, Prague.

Novák, P., J. Kostelecký, and L. Skořepa (1994). Analysis of DOPNUL campaigns in the ETRF-89. Research report of the Research Institute of Geodesy, Topography, and Cartography, Prague.

Novák, P. (1994). Czech and Slovak reference network of the zero order. Research report of the Research Institute of Geodesy, Topography, and Cartography, Prague.

Novák, P. (1995). Analysis of GPS data in geodesy. Presented at the geodetic workshop "Applications of GPS in Geodesy", Prague, June 1995.

Kostelecký, J., *P. Novák*, L. Skořepa, and J. Šimek (1995). Analysis of continuous GPS observations for geodynamics purposes. Presented at the XXI. general assembly of the International Union of Geodesy and Geophysics, Boulder, July 1995.

Vaníček, P., M. Najafi, *P. Novák*, and J. Huang (1997). Evaluation of boundary values in the generalized Stokes-Helmert's problem. Contract report for the Geodetic Survey Division, Natural Resources Canada, Ottawa.

Vaníček, P., *P. Novák*, and J. Huang (1997). Atmosphere in Stokes-Helmert's solution of the geodetic boundary-value problem. Contract report for the Geodetic Survey Division, Natural Resources Canada, Ottawa.

Vaníček, P., J. Huang, and *P. Novák* (1997). DOWN'97. Discrete Poisson's downward continuation package for 5 x 5' data. Contract report for the Geodetic Survey Division, Natural Resources Canada, Ottawa.

Vaníček, P., *P. Novák*, and J. Huang (1998). Stokes's integration as a solution to the geodetic boundary-value problem. Contract report for the Geodetic Survey Division, Natural Resources Canada, Ottawa.

Vaníček, P., J. Huang, and *P. Novák* (1998). Effect of topographical mass density variations on gravity and geoid in the Canadian Rocky Mountains. Contract report for the Geodetic Survey Division, Natural Resources Canada, Ottawa.

Novák, P. and P. Vaníček (1998). Atmospheric corrections for the evaluation of mean Helmert's gravity anomalies. Presented at the annual meeting of the Canadian Geophysical Union, Quebec City, May 1998.

Novák, P. and P. Vaníček (1999). Effect of distant topographical masses on geoid determination. Presented at the annual meeting of the Canadian Geophysical Union, Banff, May 1999.

Vaníček, P. and *P. Novák* (1999). Comparison between planar and spherical models of topography. Presented at the annual meeting of the Canadian Geophysical Union, Banff, May 1999.

Novák, P., P. Vaníček, M. Véronneau, W. E. Featherstone, and S. A. Holmes (1999). On the accuracy of Stokes's integration in the precise high-frequency geoid determination. Presented at the semi-annual meeting of the American Geophysical Union, Boston, June 1999.